USDA/NIFA Nanotechnology Grantees' Conference
December 10- 11, 2010, Washington, DC.

Nanoscale analysis of chemical residues in foods using whispering-gallery-mode miniature sensors

Zhixiong Guo, Lei Huang, Qiulin Ma and Tobias Rossmann

Department of Mechanical and Aerospace Engineering
Rutgers University – New Brunswick/Piscataway
New Jersey, 08854, USA

THE STATE UNIVERSITY OF NEW JERSEY
RUTGERS

Outline

- **Introduction:**
  - -- What is Whispering-Gallery Mode (WGM)?
  - -- Motivation
- **Approach and experimental setup**
- **Results and discussion**
- **Conclusions**
- **Acknowledgment**

Optical Whispering-Gallery Mode (WGM)

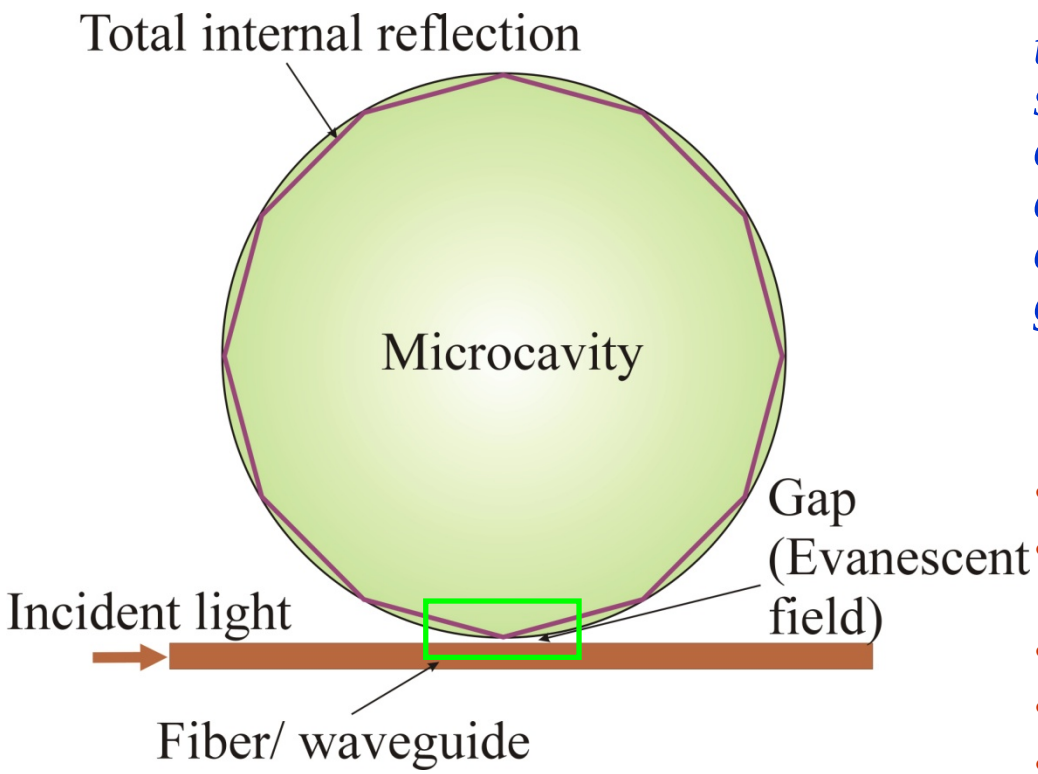

WGM occurs when light, confined by total internal reflections, orbits near the surface of a dielectric medium of circular geometry and returns in phase after each revolution. The electromagnetic field can close on itself, giving rise to resonance.

- Gap < λ: Photon tunneling in the gap
- Matter-radiation interactions in the evanescent field
- Morphology-dependent resonance
- Miniature in size
- Manufacturable

$$\Delta f / f \approx -(\Delta R / R + \Delta n / n)$$

Motivation

- **W**GM microsensor can reach an ultra high quality factor (> 10^{10}) in a small mode volume, which in turn gives a high resolution
- **W**GM microsensor is miniature in size and very easy to fabricate
- **P**rior studies have explored WGM resonances for various detections:

  -- Arnold *et al.* [2002,2003] have demonstrated the detection of protein molecules within an aqueous solution ;

  -- Quan and Guo [2007] proposed and analyzed the detection of a single molecule.
- **H**ere we explore a potential WGM gas-sensing method, using water vapor, which is essential to monitor for food safety, pharmacy, etc., as a gas-phase example
- **F**ew methods have demonstrated reliable detection of water vapor at humidity level below 10%

Approach

- Coating of nanostructured layers of SiO_2 nanoparticles has been employed.
- The adsorption and desorption of water in the coated layer introduce effective refractive index changes of the coating layer, which in turn induce resonance frequency shifts.
- Preparation of the coating: Electrostatic-self-assembly (ESA) layer by layer method.

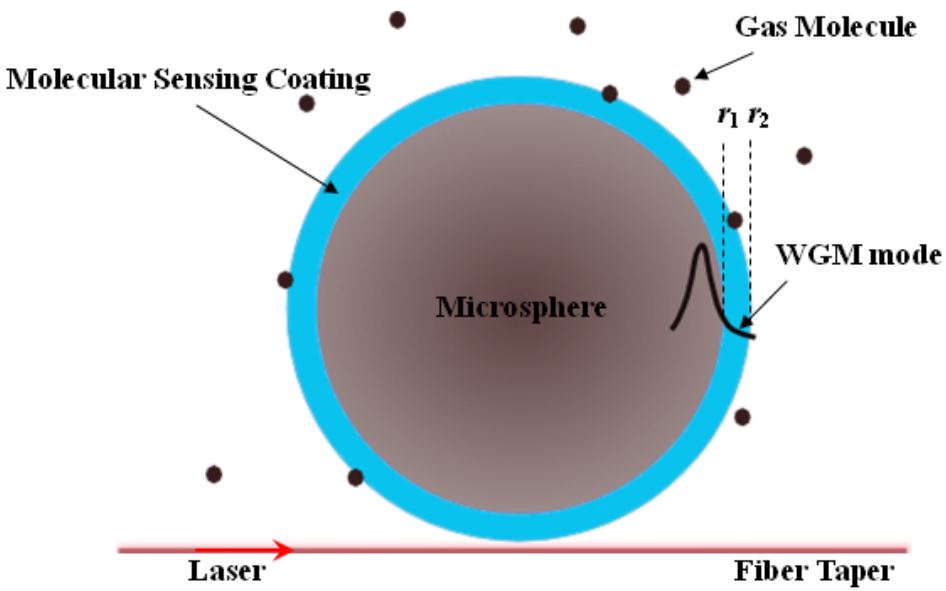

Figure 1. Schema of the sensing mechanism

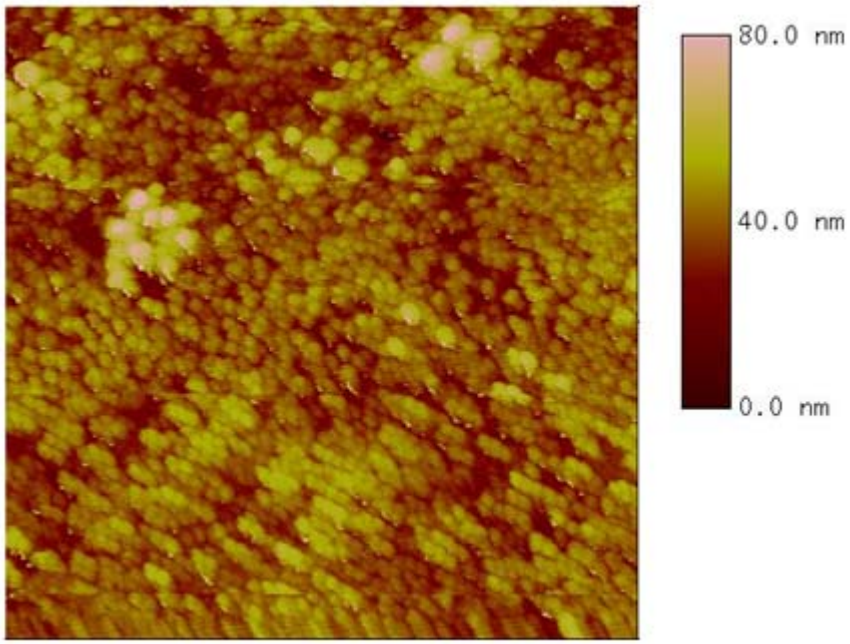

Figure 2. AFM image of the film composed of 20 monolayers of 20nm nanoparticles, coating thickness: ~330nm

Experimental setup

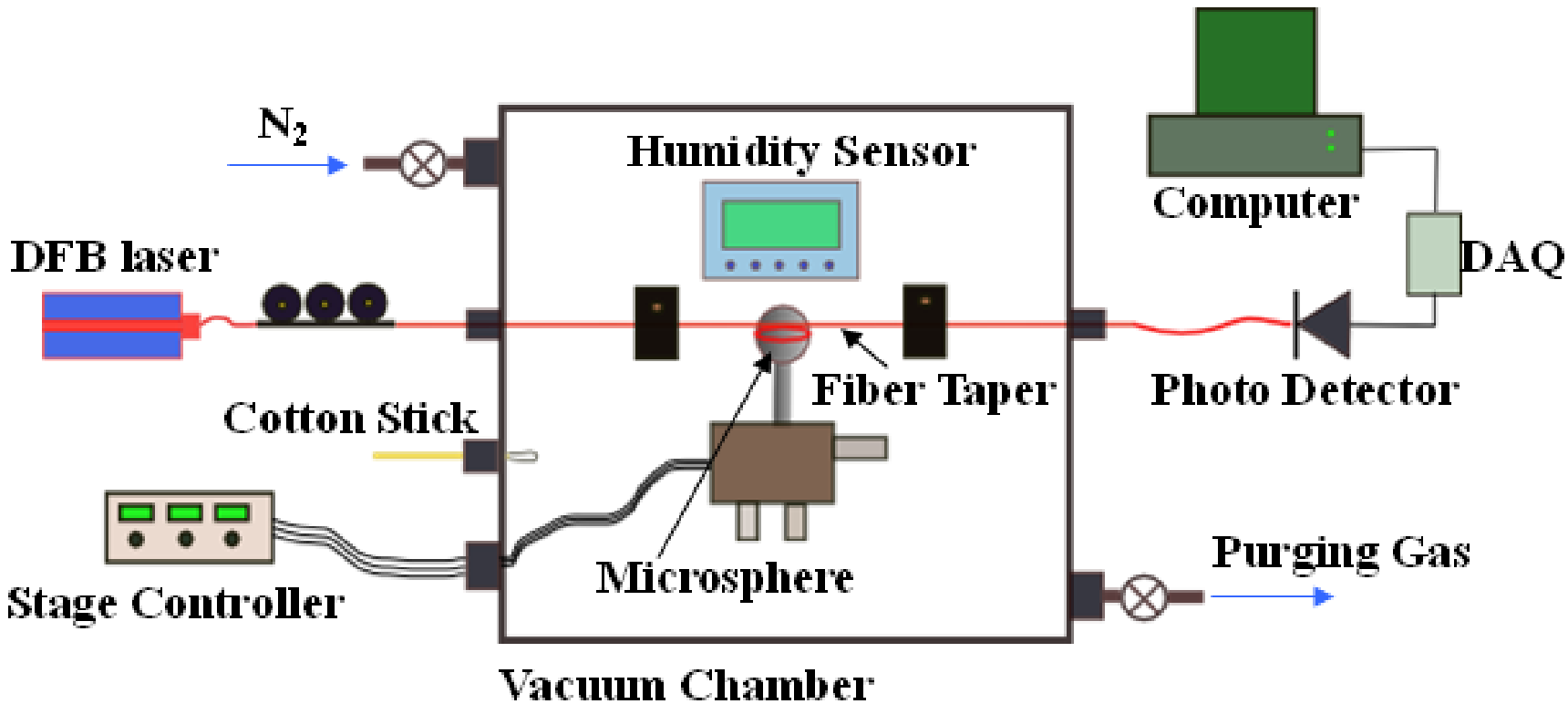

Figure 3. Experimental setup of the low-level humidity (0~10%) sensing

Results and discussion I – Theoretical analysis

- The radial distribution of the transverse electronic (TE) WGMs in the coated microsphere can be described by Mie theory.

$$E_{l,n} = \begin{cases} A\psi_l(n_1 k_0^{(n)} r) & (r \le r_1) \\ C\psi_l(n_2 k_0^{(n)} r) + D\chi_l(n_2 k_0^{(n)} r) & (r_1 \le r \le r_2) \\ B\chi_l(n_3 k_0^{(n)} r) & (r_2 \le r) \end{cases}$$

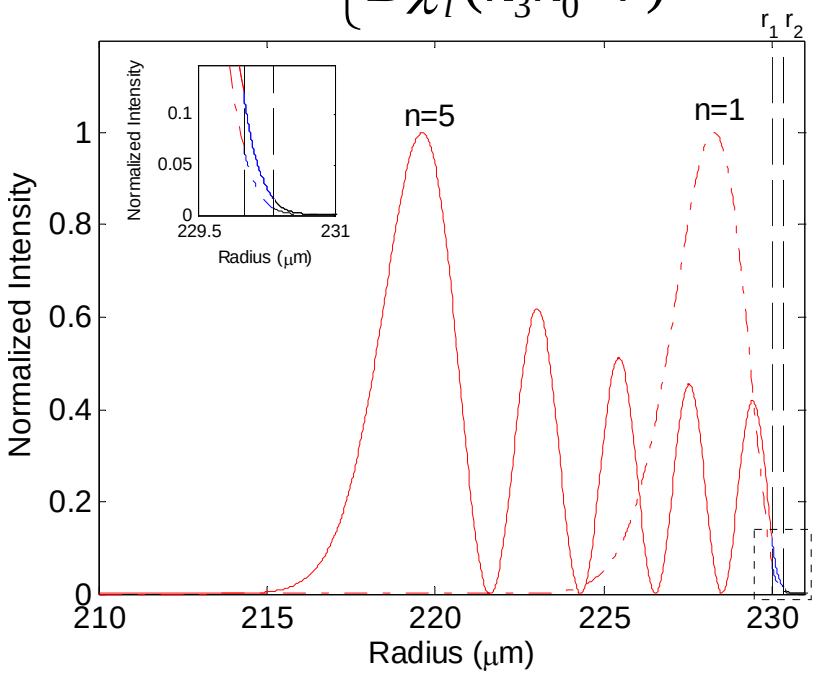

Figure 4. Intensity distribution of two TE WGMs r1=230μm and r2=230.33 μm, n1=1.4862,n2=1.22, n3=1

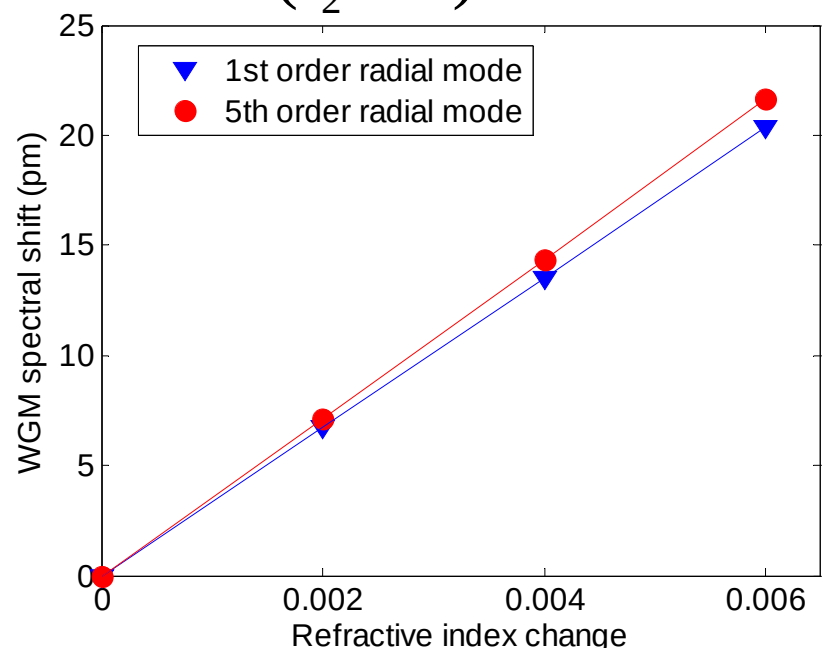

Figure 5. Simulation of the WGM spectral shift versus the refractive index change of the coating

Results and discussion II – Experiment results

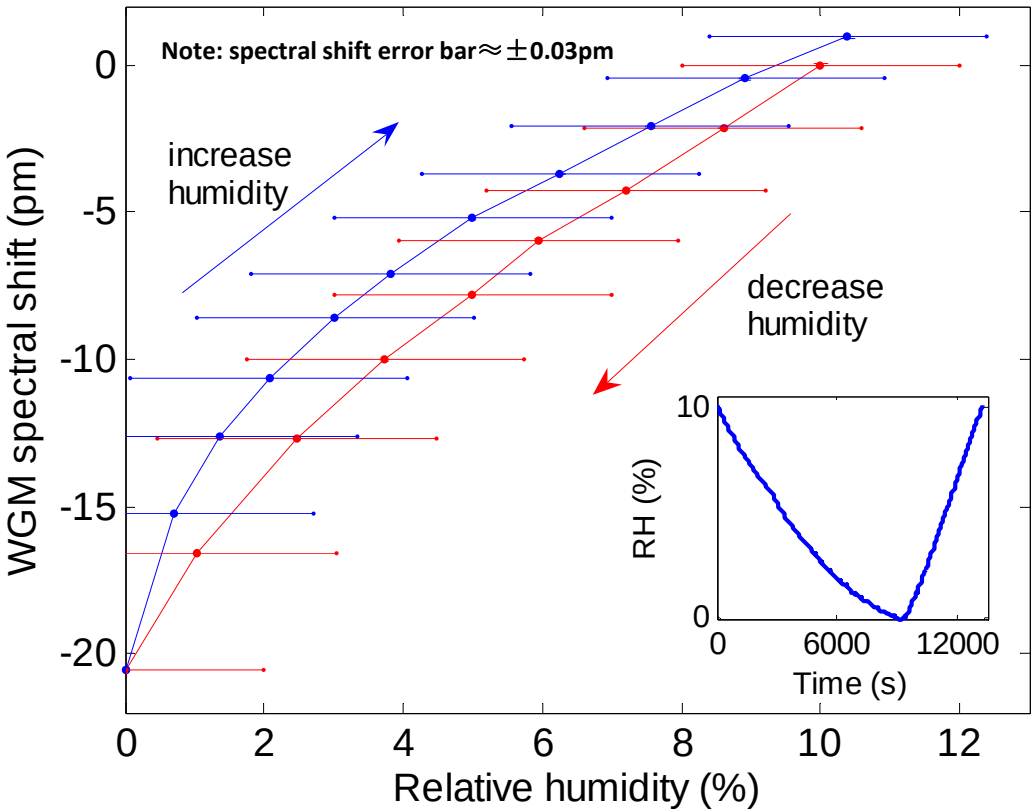

Figure 6. WGM spectral shift versus RH change at 298.2K; inset: humidity change versus time

- Both processes are slow enough to ensure that the temporal response of the commercial sensor humidity changes;
- The temperature inside the chamber is maintained at 298.2±0.1K during the test, as measured by the commercial sensor;
- The method has given a sensitivity of 2.9×10^{-4} RIU pm^{-1} ;
- A change of 1 ppm of H_2O (0.003% RH) is estimated as the detection limit;
- A significant hysteresis effect is clearly seen.

Results and discussion III – Experiment results

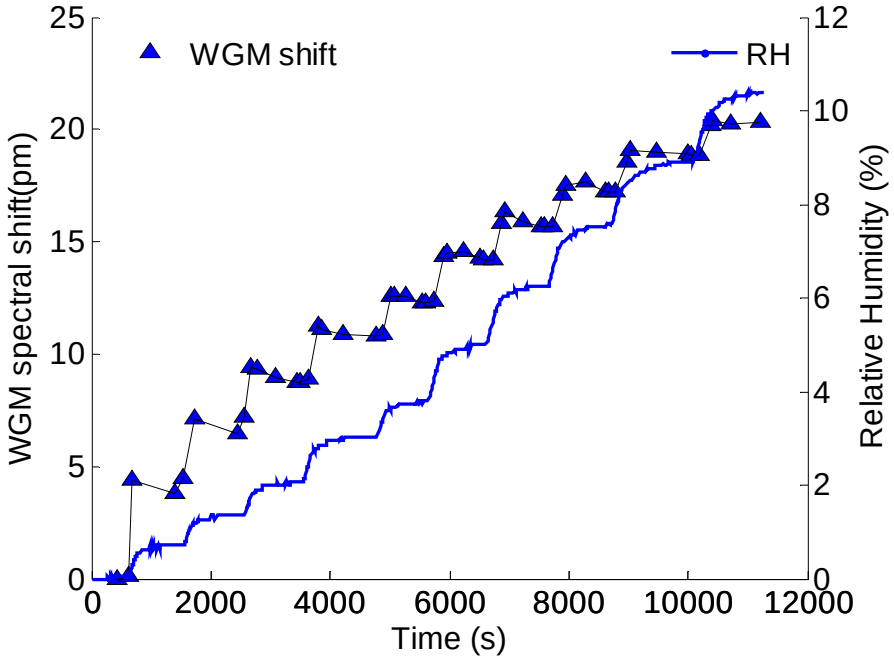

Figure 7. WGM spectral shift with a continuous step increase of humidity at 300K

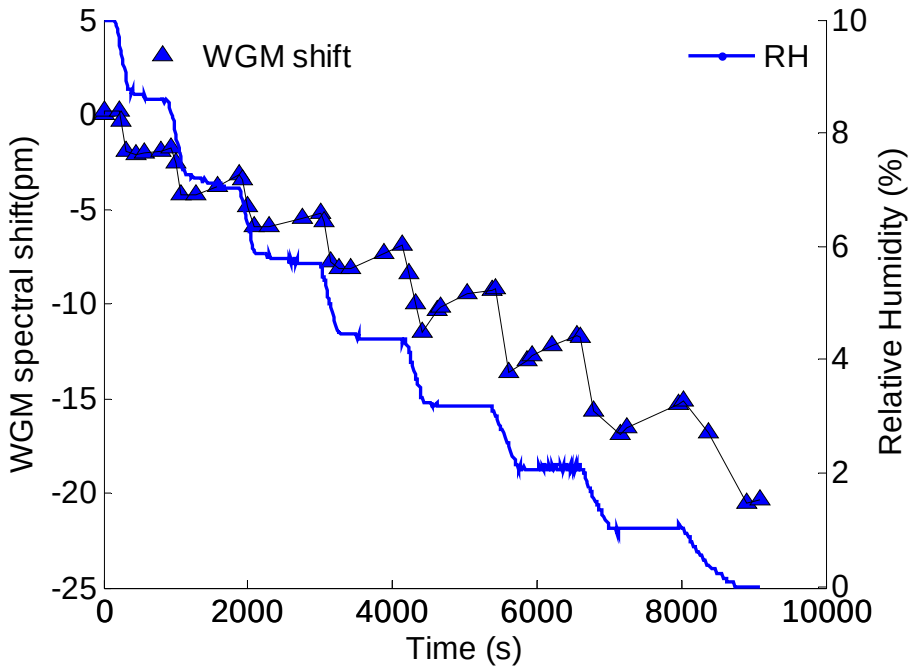

Figure 8. WGM spectral shift with a continuous step decrease of humidity at 300K

- The water vapor source is exposed to the chamber and then quickly isolated to create the step increase; An equivalent step humidity decrease is achieved by short-duration dry nitrogen purging;
- Temperature variation is maintained within 0.08K;
- The WGM shift closely follows the step change of the humidity;
- The dynamic processes tend to return to the initial water concentration level.

Results and discussion IV – Experiment results

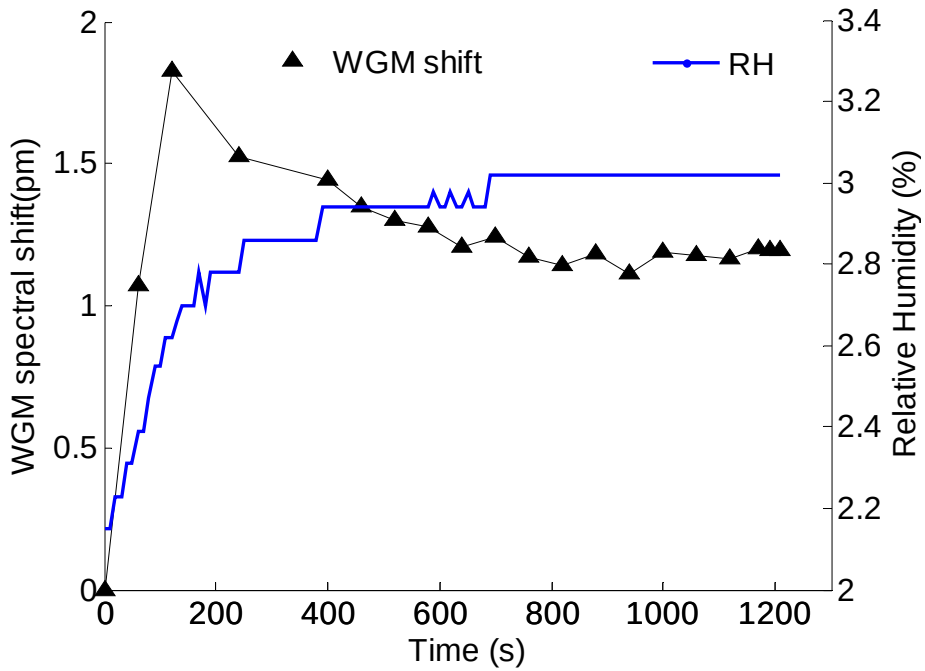

Figure 9. WGM spectral shift with a single step increase of humidity at 300K

- Temperature variation is maintained within 0.08K;
- The WGM shift closely follows the step change of the humidity;
- The WGM microsensor responses faster than the commercial sensor;
- The dynamic processes tend to return to the initial water concentration level due to the dynamic desorption and adsorption competition.

Conclusions

- The WGM spectral shift induced by a refractive index change in a transparent coating has been analyzed theoretically and experimentally.
- A nanostructured SiO_2 layer has been coated onto the surface of a silica microsphere.
- The coated microsphere in response to environmental humidity changes via the WGM spectral shift has been measured in a very low humidity level (<10%).
- The hysteresis effect was found, and the dynamic adsorption and desorption processes of water molecules interacting with the coated layer are revealed by the WGM spectral shift during the step changes in humidity.
- The method has given a sensitivity of 2.9×10^{-4} RIU pm^{-1}.
- A change of 1 ppm of H_2O (0.003% RH) is estimated as the detection limit using the current instrument.

Acknowledgment

- Support to the work by the US Department of Agriculture under CSREES award 2008-01336.
- The laboratory support of the coating process from Professor Denhardt (Rutgers University, Department of Biology).
- The AFM imaging support from Professor Qingrong Huang (Rutgers University, Department of Food Science).
- Support for the work from Rutgers University Academic Excellence Fund.

USDA NIFA Grantees Conference Progress Report

Development of Rapid Detection Technique for Pathogens using SERS with Silver Nanorod Array Substrates

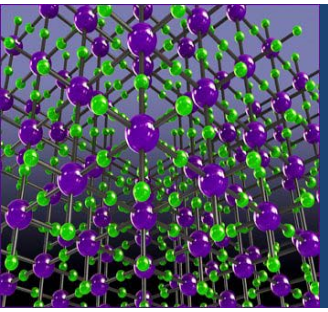

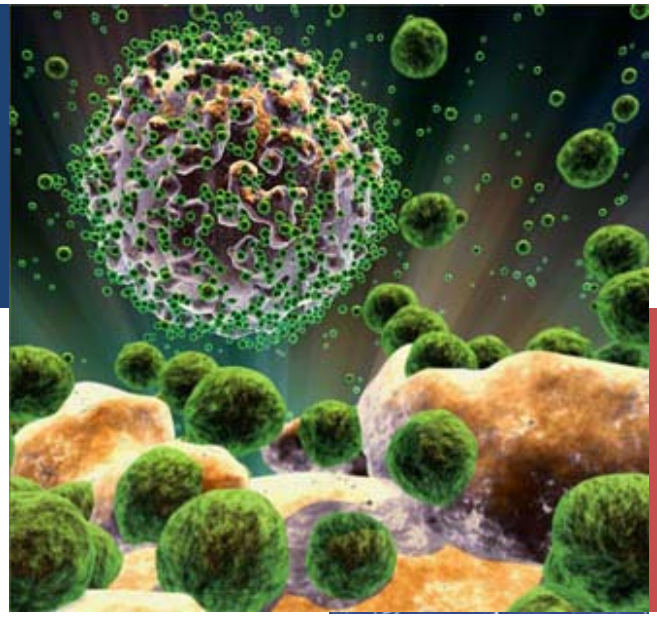

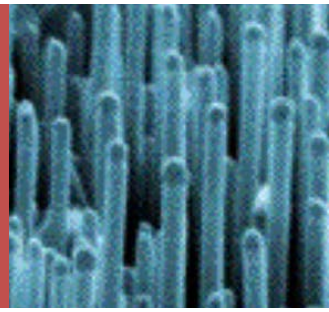

PI: Yao-wen Huang (UGA)

Co-PI: Yiping Zhao (UGA) and Bosoon Park (USDA)

Objectives

- To determine a better concentration methods by using filtration and centrifugation techniques

- To develop and determine an environment that reduces the contaminants during the SERS application

Experimental

- **Bacterial Preparation**

Salmonella Typhimurium 1925-1 (poultry isolate) in trypticase soy broth over night at 25° C to yield generally ~10^{9} CFU/ml culture.

Following incubation, the cultures were washed three times with sterilized de-ionized (DI) water before re-suspending in DI water. Desired dilutions were made with sterilized DI water.

Experiemtnal

- **SERS Measurements:**

HRC-10HT Raman analyzer system (Enware Optronics Inc., Irvine, CA).

The laser power: 30mW

λ: 785 nm; exposure time: 10s

Sample volume: 15μL

Experiemtnal

- **Data analysis**

The spectral coverage is from 200 to 2400 cm^{-1} with 785 nm excitation.

WIRE 2.0 for peak fitting.

Origin software 7.0 version for spectra processing, including spectra plotting, baseline correction and peak detection.

Experimental

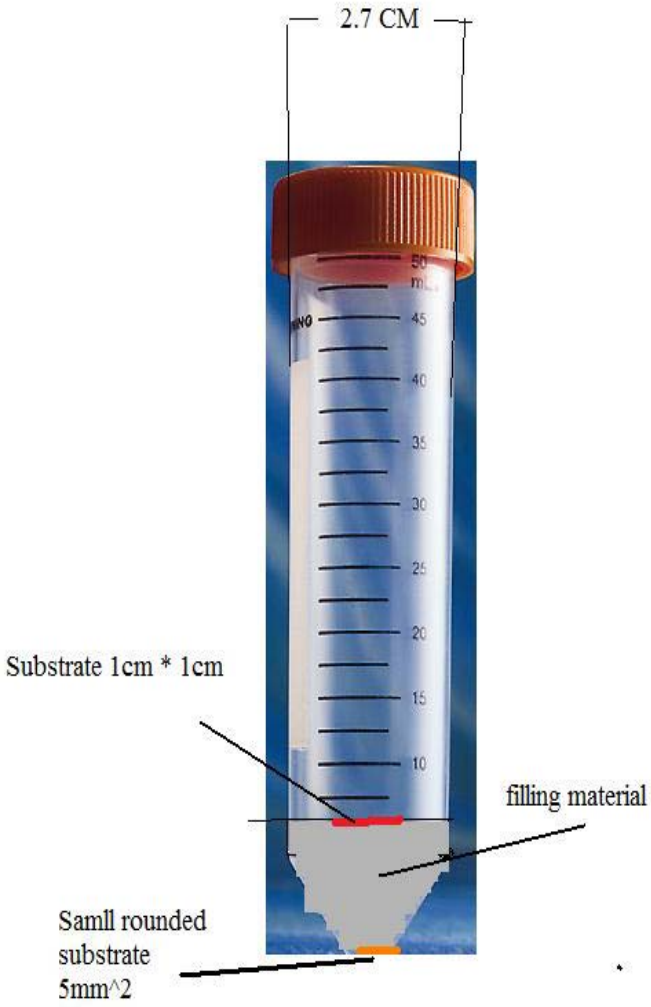

Pipette Method:

2 or 15 μl bacteria samples are directly pipette onto the substrate. SERS measurements are taken after drying.

Centrifuge Method:

10 or 40 ml bacteria solution is centrifuged in a substrate containing tube. Bacteria are tightly applied onto the substrate by centrifuge force and concentrated at the same time.

Two step filtration method

First filtration:

250 ml salmonella sample (10^5, 10^4, and 10^3 CFU/ml) was filtered through vacuum filtration system with a filter membrane of 0.22 μm pore size. Then, the filter membrane was collected and vortex for 15 sec with 2 ml DI water, based on Wolffs procedure.

Second filtration:

2 ml solution from first filtration was added to the centrifugal filter. After centrifuge at 6500 rpm for 7 min. Only bacteria were left on the membrane (0.2 μm pore size). 50μl water was added to re-suspend the bacteria. 15 μl solution is added on substrate for SERS measurement.

Results: centrifuge method

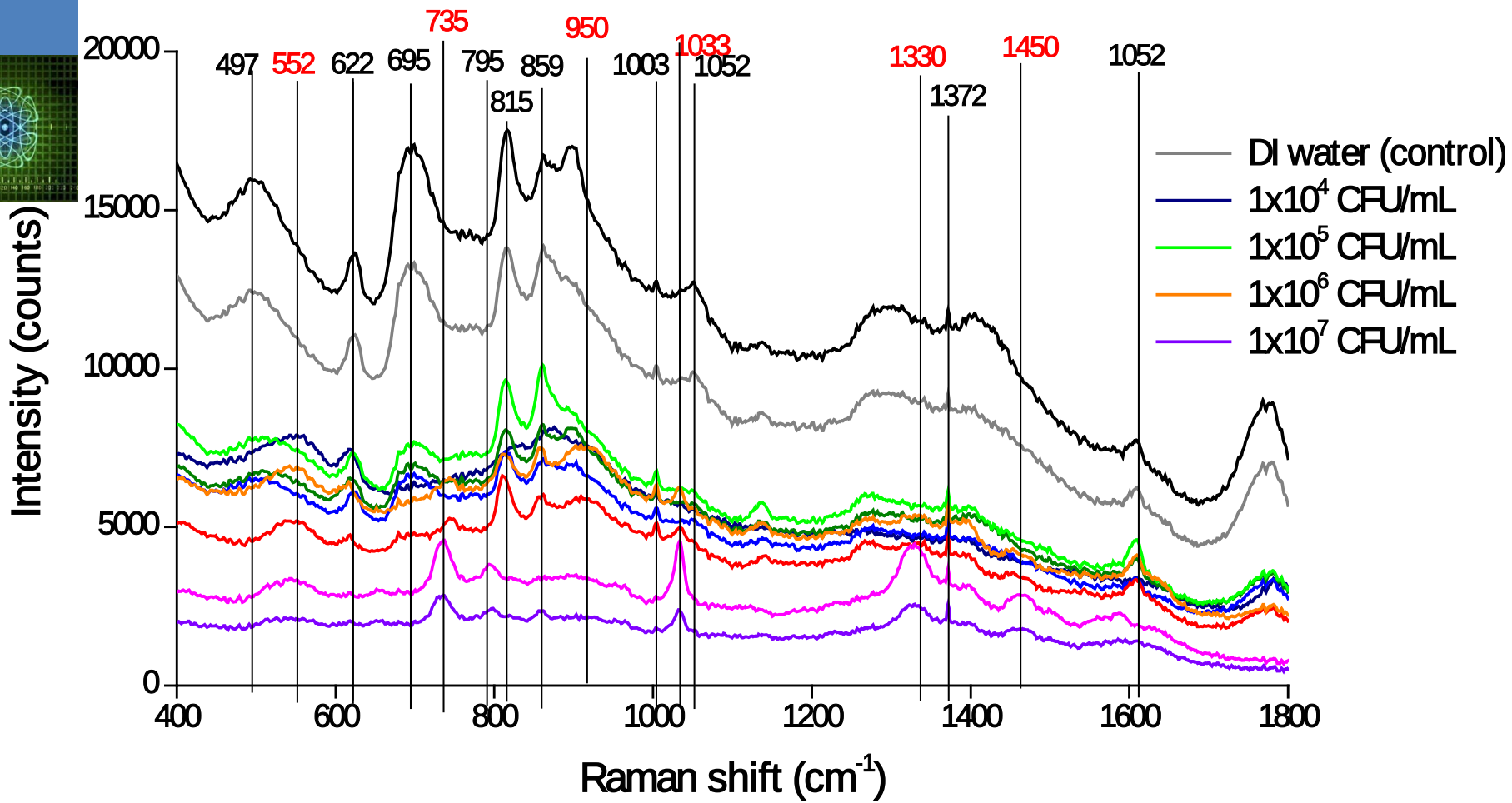

Raman spectra of *Salmonella* Typhimurium with centrifuge method at different concentration. Number in red shows the peak from bacteria, while number in black shows peak from background. (30 mW and 10 s)

Data analysis

DI water samples at the same band region, from 715-755 cm^{-1} were baseline corrected using Origin 7.0 by 10 points baseline with smoothing.

The baseline subtracted data were used to calculate the average standard deviation.

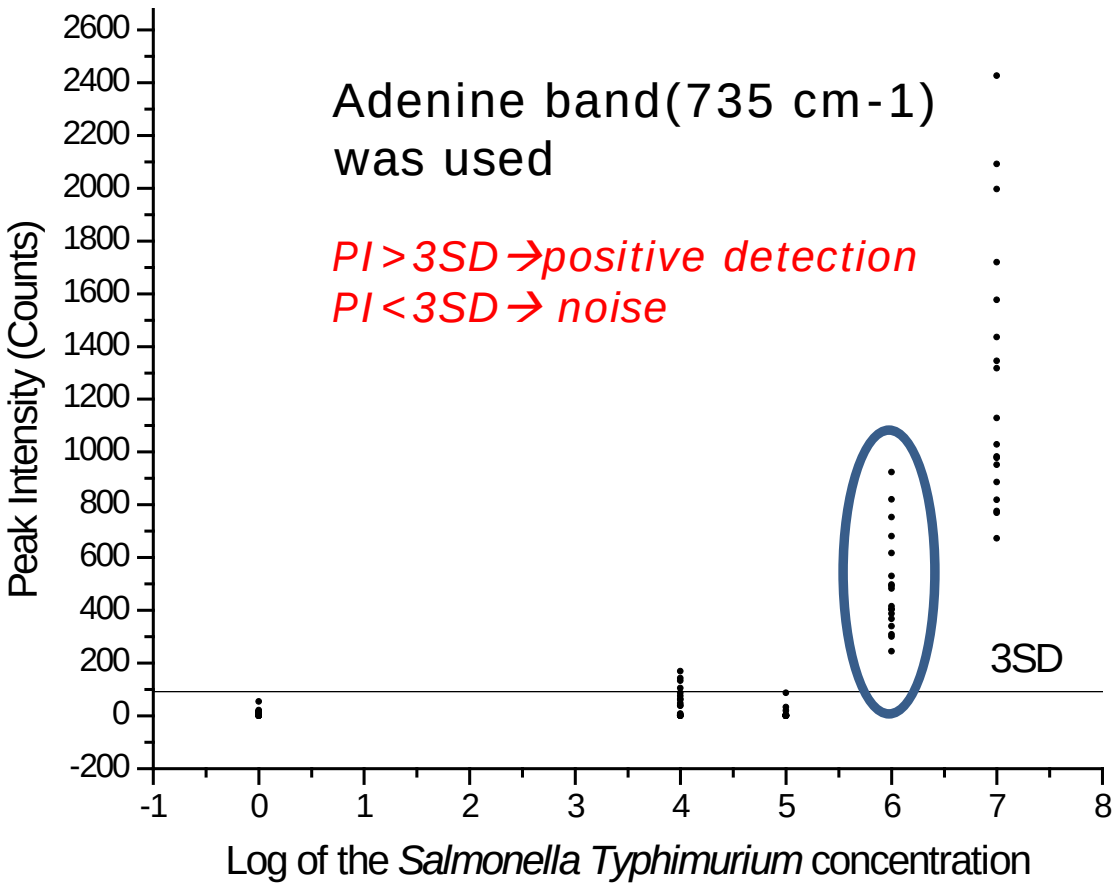

Peaks intensity of ~735 cm^{-1} band as a function of the concentration of *Salmonella* Typhimurium samples prepared by centrifuge method

SEM image of pipette samples

"Ring effect" due to the surface tension

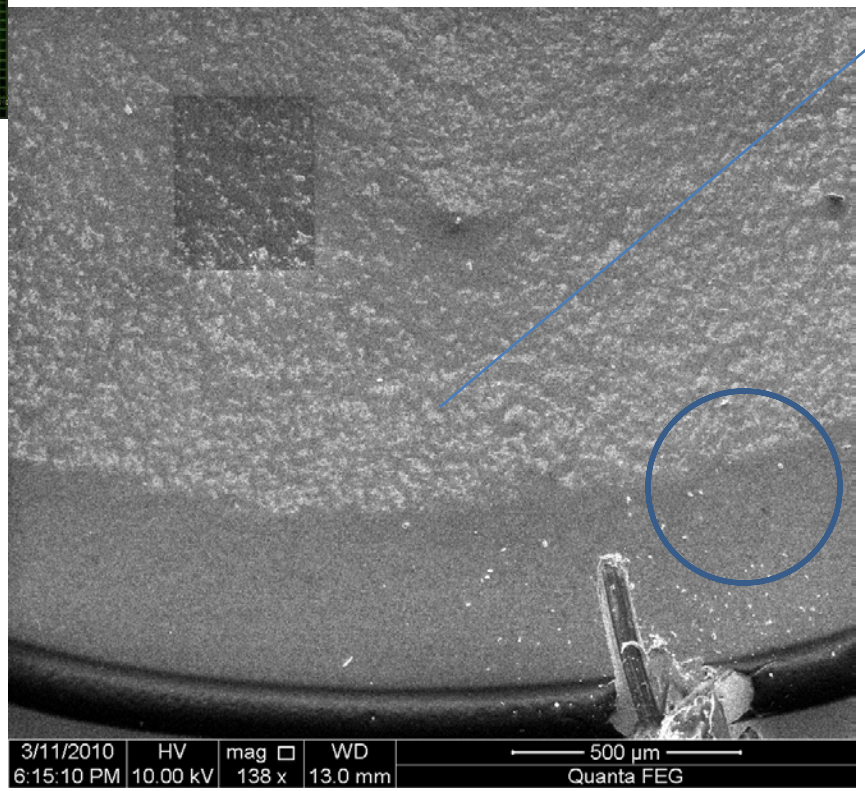

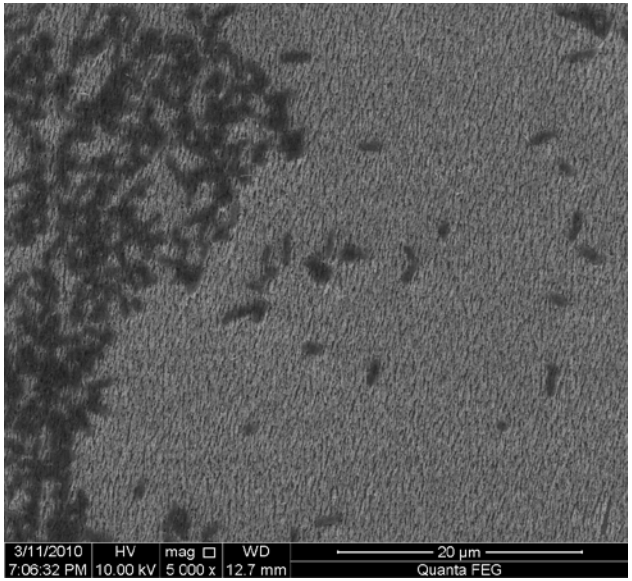

Uneven distribution of bacteria on substrate using pipette method

SEM image of centrifuge samples

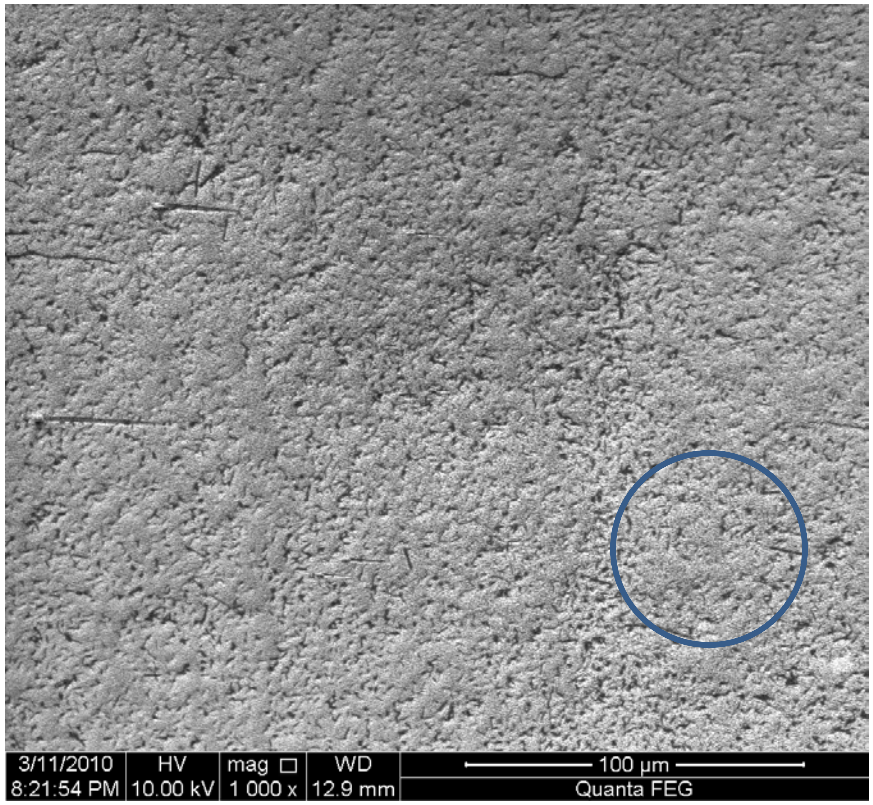

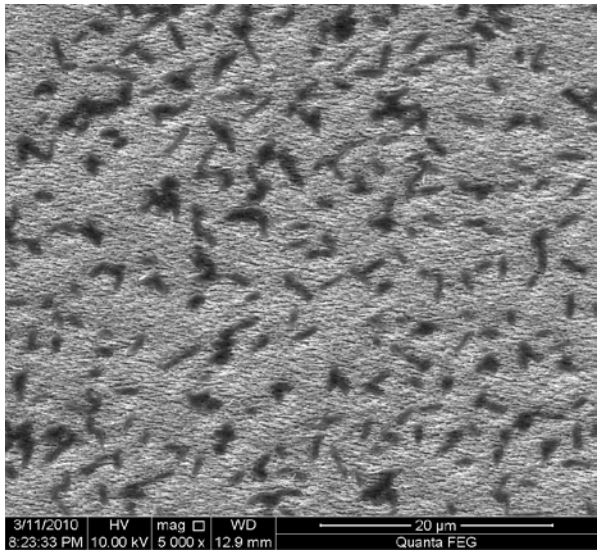

Evenly distribution of bacteria on substrate using centrifuge method

Ring effect illustrated by PolyStyrene

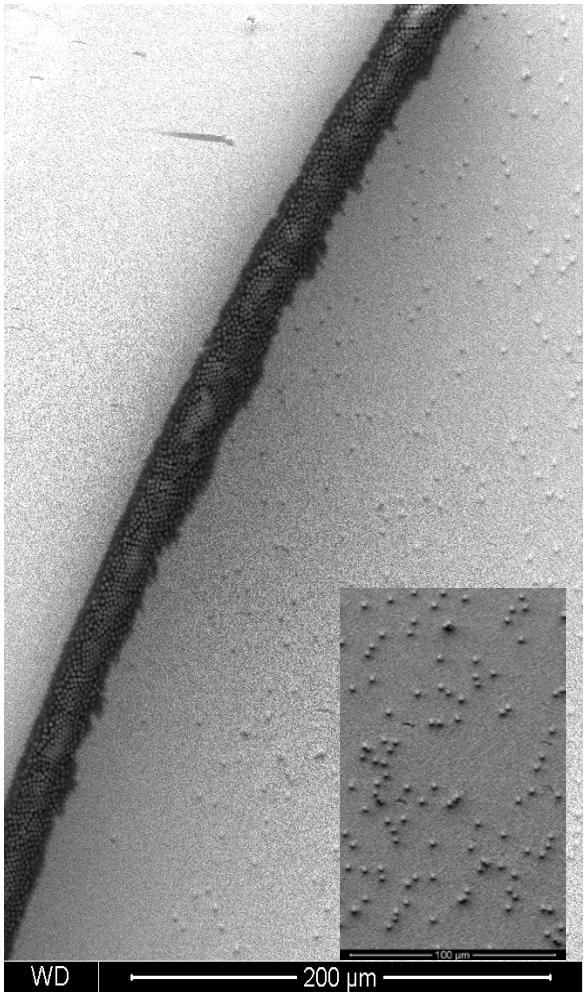

pipette method

centrifuge method

The “Ring” effect

Result: two step filtration method

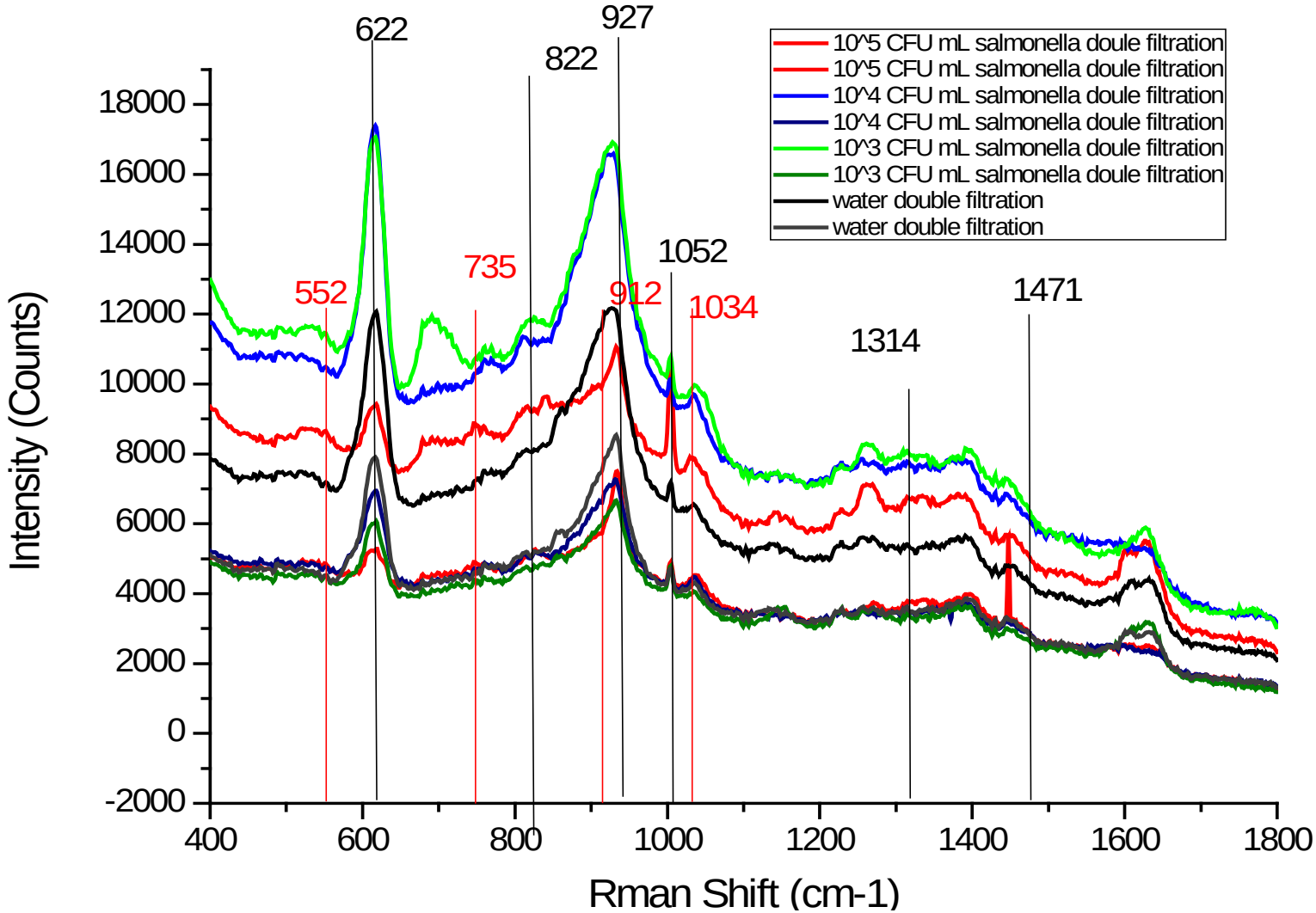

Data analysis

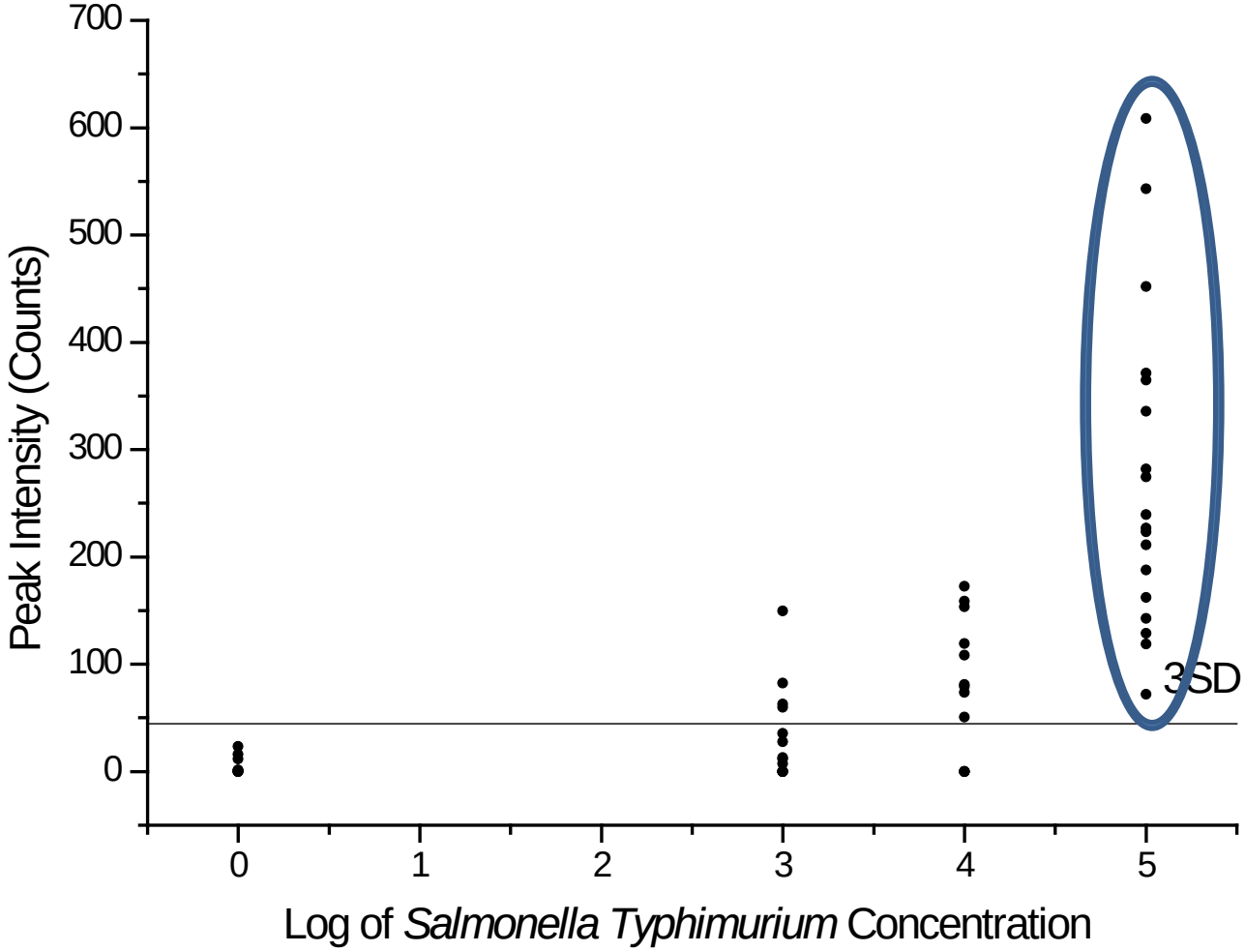

The LOD is 10^5 CFU/ml

Cleaning substrate with Plasma

- Used commercial Harrick Expanded Plasma Cleaner in cleaning room

Procedure:

1.Clean the chamber with IPA
2.Load sample
3.Pump down to purge air out of Chamber (usually reaches 10mTor)
4. Pump up with Ar to desired pressure
5. Turn on RF plasma for cleaning

Disadvantage:

1.Only have 3 levels of RF power setting
high=29.6W medium= 24.5W low=10.2W
2. No monitor of the reflected power, so no true value of the RF power is indicated.
3. Poorly vacuum condition.

Plasma cleaning with BPE

BPE scans: The intensity of BPE spectra dropped around 90%.

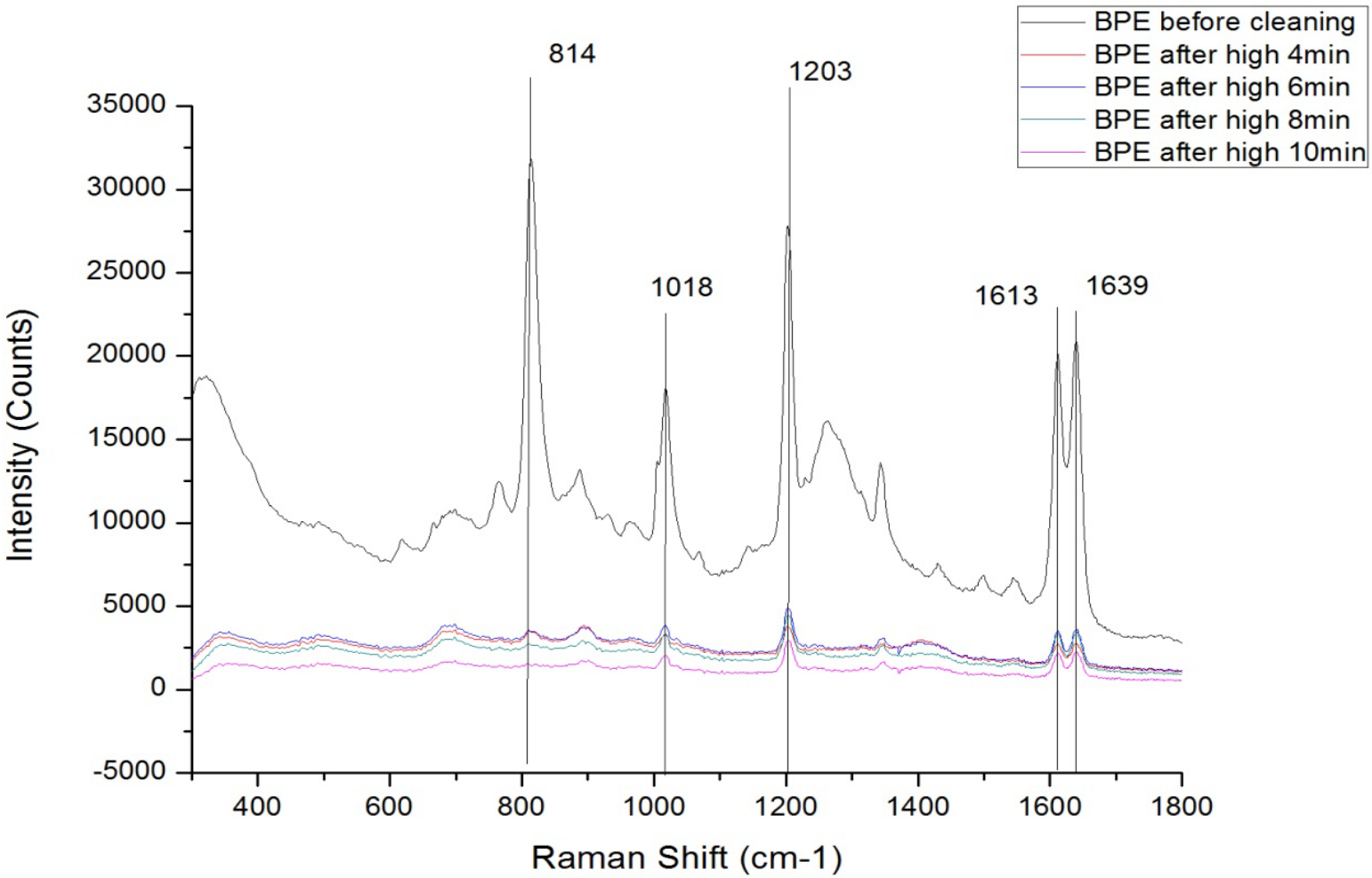

Plasma cleaning with BPE

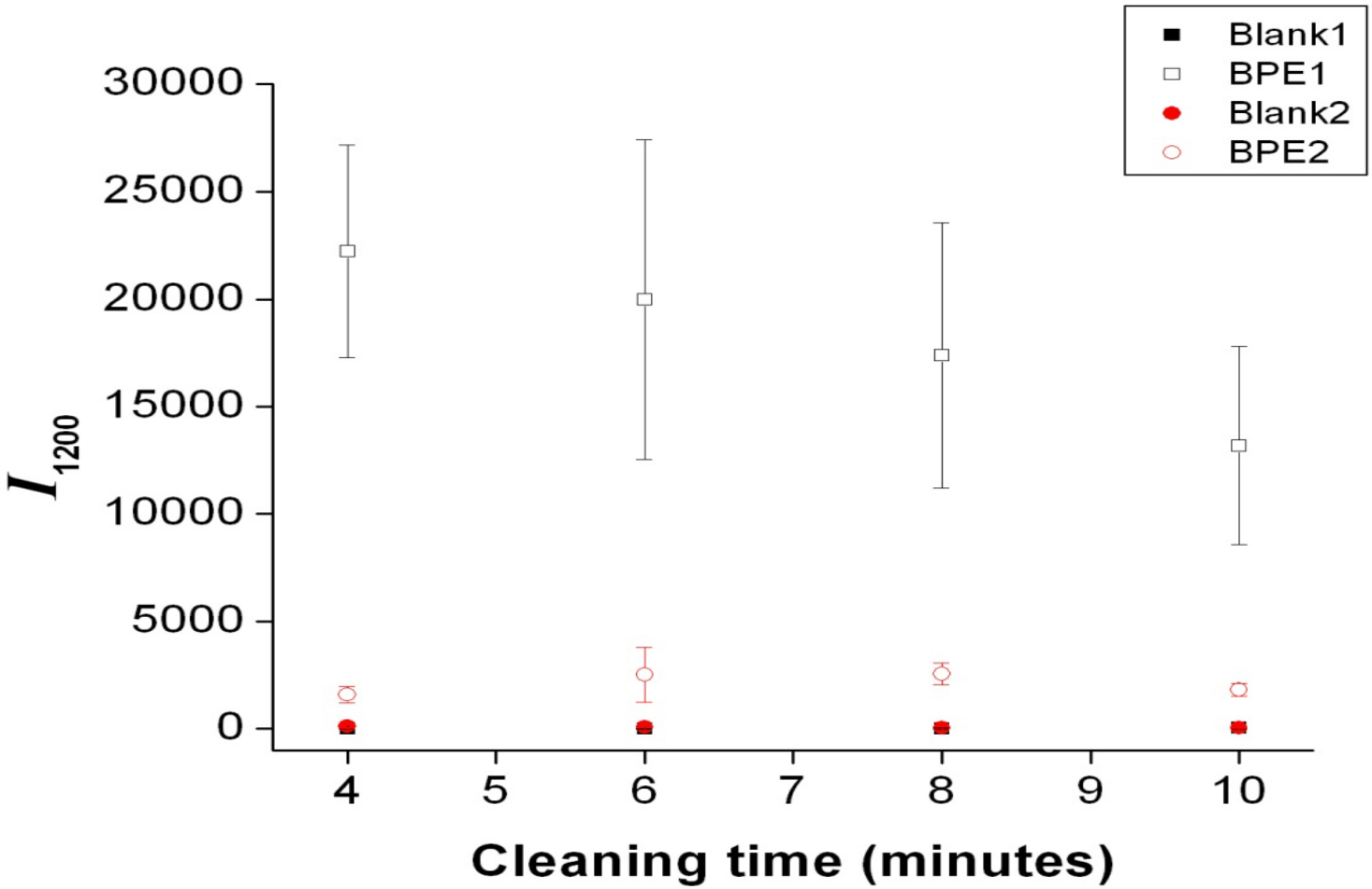

The cleaning time was too long and the AgNRs structure was compromised

Plasma cleaning with MPS

- 3-Mercapto-1-prpanesulfonic acid, sodium salt (MPS)

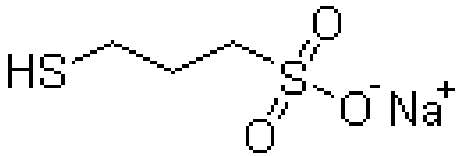

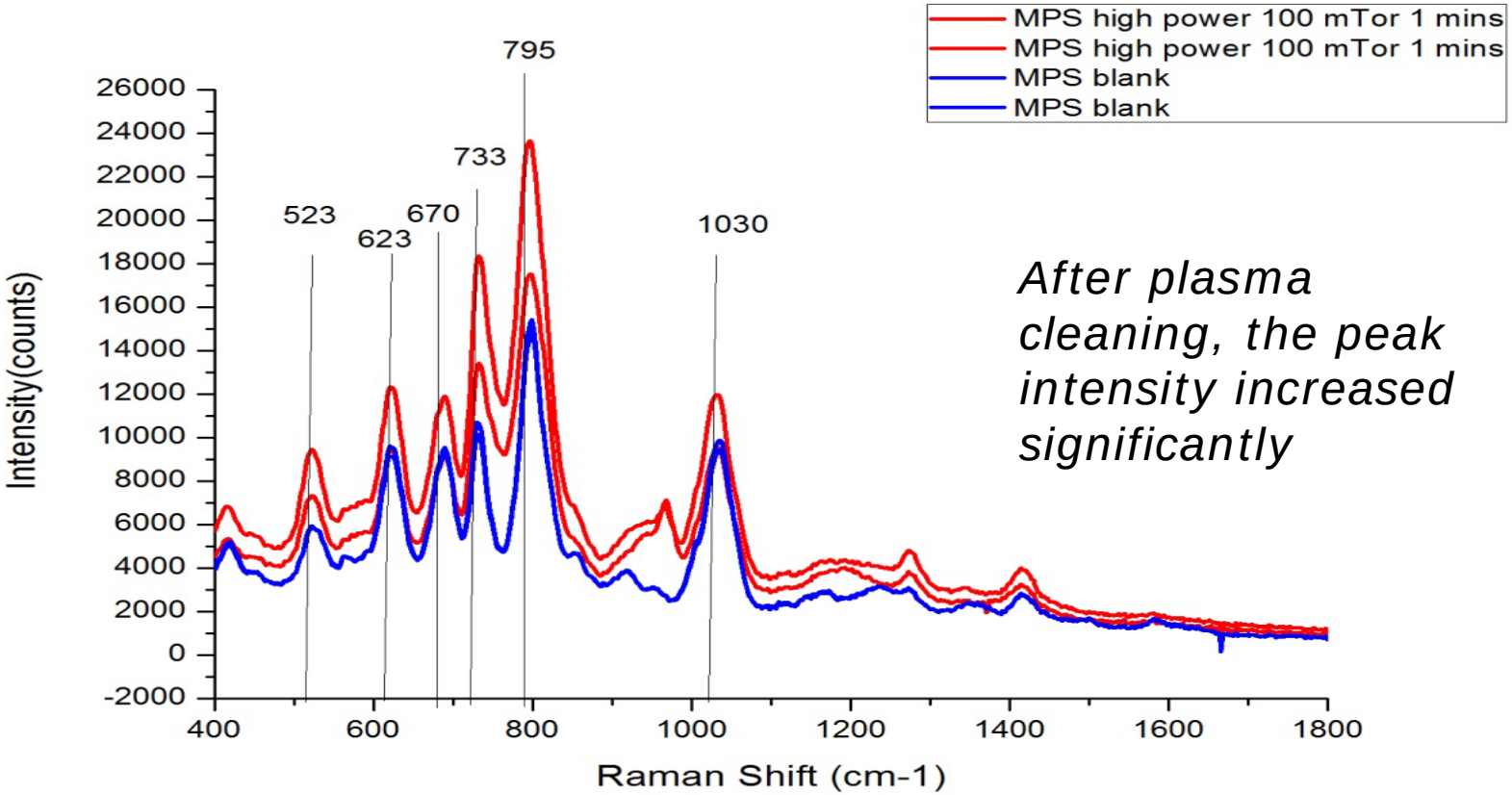

After plasma cleaning, the peak intensity increased significantly

Plasma cleaning with MPS

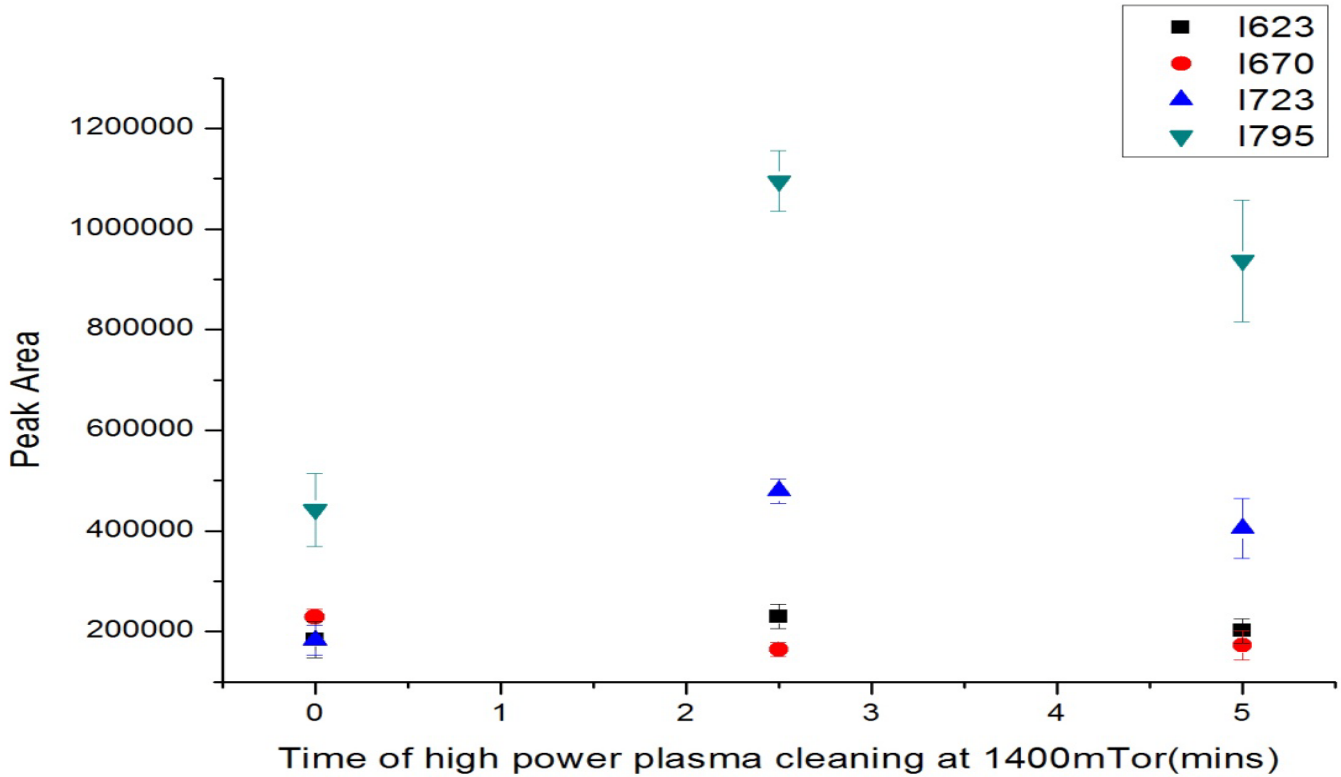

1. One of the explanations was molecular crunching. Molecular experssed more easily after multi layers were removed more plasma.
2. Or due to some chemical reaction under plasma condition.

Plasma cleaning with MP

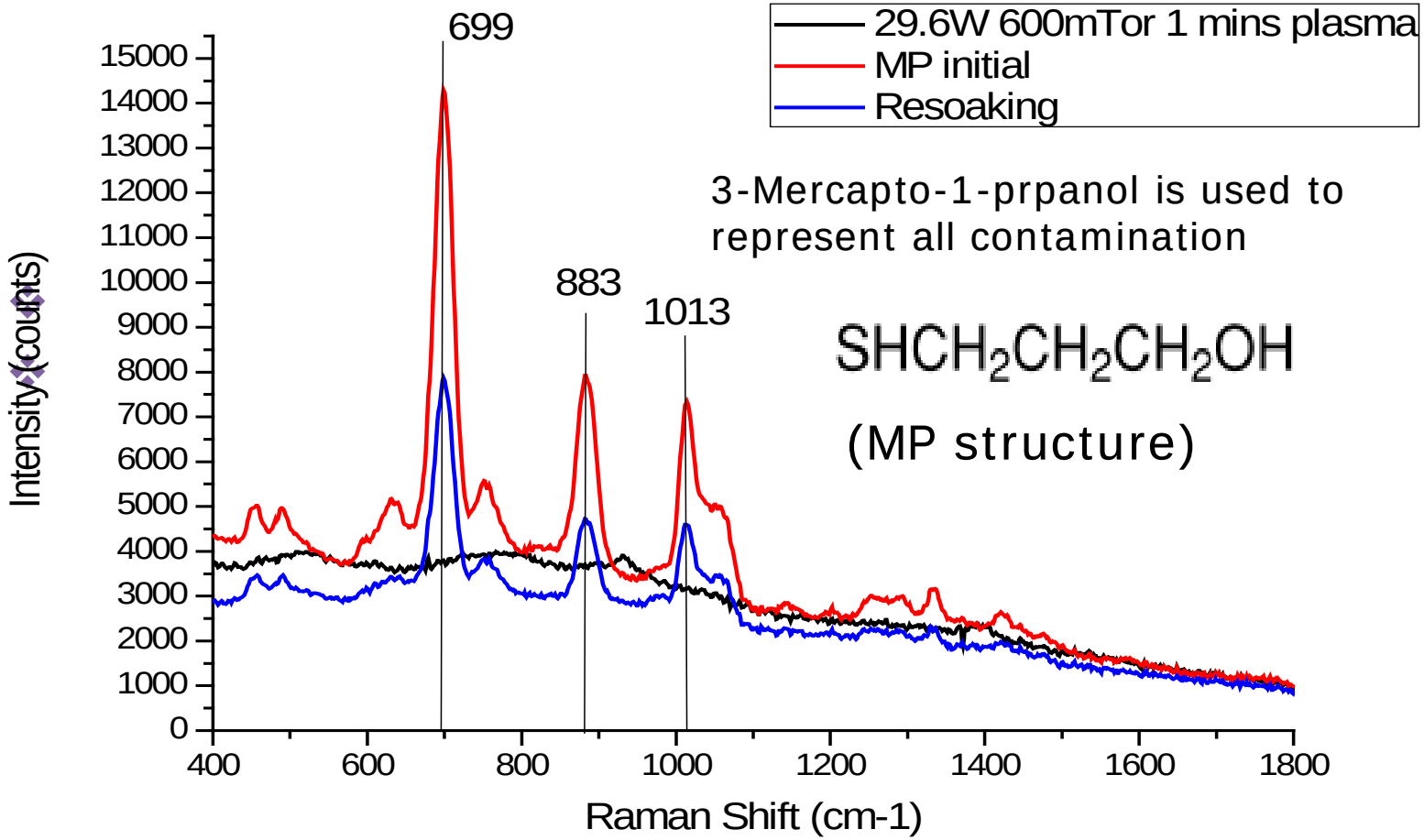

After plasma cleaning, a smooth “clean ” spectrum is obtained, indicated all MP is removed

Plasma cleaning with MP

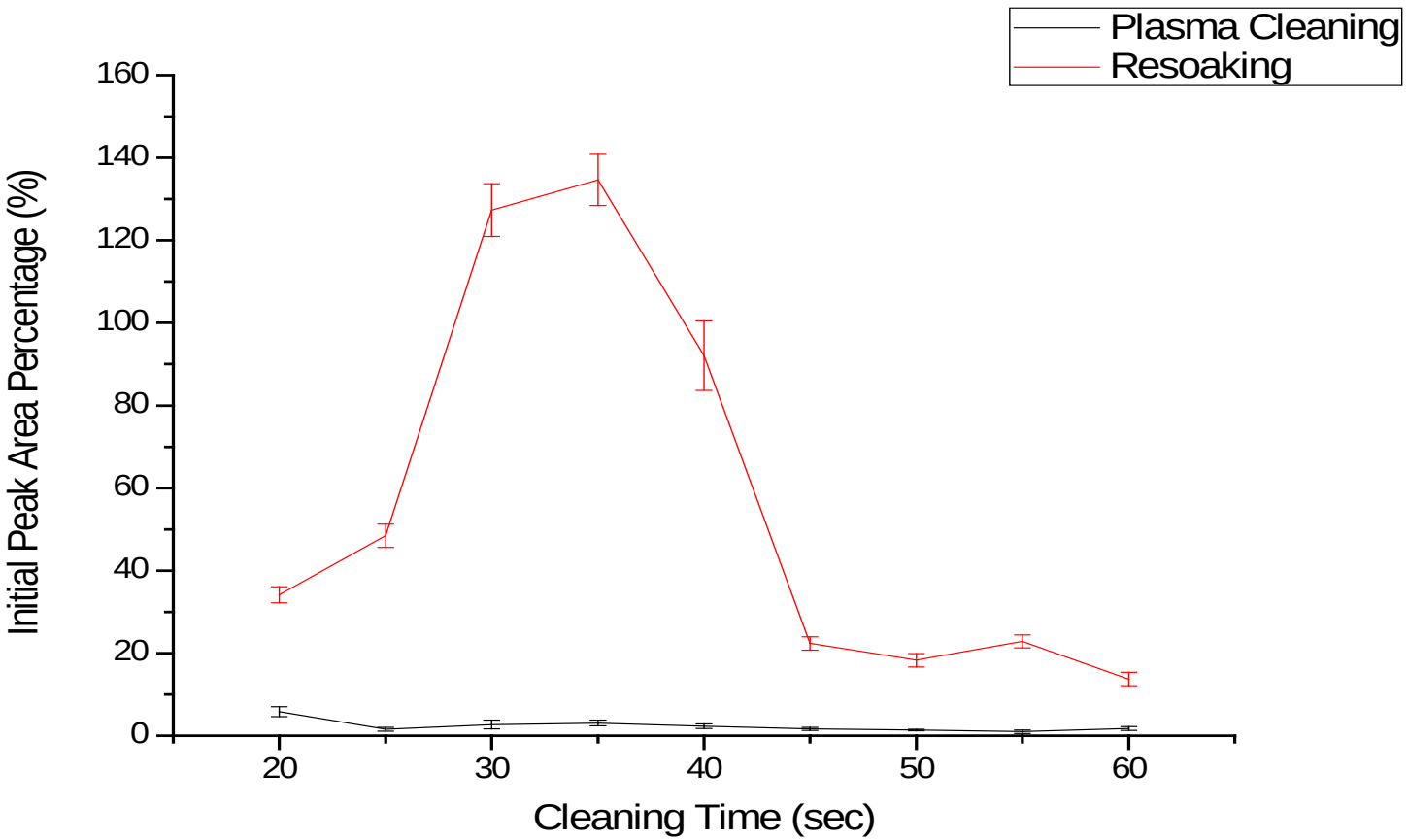

Percentage Peak area regenerated after re-soaking as a function of cleaning time. At time 30 sec and 40 sec, the MP peak intensity was even greater than those of the initial measurement.

Plasma cleaning with MP

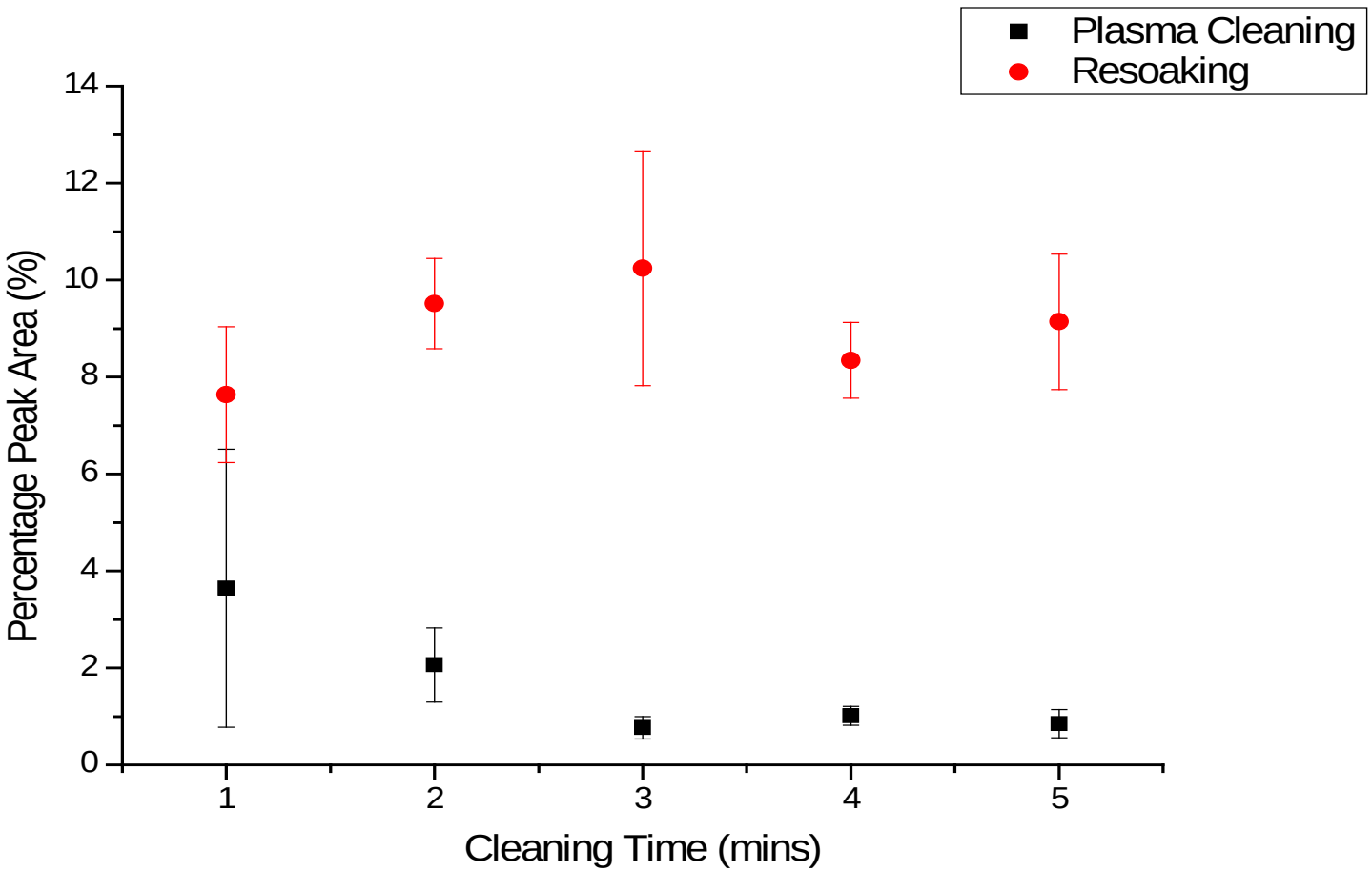

Percentage Peak area regenerated after re-soaking as a function of cleaning time. It showed that 1 min cleaning time is still too long to prevent any damage to the AgNRs Structure.

Customized Plasma Cleaner

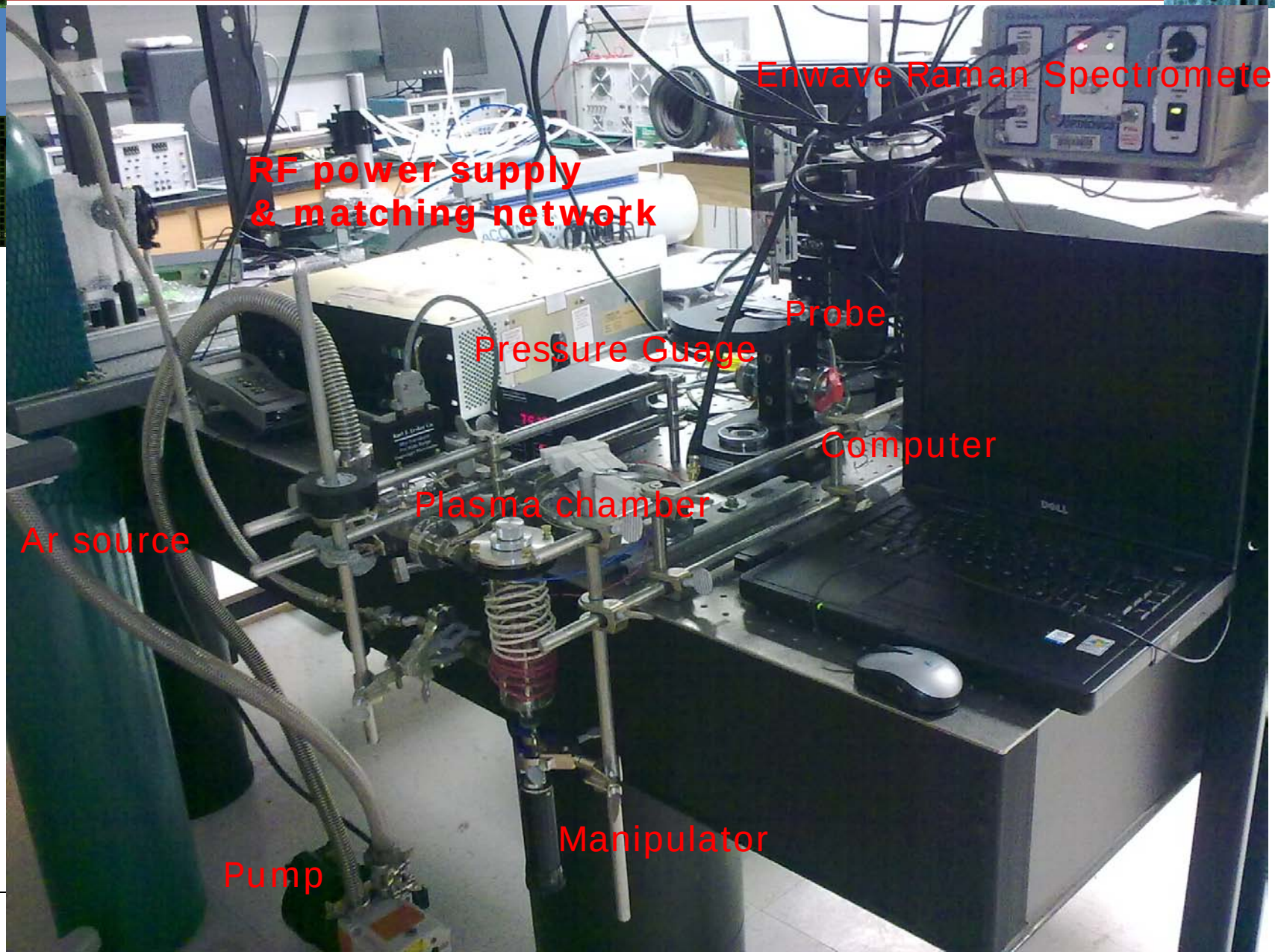

Customized Plasma Cleaner

Controlled environment: Ar flow prevent contamination form atmosphere. RF power adjusted: resolution as low as 1 Watt Matching network can lower the reflected power to 1 Watt. So true power used can be calculated. Can do *in situ* SERS measurement

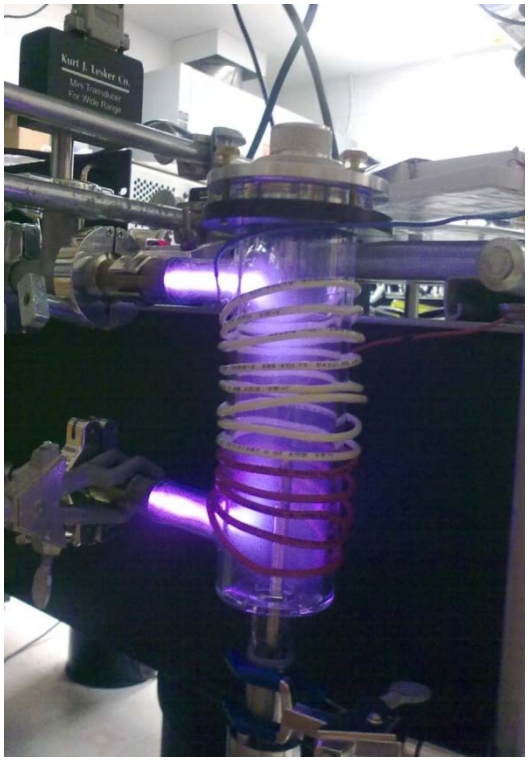

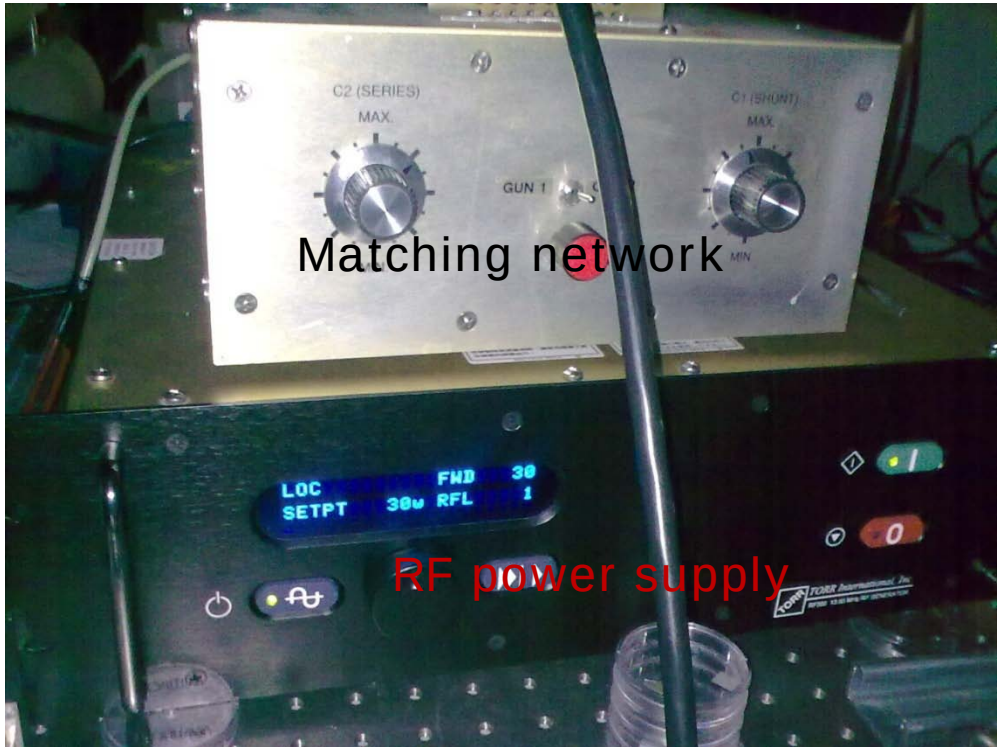

Plasma cleaner

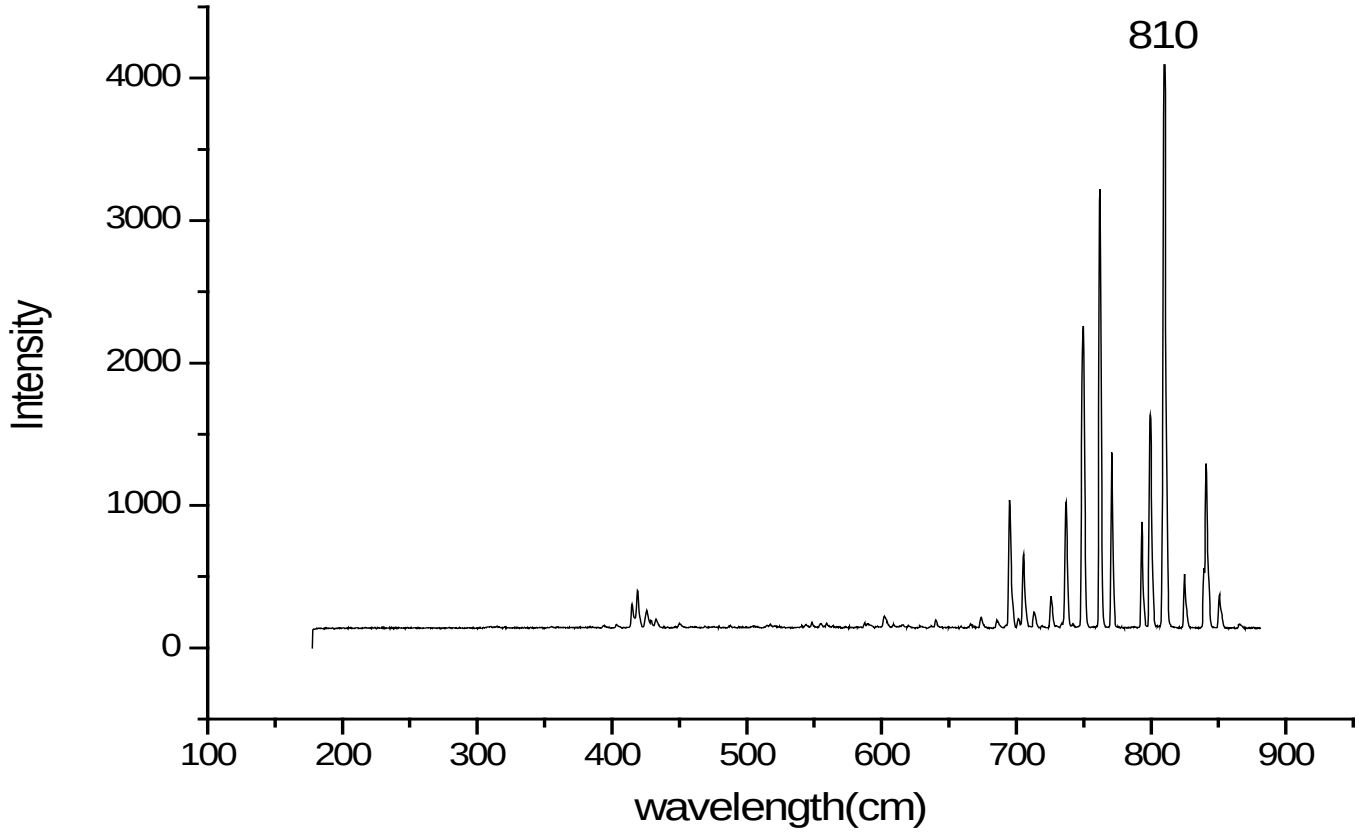

Ar+ plasma were characterized by spectrometer, and it was stable over a time period of 10 min

Plasma cleaning with MeOH

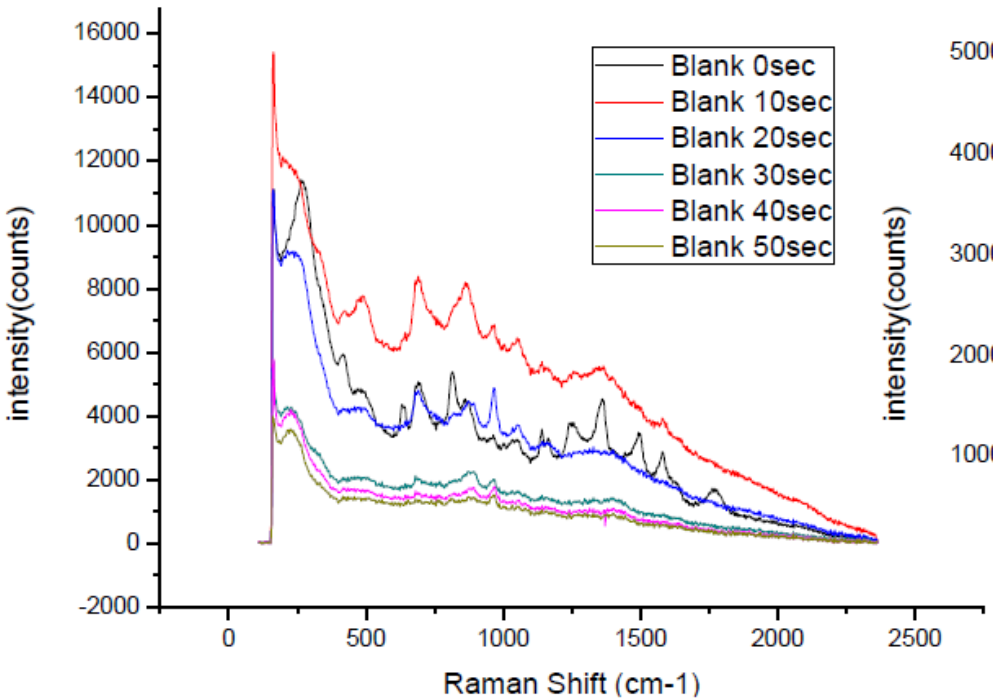

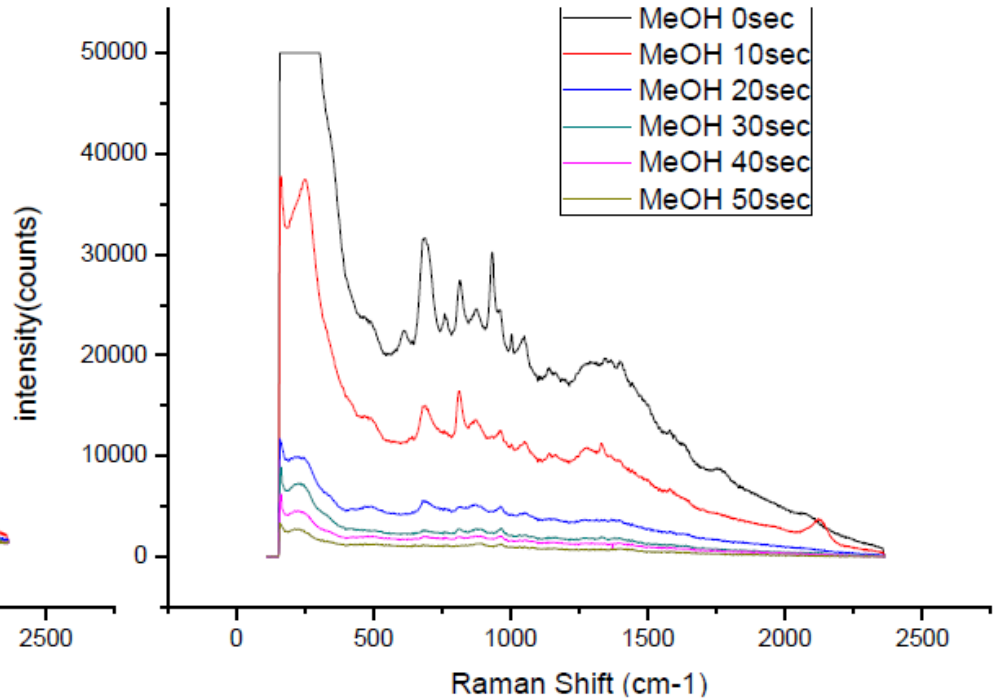

After 20 sec of plasma cleaning, adding MeOH didn't have a effect on the intensity, which indicated most of the contamination was removed, so dissolving won't make a difference.

Plasma cleaning with BPE

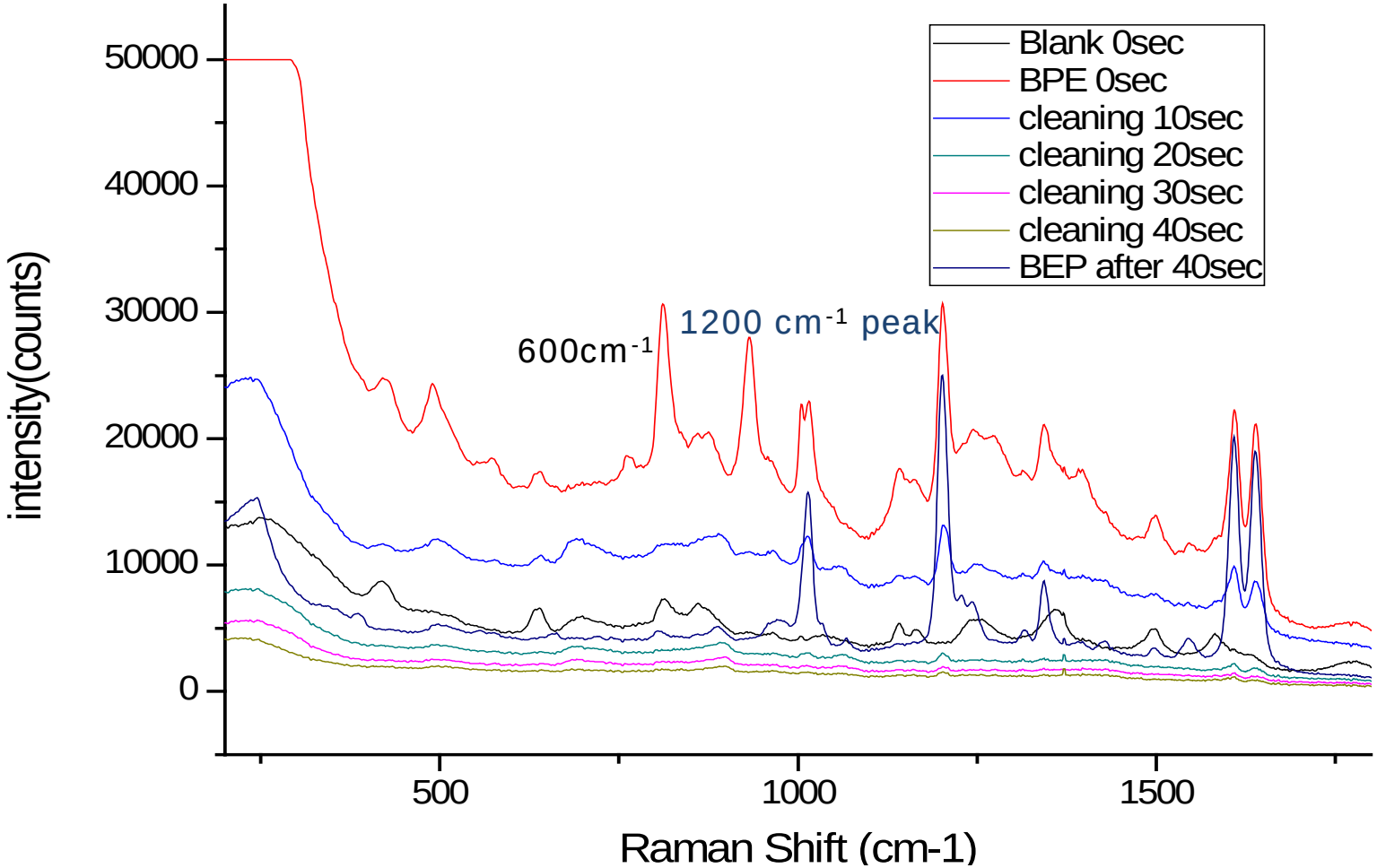

2 μl of 10^{-5} M BPE was applied to a substrate. Each time, 10 sec of Ar plasma cleaning (600mTor and 30W RF) treatment followed by SERS measurement was used for a total of 40 sec.

Data analysis

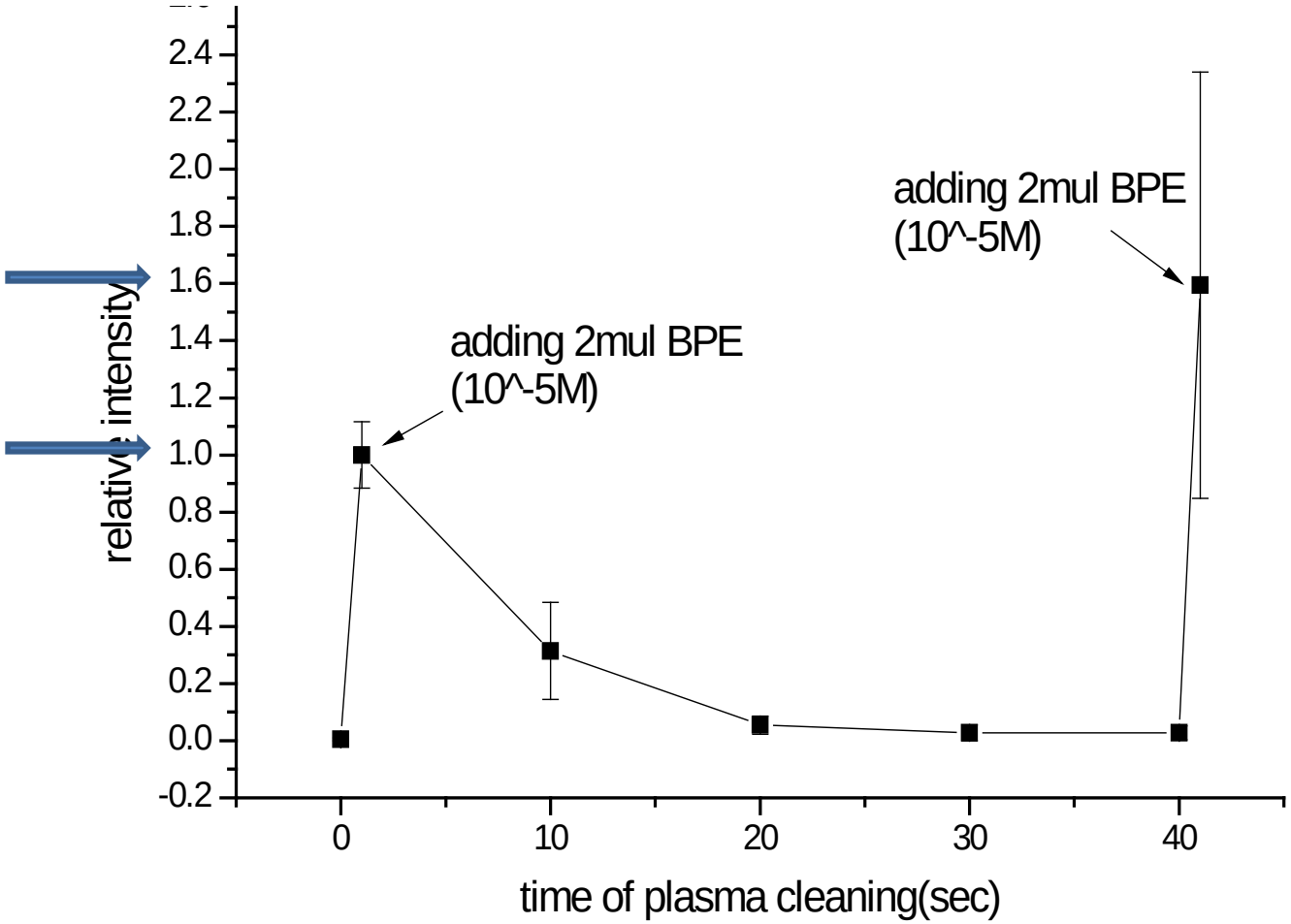

1200 cm^{-1} peak was used to show the effect of plasma cleaning as a function of time. The BPE 1200 cm^{-1} peak intensity before any plasma cleaning was considered as 1.0

Plasma cleaning with MP

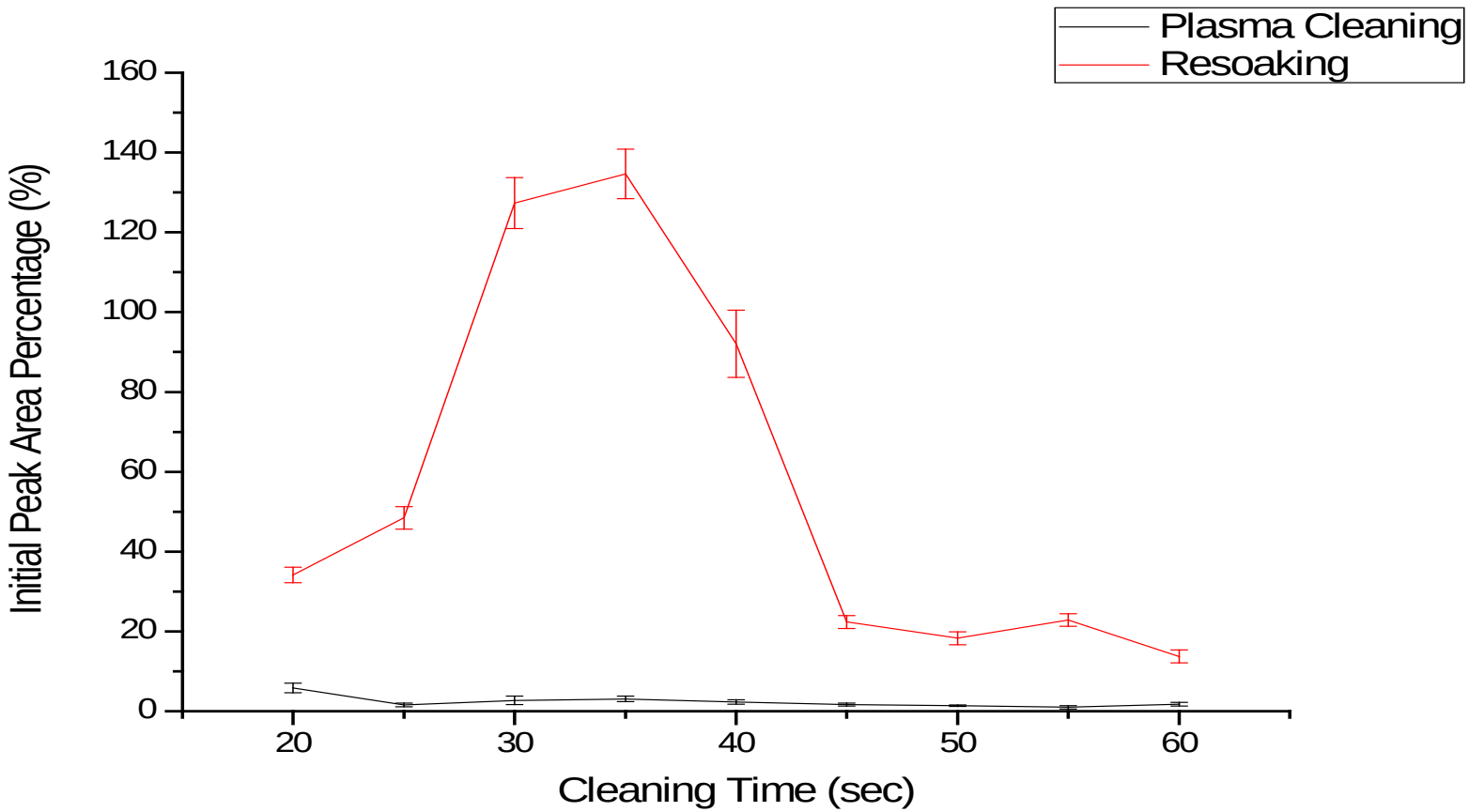

Percentage Peak area regenerated after re-soaking as a function of cleaning time. At time 30 sec and 40 sec, the MP peak intensity was even greater than those of the initial measurement.

Change of baseline

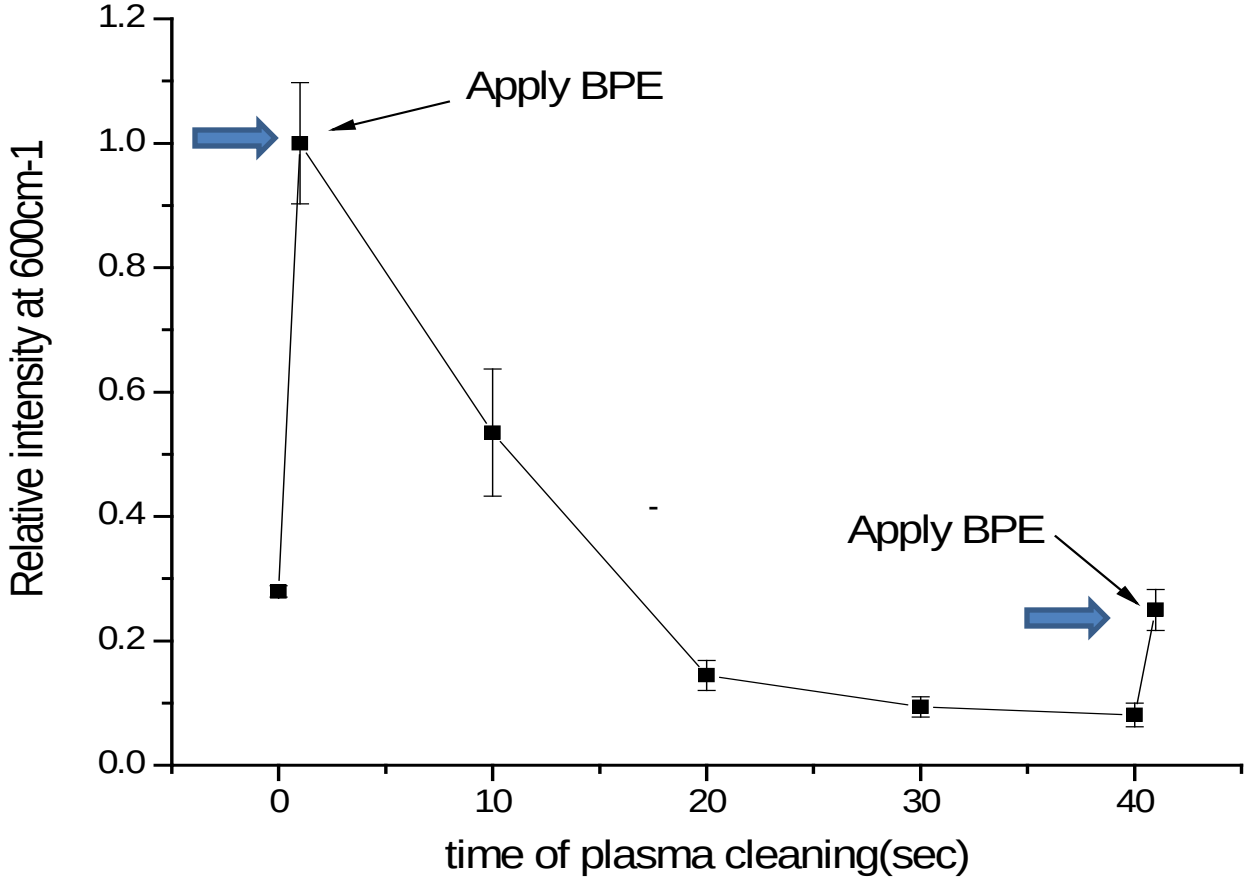

At 600cm^{-1} there was no peak at any time, so the change of intensity at 600cm^{-1} was served as the representative of the change of baseline as a function of time.

Conclusions

- Centrifugation technique

  achieved 10^6 on limit of detection more evenly distribution

- Filtration technique

  lowered the LOD to 10^5 CFU/ml

  could be used to separate bacteria from food matrix

- Plasma Cleaning

  controlled environment: eliminated interference from atmosphere remove contaminations

Future Perspectives

- 1. Confirmation of bacteria detection with plasma cleaned substrates and in a controlled environment
- 2. Detection of target bacteria with magnetic beads
- 3. Detection of bacteria in real food samples (ie. produce) using filtration method
- 4. Detection of a mixed bacteria culture

Q&A

Thank You for Your Attention

Nanowire Switch and Nanoelectrode/nanochannel Based Impedance Biosensor for Rapid Screening of Avian Influenza

Yanbin Li[1], Tony Huang[2], Huaguang Lu[3], Chuanmin Ruan[1]

[1]Department of Biological & Agricultural Engineering, Center of Excellence for Poultry Science, University of Arkansas

[2]Departments of Engineering Science and Mechanics, and [3]Animal Diagnostics Laboratory, Pennsylvania State University

USDA/NIFA Nanotechnology Grantees' Meeting
December 10-11, 2010, Washington, DC

Highly Pathogenic Avian Influenza (HPAI) H5N1

- **Reported HPAI H5N1 outbreaks**
  (WHO, 11-19-2009)
  - 62 countries had outbreaks in poultry;
  - 15 countries had human cases, 508 people infected, 302 died since 2003.
- **Cost (FAO, 2006):**
  - Over150 million poultry dead/culled/depopulated;
  - $10 billion economic losses
- **Predicted HPAI Pandemic occurs:**
  - 89,000 to 207,000 deaths and 20 to 47 million illnesses in US in few months (CDC, 1999);
  - 2 to 7.4 million people could die from a global flu pandemic (WHO, 2005).

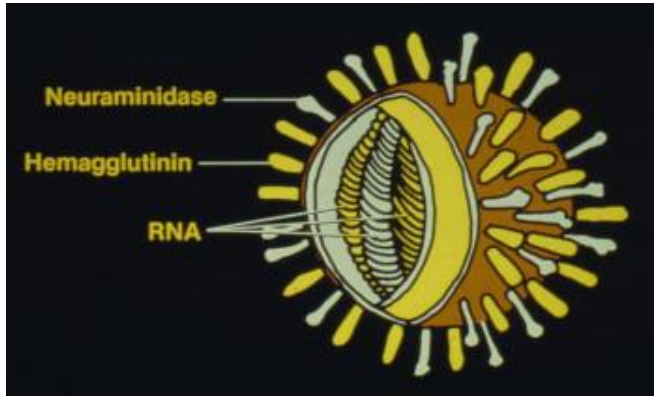

Hemagglutinin subtypes: 16 (H1–H16)
Neuraminidase subtypes: 9 (N1–N9)

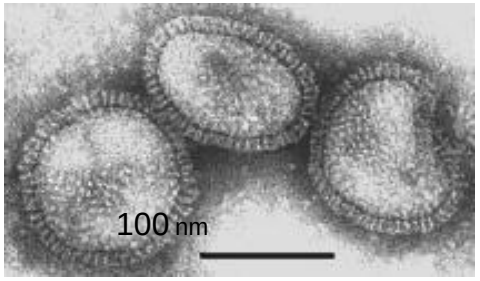

Current AI Detection Methods

- **Virus Isolation:**
  - **Advtg:** Specific and sensitive;
  - **Dis-advtg:** time-consuming (3-7 days)
- **Standard/Gel PCR, Real-time PCR:**
  - **Advtg:** A same day rapid test, specific and sensitive;
  - **Dis-advtg:** Requires expensive equipment, very complex sample preparation and well-trained laboratory technicians
- **Ag-ELISA:**
  - **Advtg:** Relatively rapid (4-8 h);
  - **Dis-advtg:** low sensitive and subject to false positives
- **Ag-capture Strips:**
  - **Advtg:** Rapid (1-3 h), simple and inexpensive
  - **Dis-advtg**: low sensitive, false positives

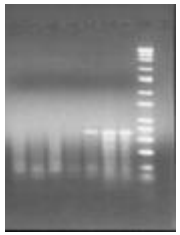

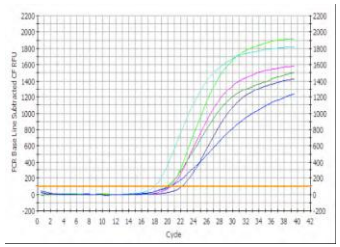

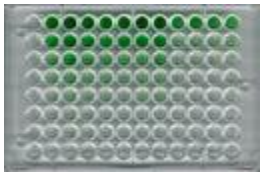

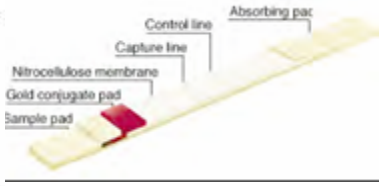

Justification for AI Diagnostic Research

"The technology for diagnosing human H5N1 infections is mature, but many tests are complex, some are liable to error, and some can be performed safely only in biosafety level 3 facilities. A simple, rapid, robust and reliable test, suitable for use in the field or at the patient's bedside, is urgently needed."

— WHO, 2006. Influenza Research at the Human and Animal Interface. Report of a WHO working Group. September 21-22, 2006, Geneva, Switzerland. (The first paragraph of the Executive Summary on page 2)

AI false (+) or (-) diagnostics is NOT acceptable, NOT affordable!

Urgent Needs for In-Field Tests

What are we faced with now?

- Monitor wild birds worldwide (e.g., a DOI project for tests in Alaska, $29 million, 50,000-75,000 samples)
- Routinely check each poultry flock (US Poultry industry is testing >10 samples/flock before processing)
- Have frequent tests on open poultry farms in remote areas (Indonesia, Vietnam, Thailand, China, etc.)
- Test live bird market and auction birds (in US)

What do we need now?

- In-field rapid screening tests: <1 h
- Reliable method: specific, sensitive
- Simple instrument: portable and automated
- No need for specifically trained operators
- Low cost per test
- Quickly adaptable to mutated subtypes

Objectives

- **Major Goal** is to develop a nanomaterials- and nanostructures-based **nano-biosensor** for rapid detection of avian influenza virus (AIV).
- **The specific objectives are to:**

1. Coat **magnetic nanobeads with anti-H5 monoclonal antibodies** for highly efficient capture, separation and concentration of target virus in poultry swab samples;
2. Design and fabricate interdigitated **nanoelectrode and nanochannel**, and integrate them into **a nano-microfluidic-chip** for ultra-sensitive impedance measurement ; immobilize anti-H5 monoclonal antibodies in the nanochannel for more specific binding target virus;
3. Synthesize, functionalize, surface-modify and characterize gold nanowires; conjugate the gold nanowire with anti-N1 monoclonal antibodies for “switch” function in the nano-biosensor;
4. Evaluate the nano-biosensor for screening of H5N1 and other H5 subtypes of AI virus in comparison with gold standard methods.

Advantages of Nanomaterials and Nanostructures

- **Magnetic nanobeads:**
  - Higher surface area to volume ratio
  - Stronger penetration ability
  - Less interference in detection
- **Interdigitated nanoelectrode/nanochannel:**
  - Lower energy requirement
  - Smaller volume of testing sample
  - Less binding time
- **Nanowire switch:**
  - Least false positive/negative signals
  - Easier fabrication for required diameter and length

Design of Nano-Biosensor for AI Detection

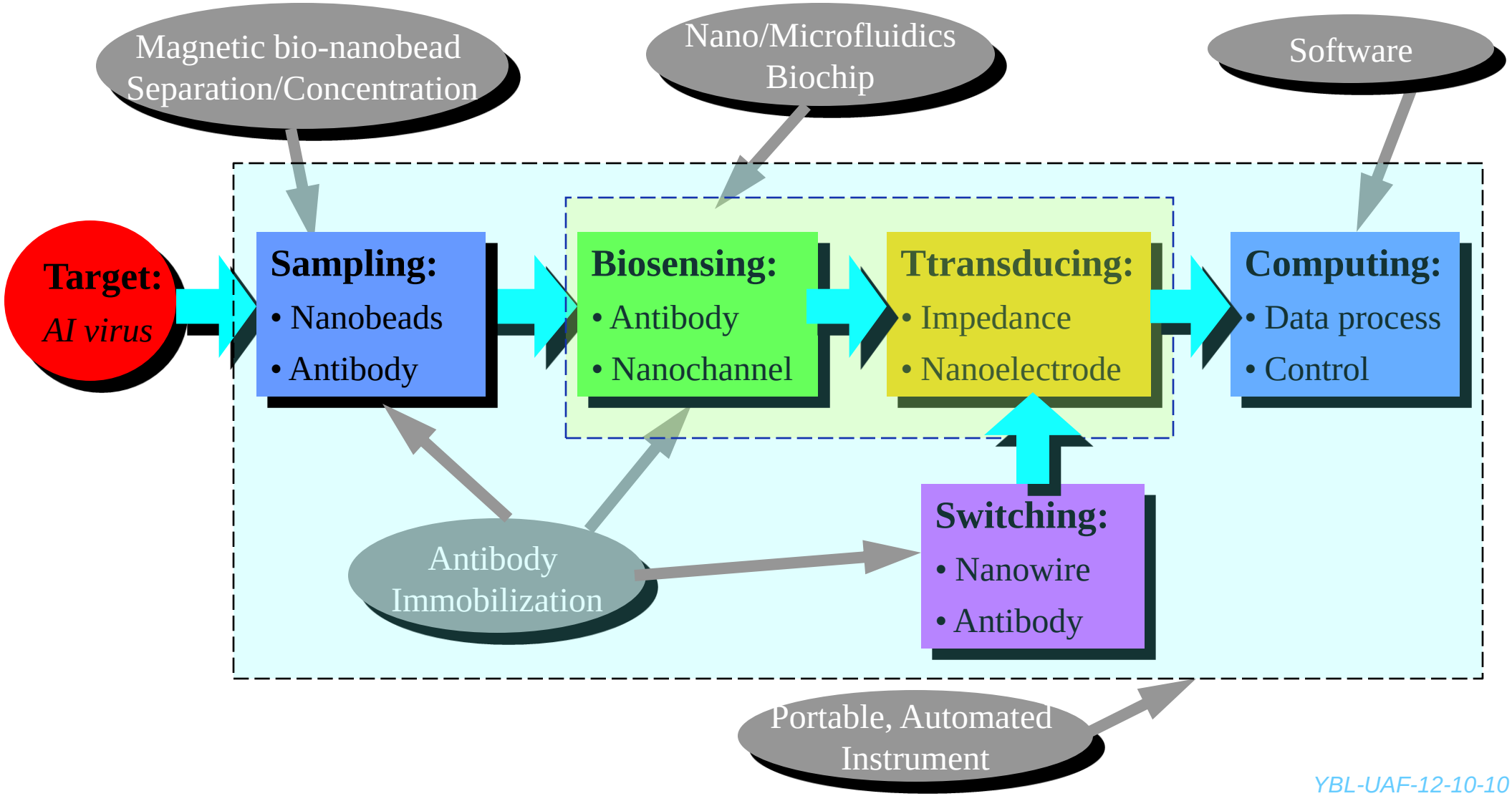

Separation of AI H5N1 Using Magnetic Nanobeads

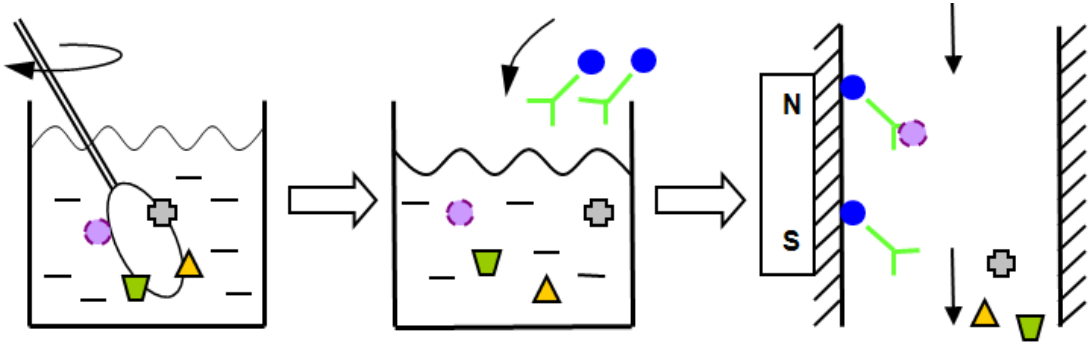

Magnetic bio-nanobeads separation

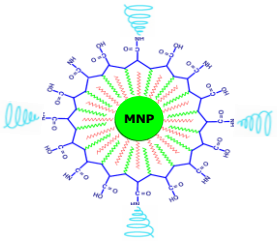

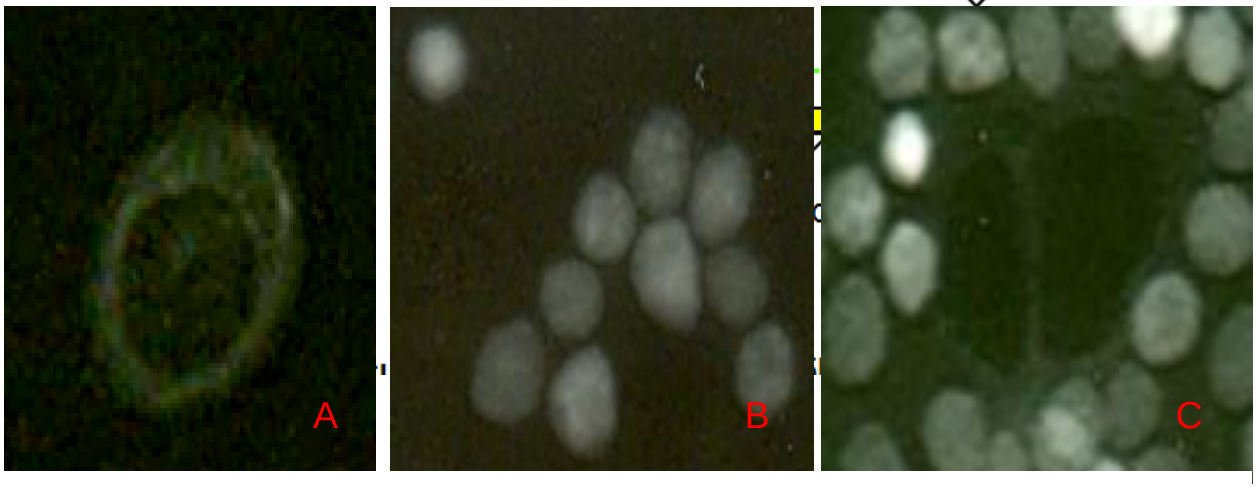

TEM (100,000×) of (A) avian influenza virus H5N1, (B) 30 nm magnetic nanobeads and (C) 30 nm nanobeads captured H5N1 viruses.

Measurement of Impedance Using Nanoelectrodes

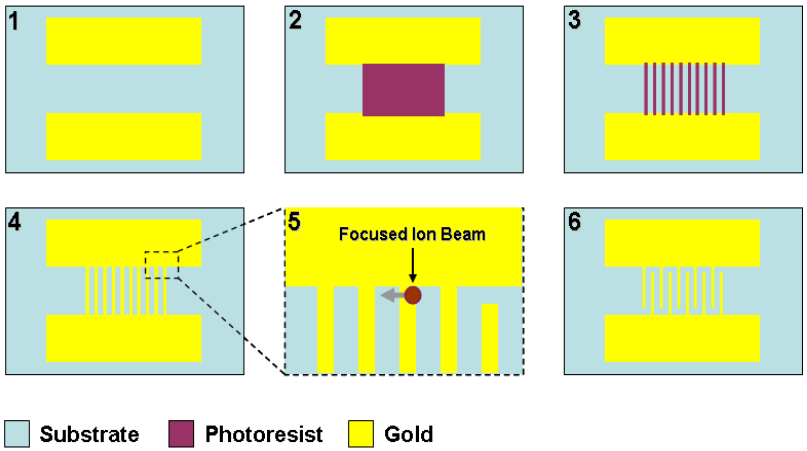

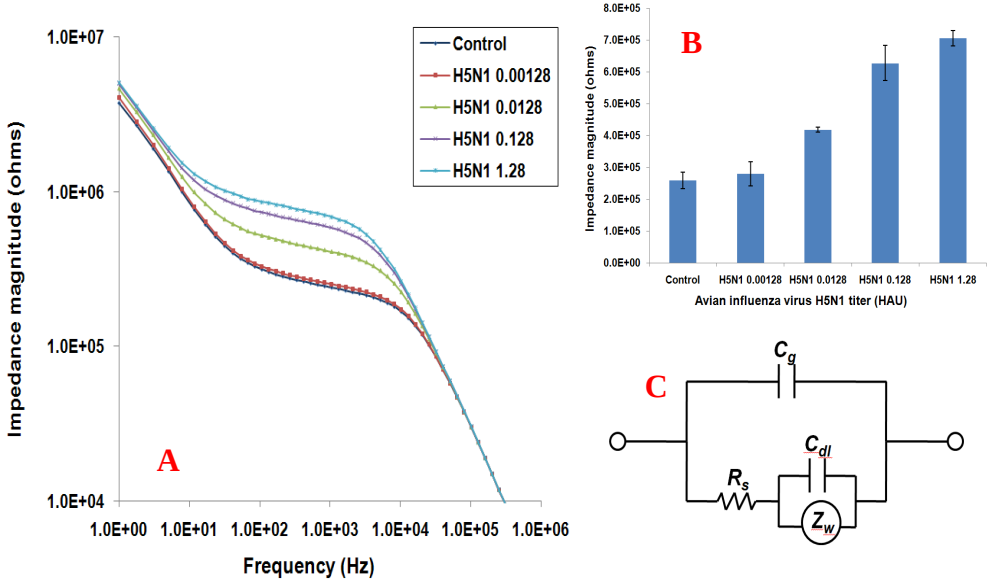

Fig. 5. (A) The typical impedance spectra of the impedance biosensor for detection of AIV H5N1; (B) All test results; (C) Equivalent circuit.

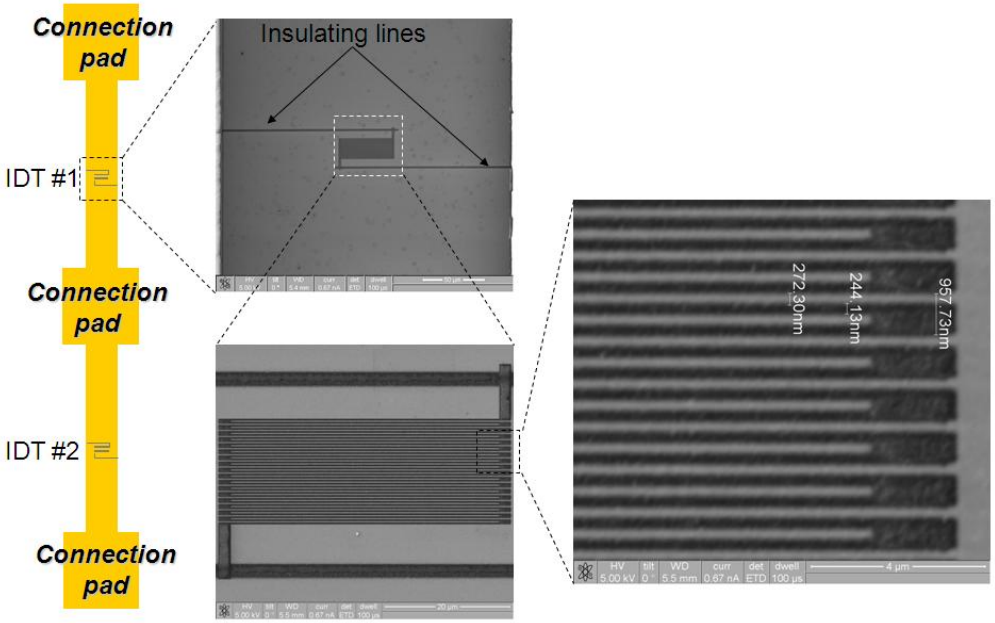

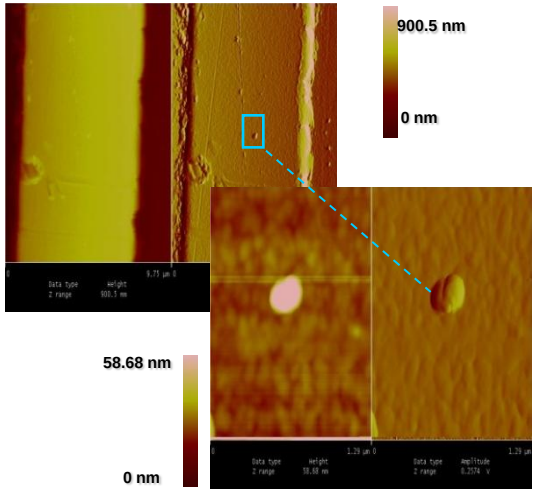

AFM images of captured AIV H5N1 virus on the surface of Au microelectrode,

Detection of AI Virus Using Nanowire Switch

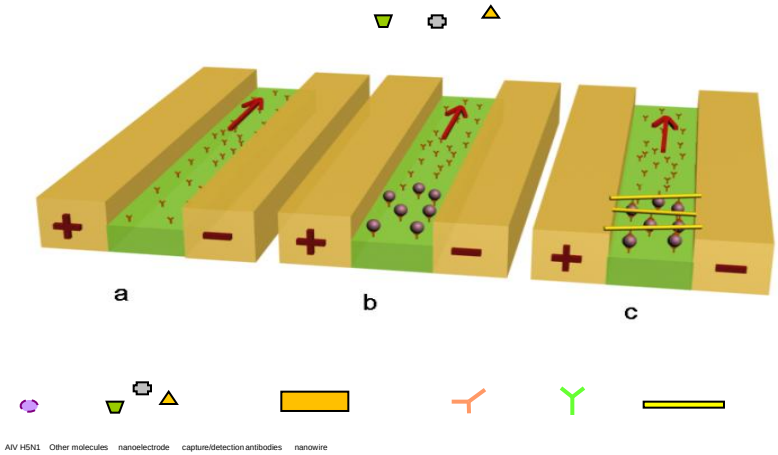

Assay steps for nanofluidic biosensor with conducting gold nanowires as bridges. (a) antibody modified nanochannel/ nanoelectrode; (b) AIV bound in the nanochannel; (c) gold nanowire conjugated with antibody bound with AIV.

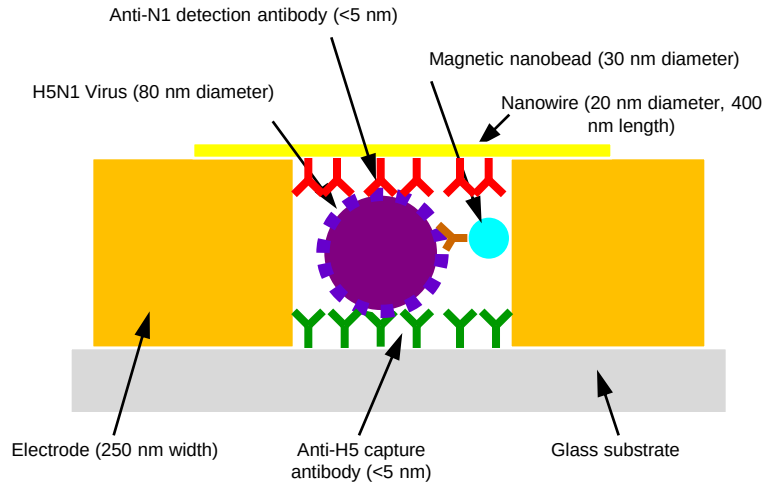

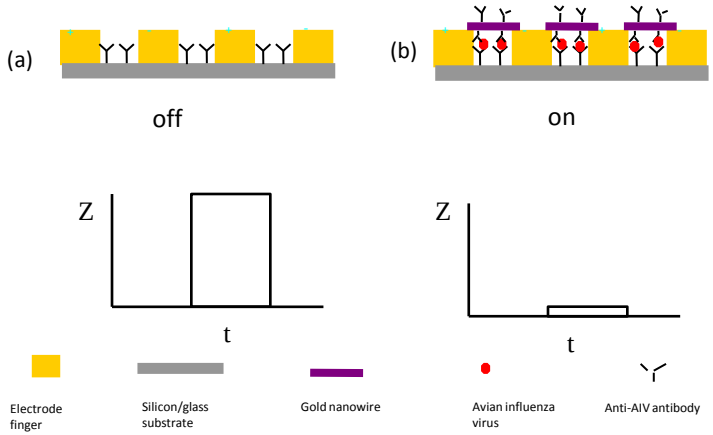

Mechanism of the conductive colloidal gold nanowire-based impedance biosensor for screening of AIV. (a) without target virus; (b) with target virus.

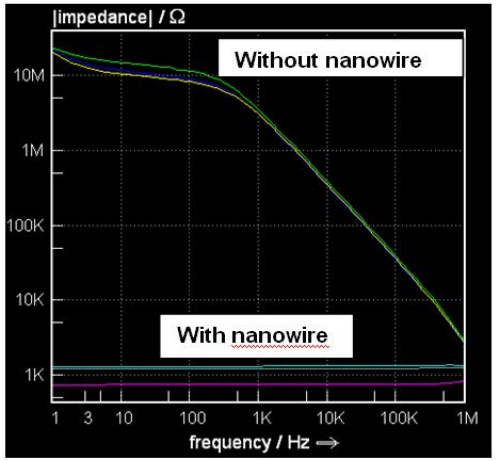

Fig. 5. Impedance spectrum of gold nanowire switch "on"/"off" on the interdigitated nanoelectrode-based impedance biosensor.

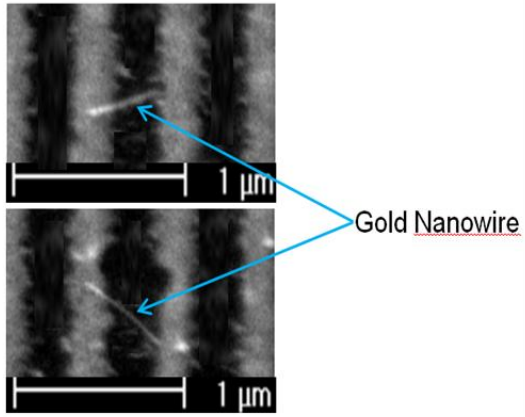

Fig. 6. SEM images of the gold nanowire crossed between two fingers on the interdigitated nanoelectrode.

Mechanism of of AI Virus Detection

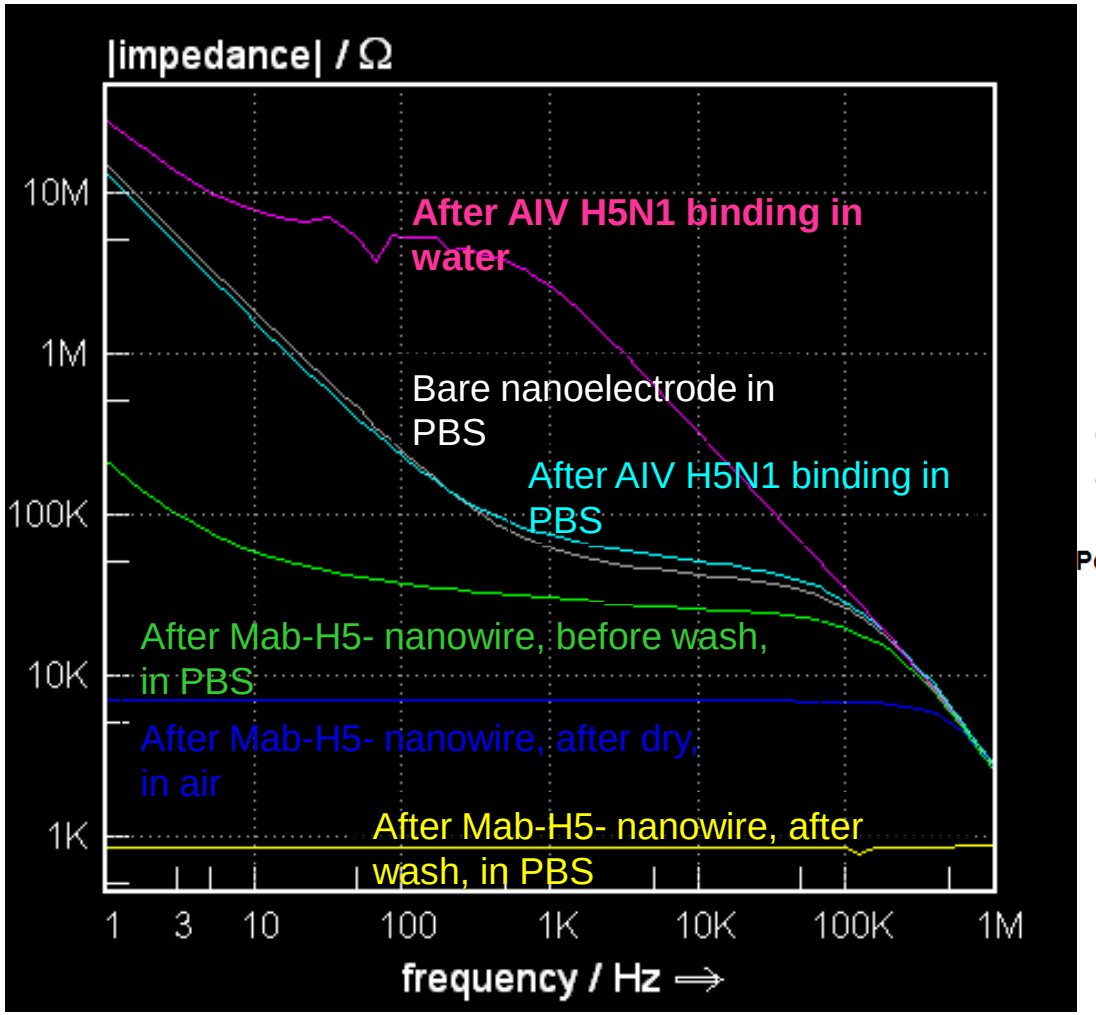

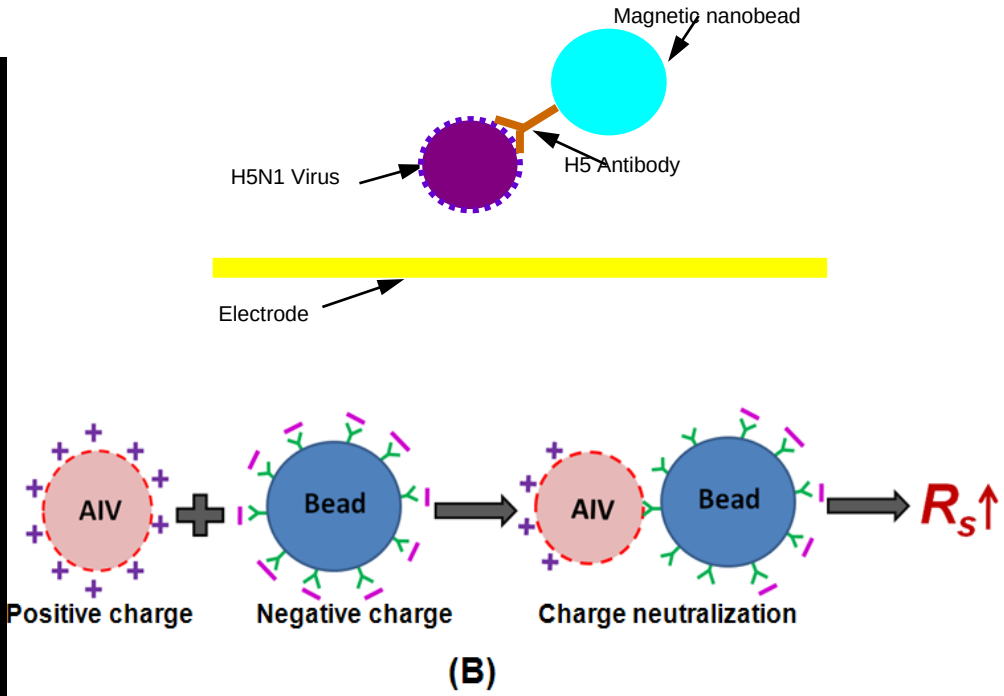

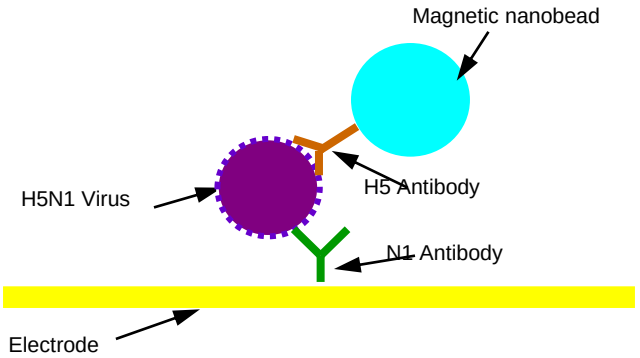

Design of AI Biosensor Instrument

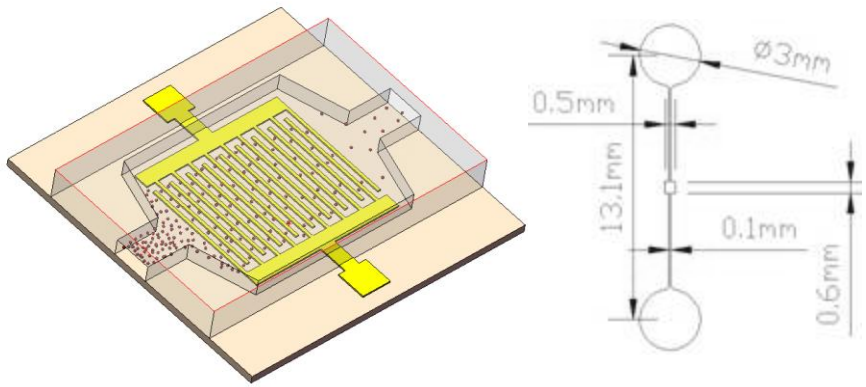

Design of the interdigitated nanoelectrode/nanochannel.

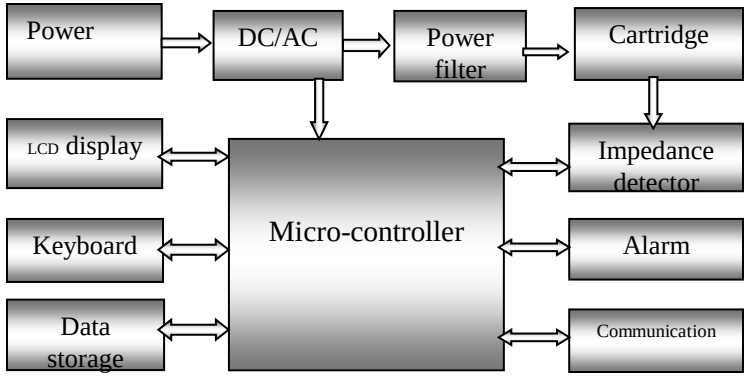

Design of the hardware.

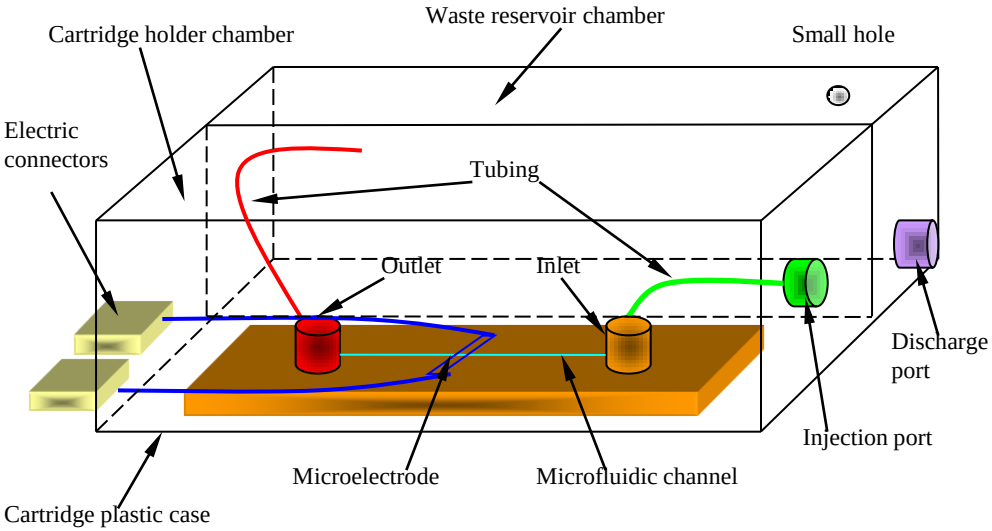

Design the testing chip.

Research Prototype of the biosensor

Results of Testing Inactivated H5N1 AIV at PSU Lab

Table 2. Results of testing inactivated H5N1 AIV mixed in chicken swab samples using both the biosensor and real time RT-PCR at PUS Lab

Sample	Concentration of AI virus used in swabs	Biosensor		Real time RT-PCR
		Reading (kΩ)	Positive/negative	
Inactivated H5N1 dilutions mixed with swab samples	10^{-2}	5.12	+	+
	10^{-3}	3.81	+	+
	10^{-4}	3.66	+	+
	10^{-5}	1.35	+	+
	10^{-6}	0.14	-	-
	0	0.08	-	-

**Biosensor reading is calculated as the difference between the control and the sample. Biosensor result is determined based on S/N >3, i.e., it is positive if the reading is more than 0.8 kΩ.*

Results of Testing Live H5N2 AIV at PSU Lab

Table 3. Results of testing live H5N2 AIV from chicken swab samples using both the biosensor and real time RT-PCR at PSU Lab

Sample	Swab sample	Biosensor		Real time RT-PCR
		Reading (kΩ)	Positive/negative	
Live H5N2 in chickens Day 1	Swab 1	0.55	-	-
	Swab 2	1.70	+	+
	Swab 3	0.85	+	-
Live H5N2 in chickens Day 2	Swab 1	2.70	+	-
	Swab 2	2.40	+	+
	Swab 3	2.60	+	-
Live H5N2 in chickens Day 3	Swab 1	2.20	+	+
	Swab 2	-6	-	-
	Swab 3	7.35	+	-

**Biosensor reading is calculated as the difference between the control and the sample. Biosensor result is determined based on S/N >3, i.e., it is positive if the reading is more than 0.8 kΩ.*

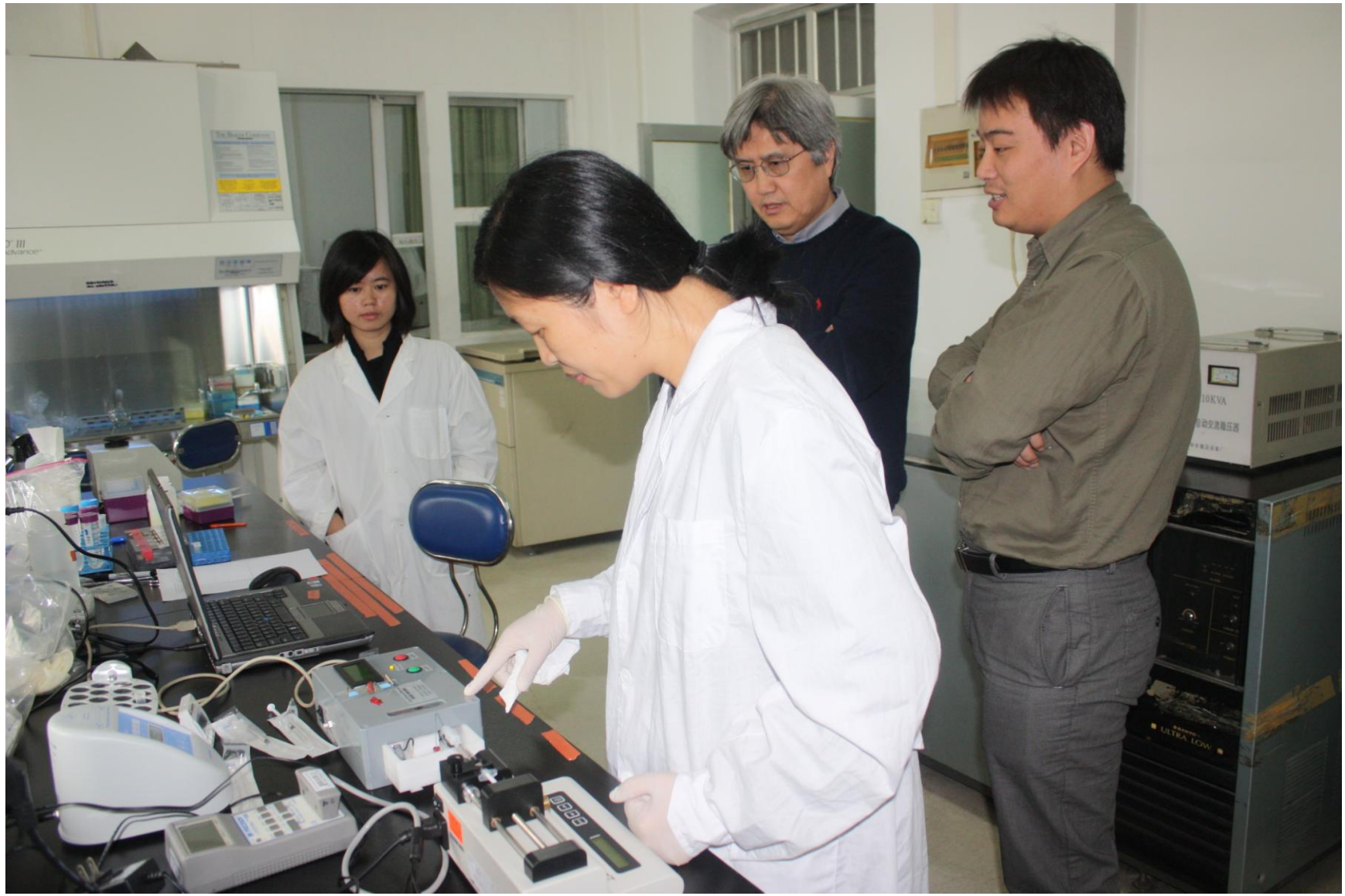

Evaluation studies of nano-biosensor for testing H5N1 AIV at Nanning Veterinary Research Institute, Nov 2010

Summary

What we have done:

- Design and fabrication of the biosensor prototype with nanowires at UofA CEPS and development of nanoelectrode and antibodies at Penn State.
- Proof-of-concept for the biosensor in labs of UofA CEPS.
- Confirmation of the biosensor with chicken swab samples in Animal Diagnostic Lab at PSU.

What the biosensor can do:

- Result can be obtained in less than 1 hr, compared to >3 hr ELISA, >6 hr RT-PCR, and >3 days virus isolation methods.
- As low as 100 EID_{50}/ml of target virus can be detected, the similar sensitivity as RT-PCR.
- Specific to H5 or H5N1 subtypes, the similar specificity as RT-PCR.

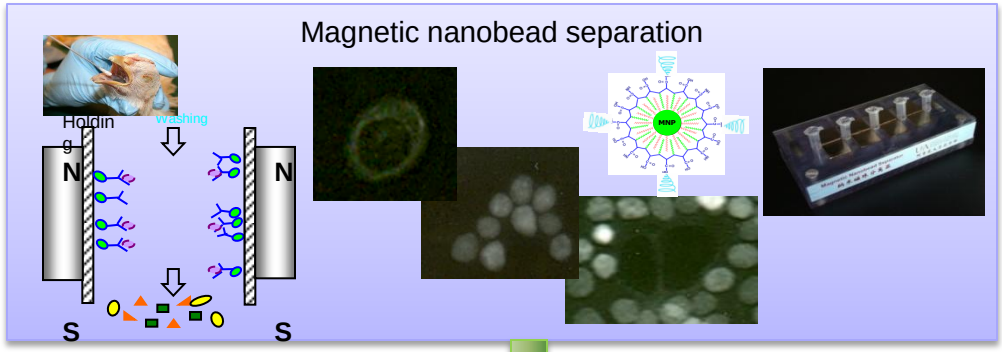

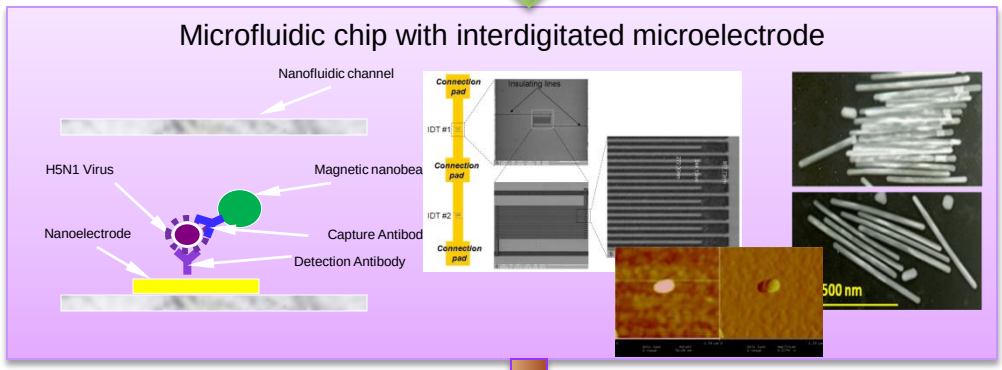

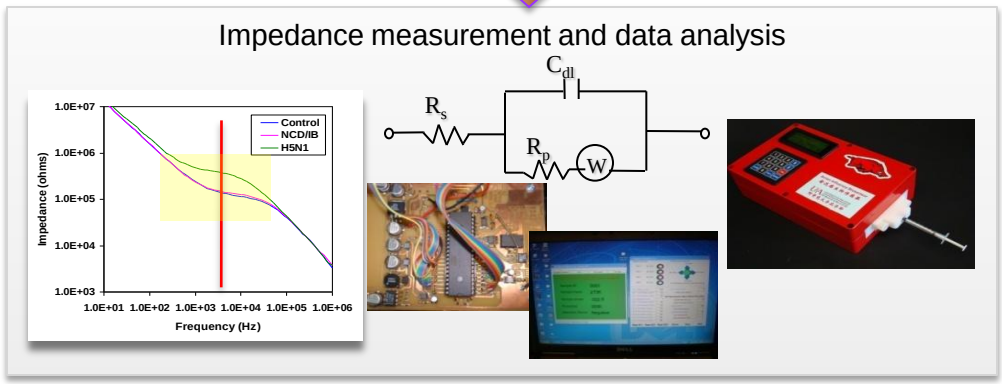

On-Going Research Studies

- Develop AIV subtype-specific Mabs against N1 and N2 subtypes, H1 and H9 subtypes for use with the nanowire switch (PSU).
- Optimize the design of nanoelectrodes/nanochannel and fabricate improved the nanochip (PSU).
- Model the electrical properties of AIV with nanowries and magnetic nanobeads in the nanochannel to better understand the mechanisms of the impedance biosensing (UofA).
- Improve immobilization of antibodies on magnetic nanobeads, nanowires and nanochannels to make them suitable for in-field use (UofA).
- Design and fabricate an integrated instrument to simplify operation (UofA).
- Evaluate the nano-biosensor with AIV positive swab samples from experimentally infected chickens (UofA and PSU).

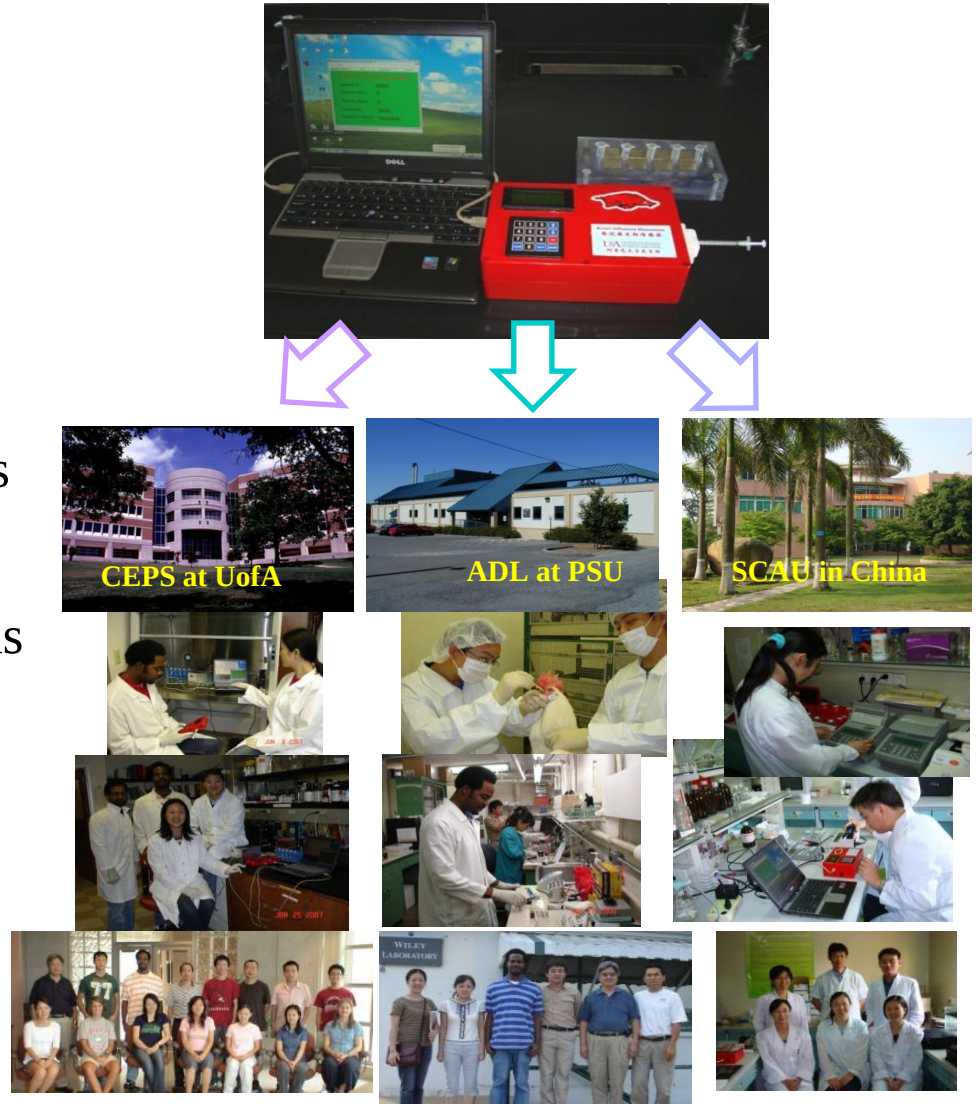

Publications

- Wang, R., J. Lin, Lassiter, K., J. Lum, B. Srinivasanm L. Lin, H. Lu, B. Hargis, W. Bottje, S. Tung, L. Berghman and Y. Li. 2010. Detection of avian influenza H5N2 from infected chickens using a portable impedance biosensor. Journal of Virology Methods (in review).
- Wang, R., Y. Li, X. Mao, T. Huang, and H. Lu. 2010. Magnetic bio-nanobeads and nanoelectrode based impedance biosensor for detection of avian influenza virus. Presented at IEEE-NanoMed 2010, December 5-9, 2010, Hong Kong, China. Paper No. 13.
- Lin, J., J. Lum, R. Wang, S. Tung, B. Hargis, Y. Li, H. Lu and L. Berghman. 2010. A portable Impedance Biosensor Instrument for Rapid Detection of Avian Influenza Virus. Presented at IEEE Sensors 2010 Conference, November 1-4, 2010, Waikoloa, Hawaii. Paper No. 1636.

Acknowledgments

- **Funding:**

  USDA/NIFA Nanotechnology

- **Research Personnel:**
  - **U of A:** Ronghui Wang, Jianhan Lin, Kentu Lassiter, Jacob Lum
  - **Penn State:** Xiaole Mao, Lin Lin
  - **CAU, SCAU & GIVR:** Maohua Wang, Ming Liao, Xiwen Luo, Peirong Jiao, Wenbo Liu, Yanfu Xie

- **Industry**:

  Ocean NanoTech, LLC

THANK YOU

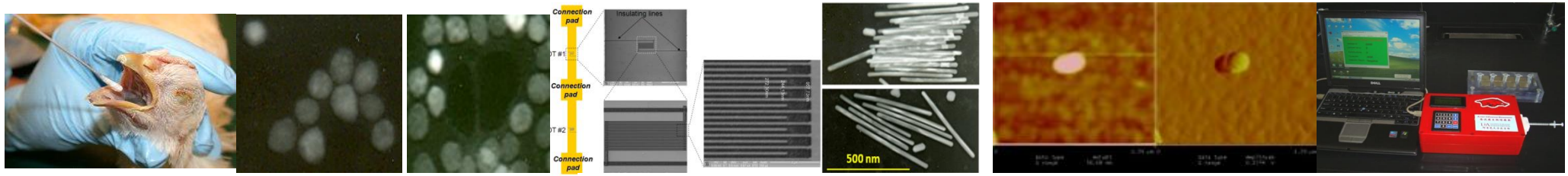
Connection pad
Insulating lines
Connection pad
Connection pad
500 nm

USDA-NRI Progress Report (12/10/2010)

Nanostructure and Nanoscale Interactions of Protein/Polysaccharide Coacervates

Project Director: Qingrong Huang

Rutgers University

Functional Foods

- Global functional food market will reach $90.5 billion in 2013;
- "foods and food components that provide a health Benefit beyond basic nutrition" – IFT expert report
- Usually accompanied by health claims for marketing purposes.

HIGH ORAC VALUE

(ORAC: *oxygen radical absorbance capacity*)

Absorption of Nutraceuticals in Gastrointestinal Track: (1) Micro/nanoencapsulation of nutraceuticals and micronutritions; (2) Controlled release at small intestine.

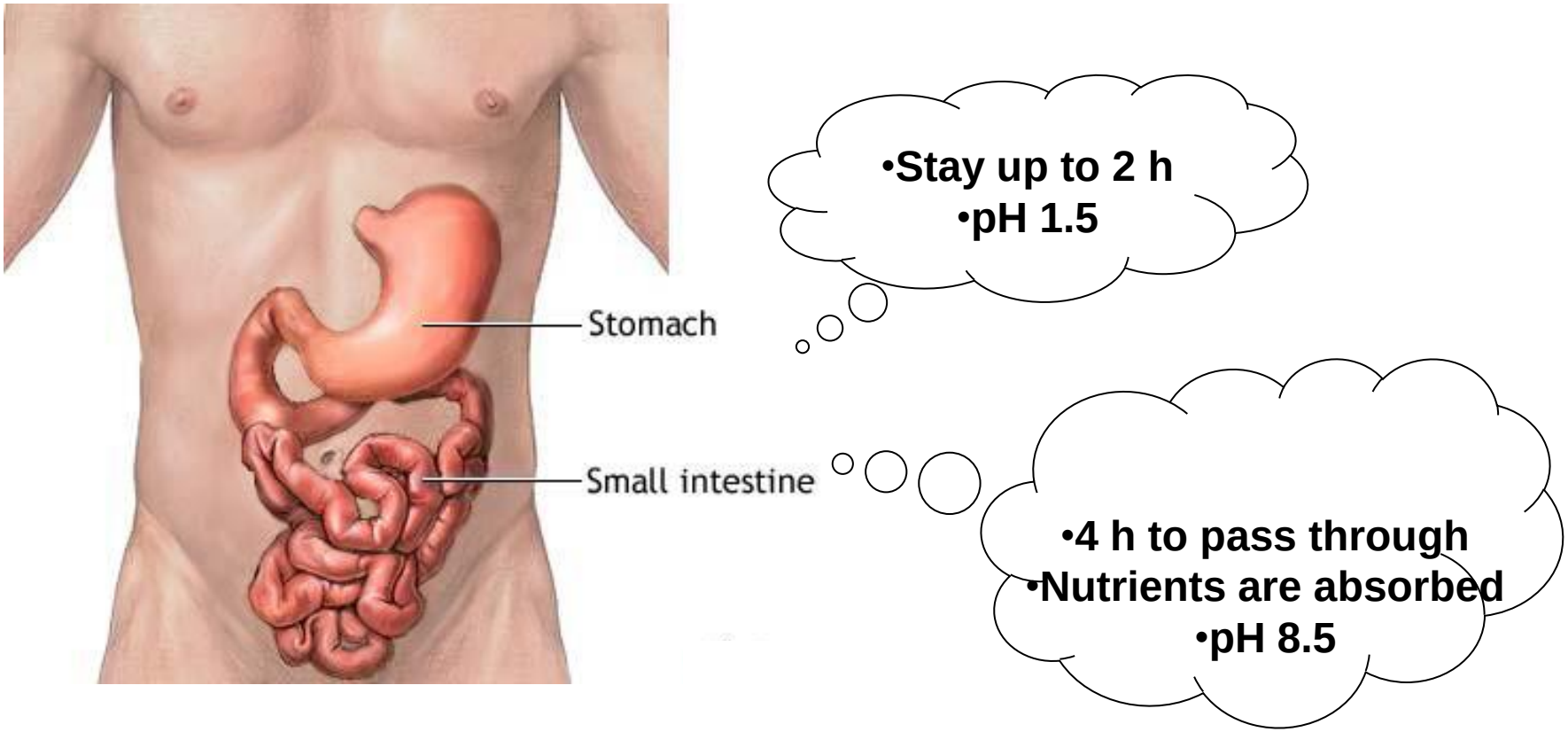

Main objective: Develop novel state-of-the-art technologies to characterize nanostructure and nanoscale interactions of protein/polysaccharide coacervates, and use the knowledge obtained to rationally design novel food delivery systems with controlled-release characteristics.

Biological Fate of Nutraceuticals

1. Solubilization

2. Absorption

3. Escape metabolism

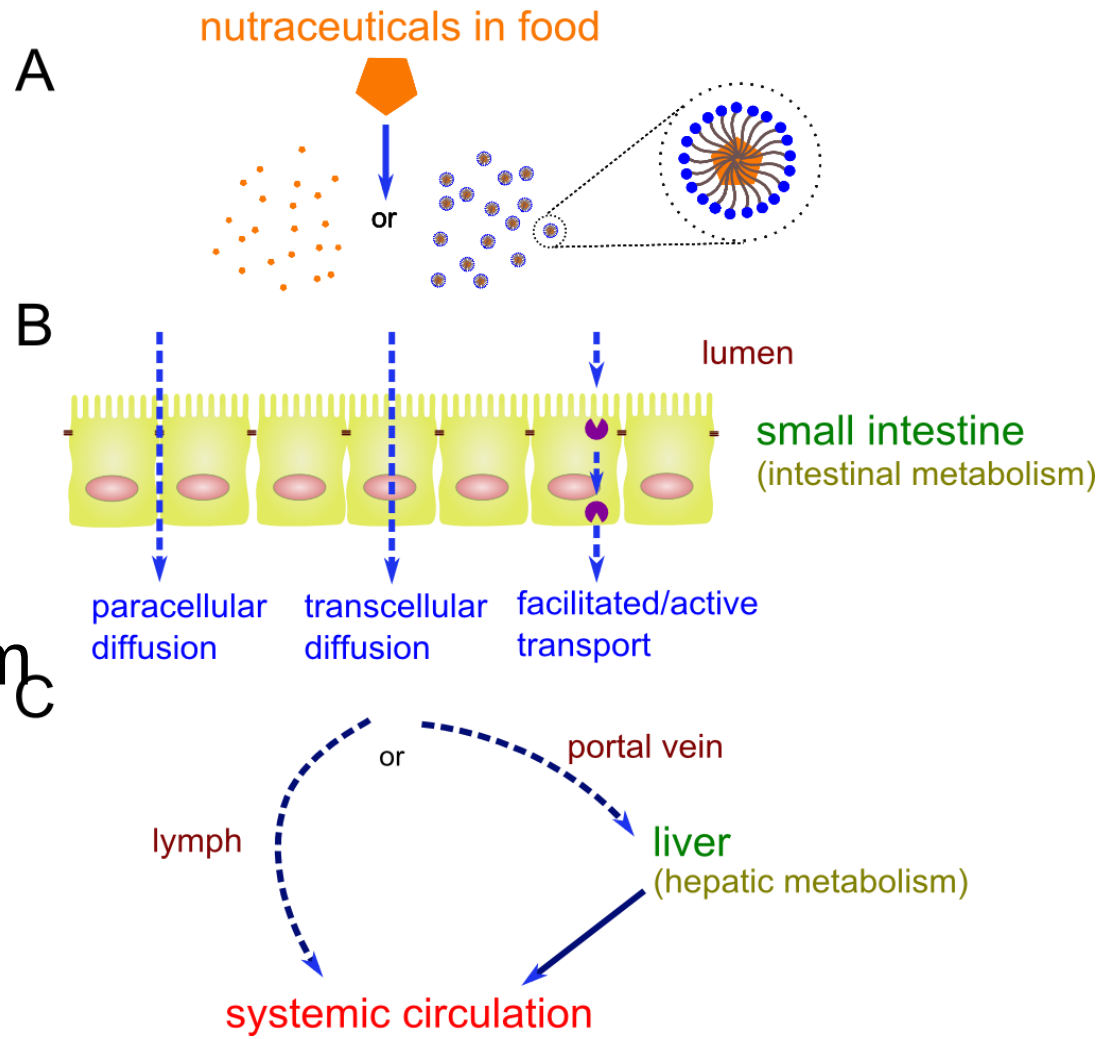

Strong Polyelectrolytes

- Carrageenans
  - Naturally sulfated polymer
  - Various kinds, difference in linear charge density(ξ)

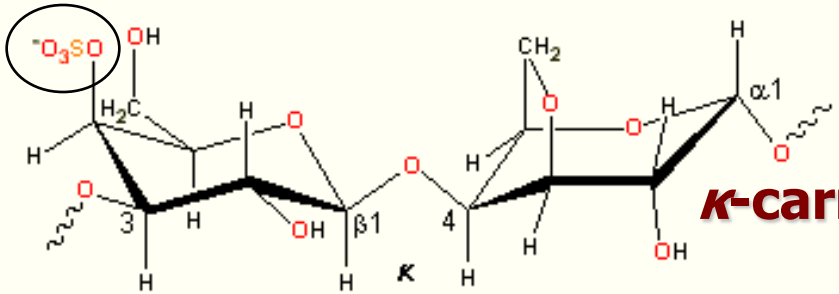

κ-carrageenan (ξ=0.92)

-(1→3)-b-D-galactopyranose-4-sulfate-(1→4)-3,6-anhydro-a-D-galactopyranose-(1→3)-

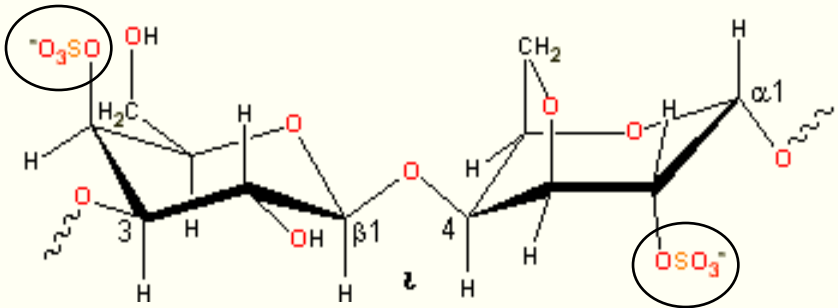

ι-carrageenan (ξ=1.53)

-(1→3)-b-D-galactopyranose-4-sulfate-(1→4)
-3,6-anhydro-a-D-galactopyranose-2-sulfate-(1→3)-

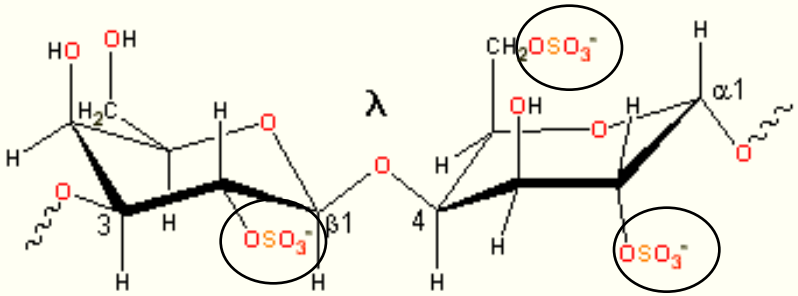

λ-carrageenan(ξ=2.07)

-(1→3)-b-D-galactopyranose-2-sulfate-(1→4)
-a-D-galactopyranose-2,6-disulfate-(1→3))-

(de Ruiter, G. A. *et al*. **1997,** *Trends in Food Science & Technology*)

Effects of Salt Concentrations

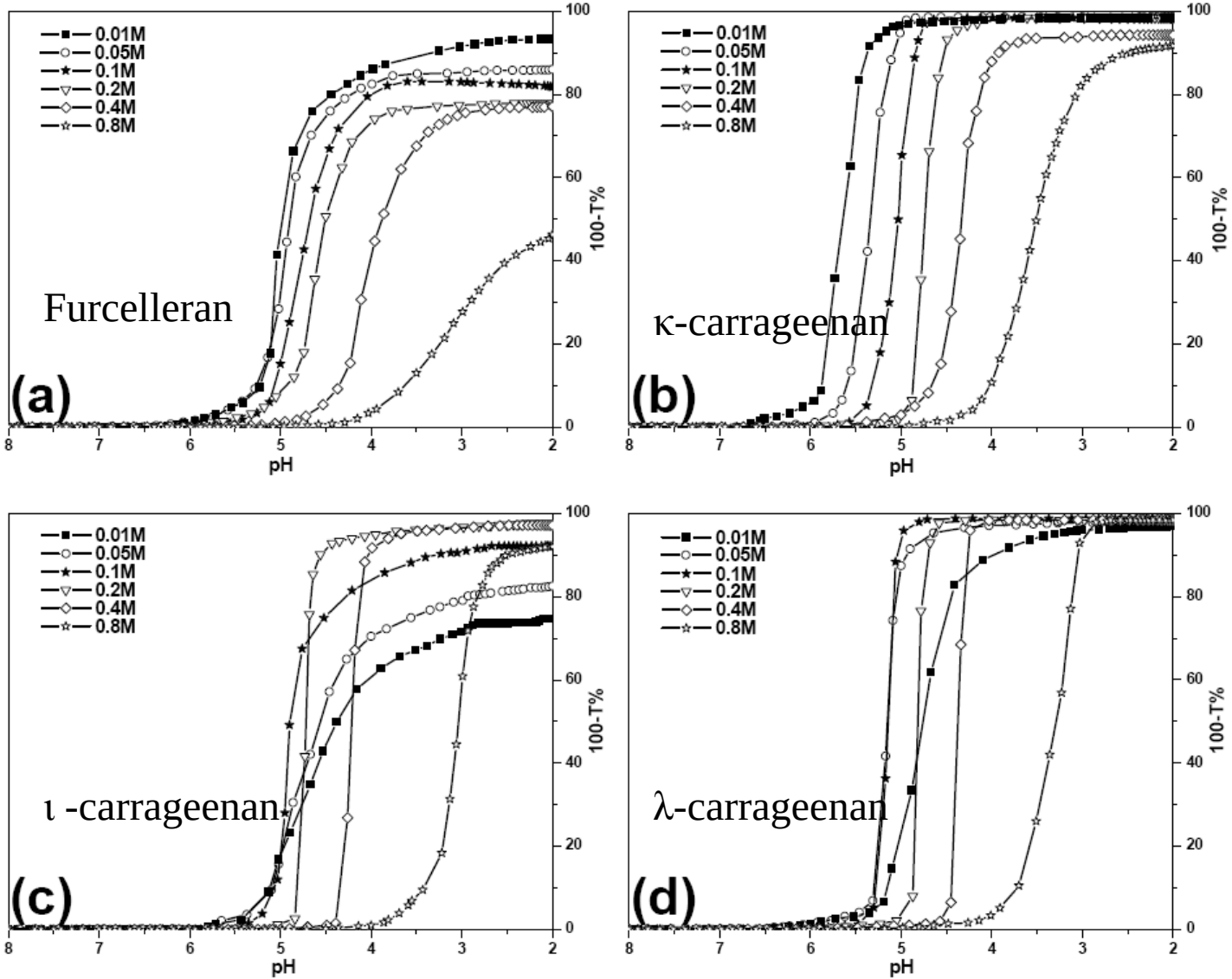

Effects of Protein/Polymer Ratios

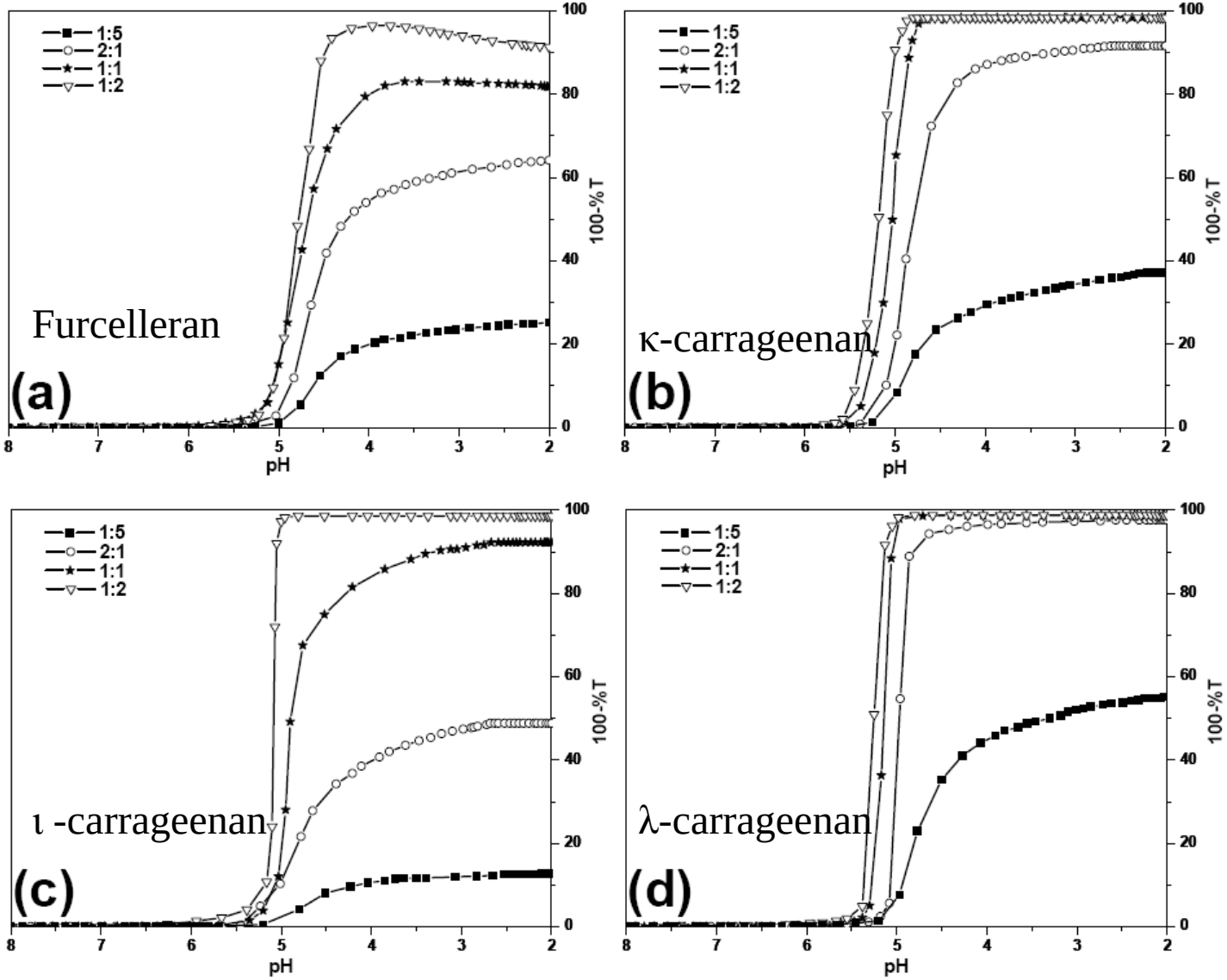

Effects of Cationic Types

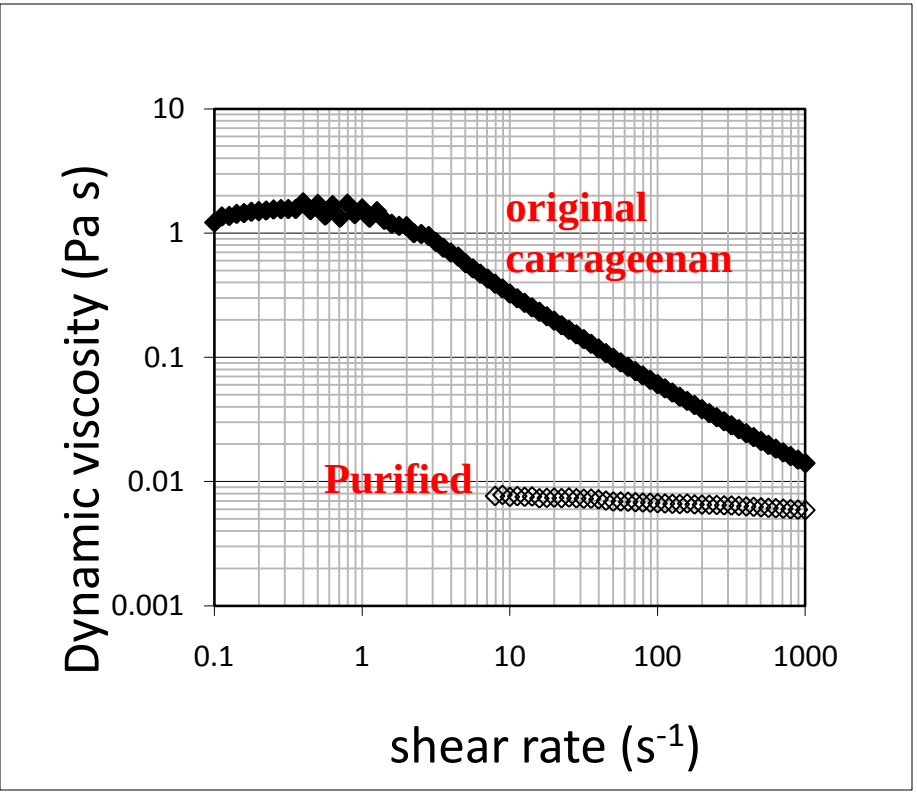

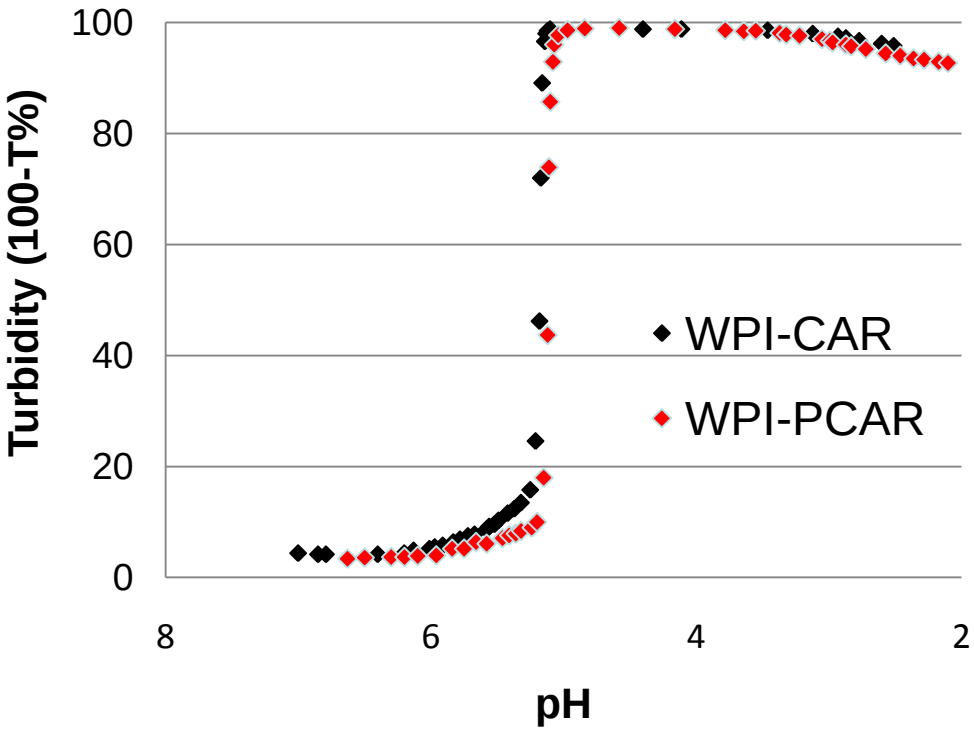

purified ι-carrageenan interactions

Cation type (Na+ vs. Ca2+) affects the rheological properties of the complexes, but has negligible effect on phase diagrams.

Phase Diagrams of WPI Fractions

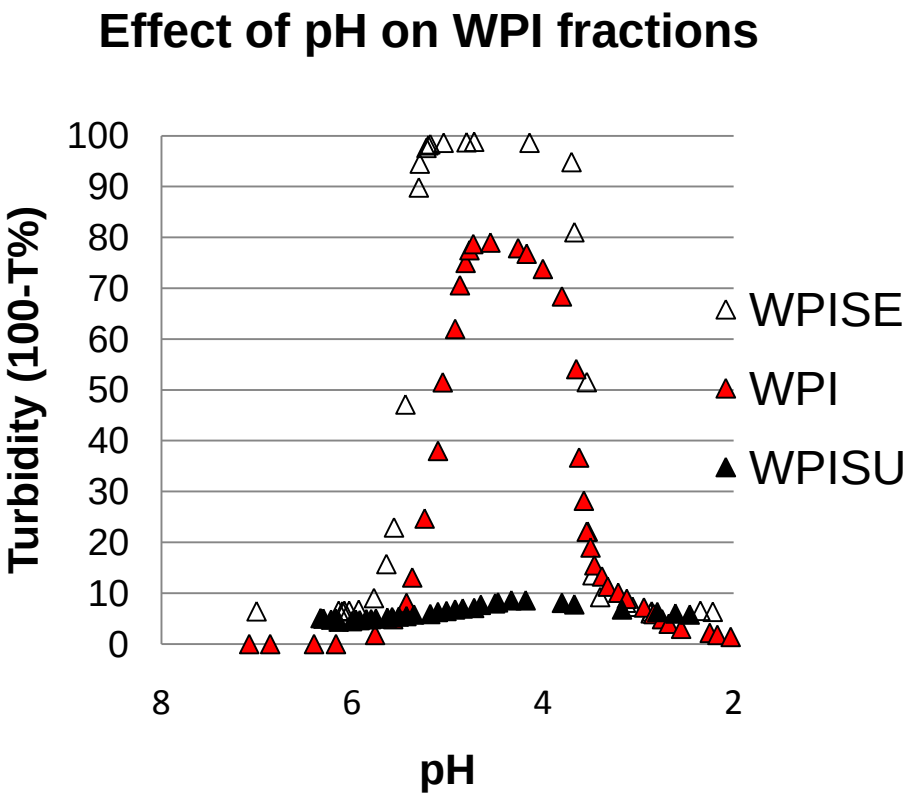

- WP treatment

Dispersion at pH 5

⇩

Centrifugation

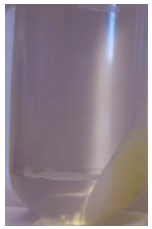

WPI

⇩

Filtration

⇩

Freeze-drying

Powder characteristics:

Supernatant : white, powder, highly soluble (WPISU)

Sediment: yellowish, grainy texture, less soluble (WPISE)

Improve In Vitro Anti-Cancer Activity of EGCG

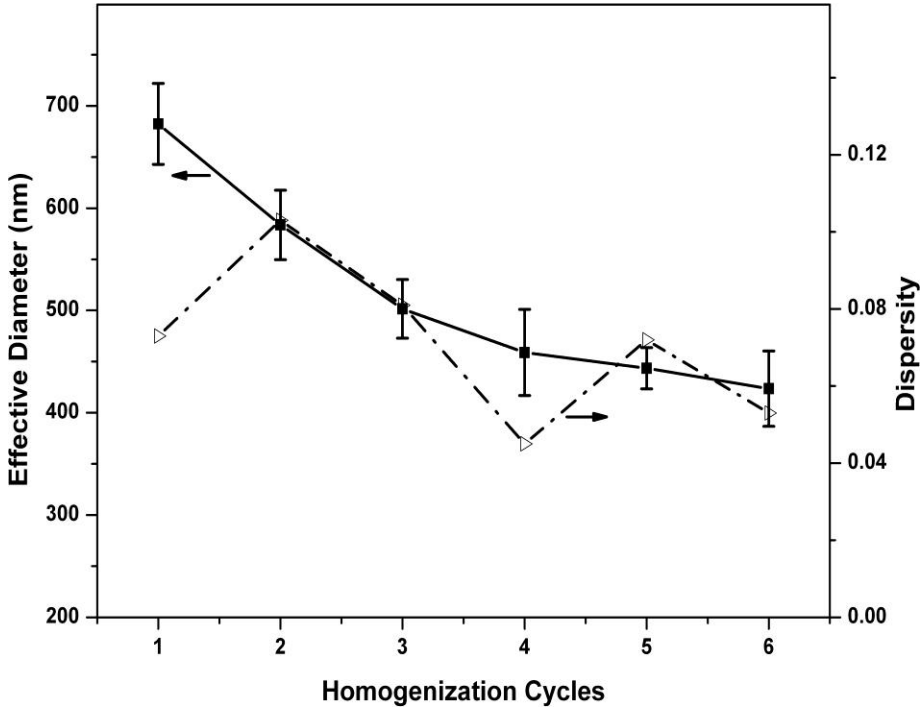

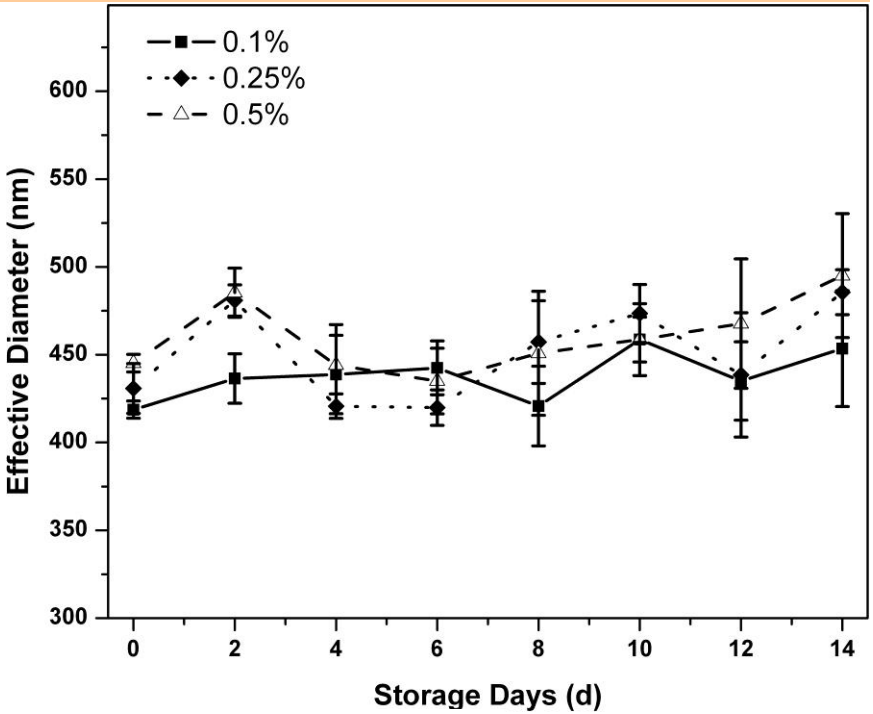

Emulsion size decreased with the increase of homogenization pressure.

Carrageenan/β-lg stabilized EGCG sub-micrometer O/W emulsion showed improved in vitro Anti-cancer activity aganist Human HepG2 cancer cells.

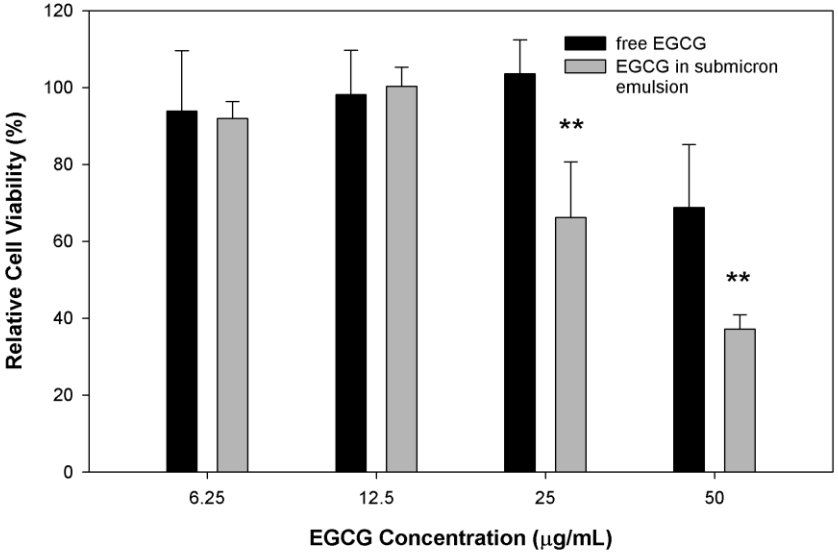

The emulsion sizes have negligible change during 14 days storage.

EGCG: epigallocatechin-3-gallate

Cationic Biopolymer:Chitosan

Chitosan is a cationic polysaccharide

is a fully or partially N-deacetylated product of naturally abundant chitin

biocompatible, biodegradable, low-toxic, bioadhesive

attract increasing attention in the fields of food, textile, cosmetics, biomedical, pharmaceutical, and other industries.

Assembly of Nanoparticles from Caseinophosphopeptides (CPPs) and Chitosan to Improve Calcium Absorption

- CPPs are bioactive peptides derived from tryptic digestion of casein;
- CPPs can enhance the mineral absorption/bioavailability in small intestine;
- CPPs contain clusters of phosphorylated seryl residues (see LC-MS data) .

Peptide sequences of CPPs.

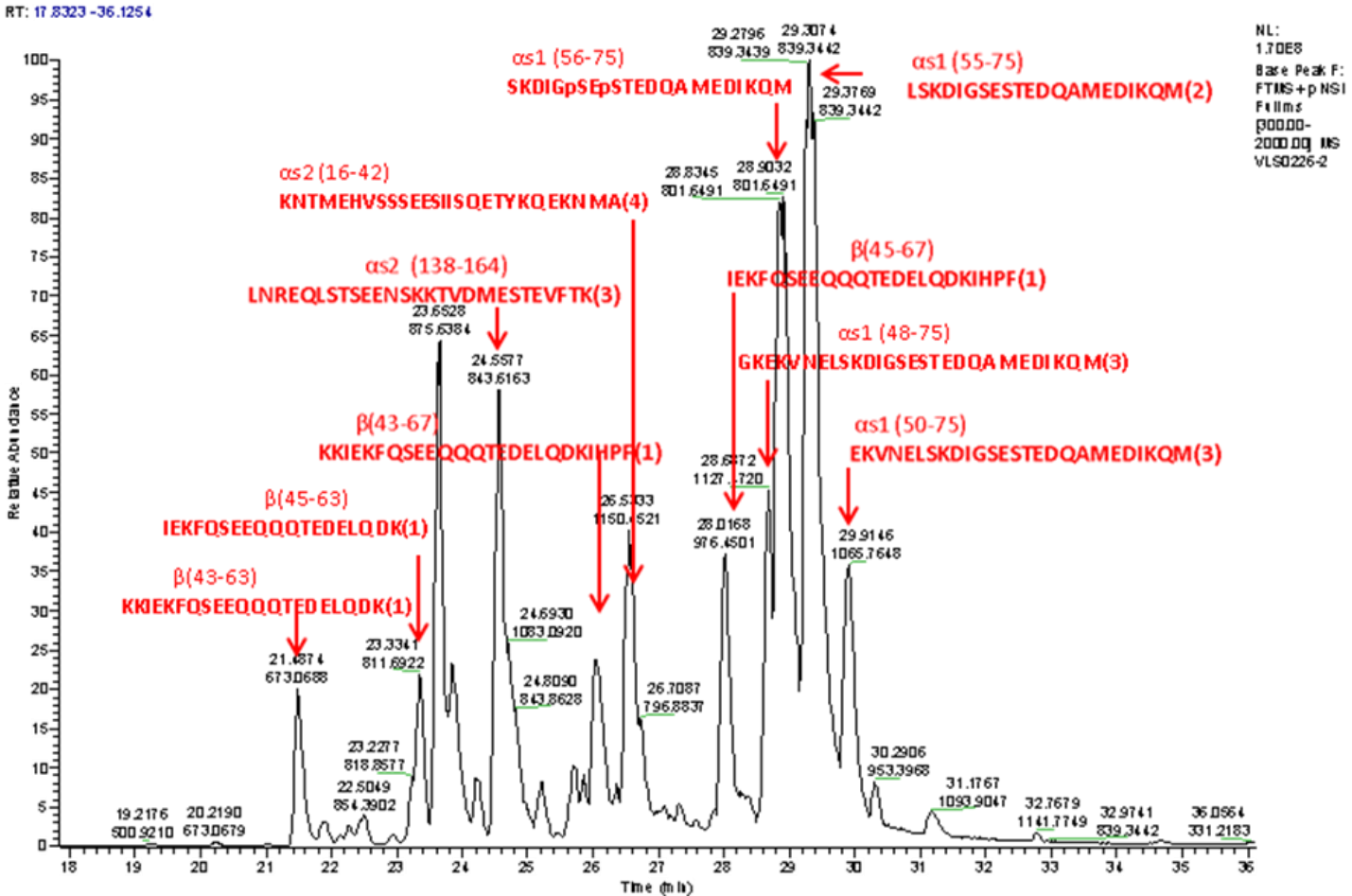

Assembly of Nanoparticles from Caseinophosphopeptides (CPPs) and Chitosan (CS): Effect of CS/CPPs Mass Ratios

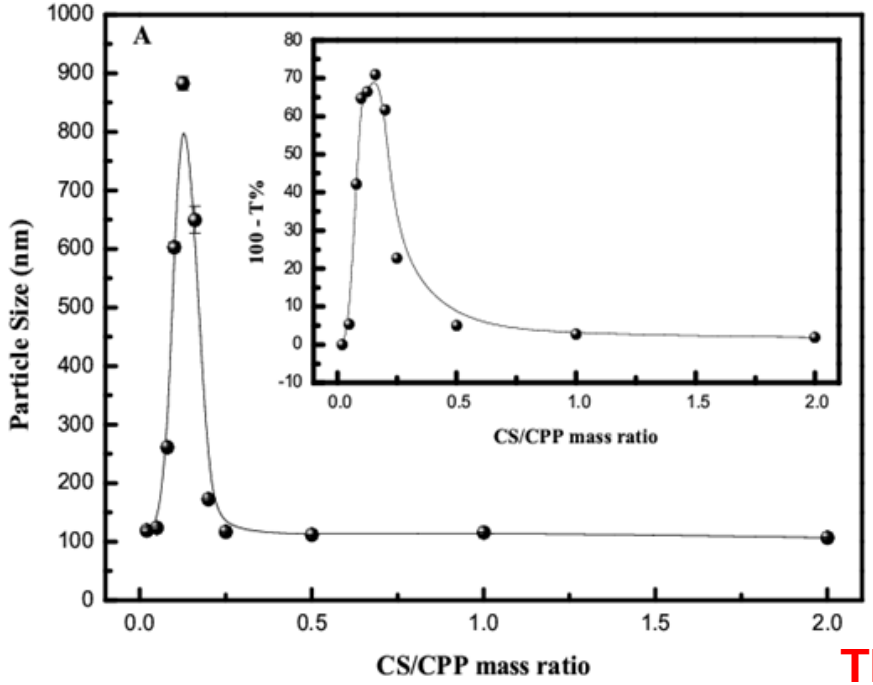

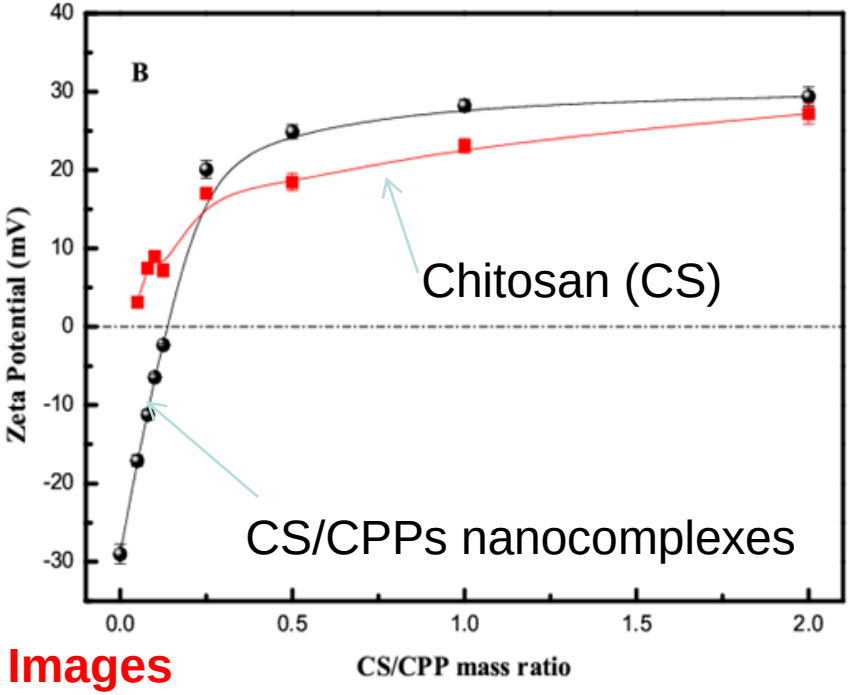

TEM Images

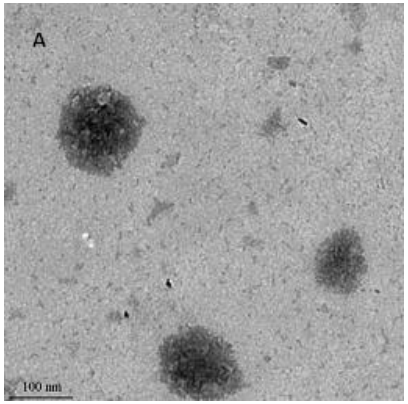

Mass ratio of CS/CPPs=0.20

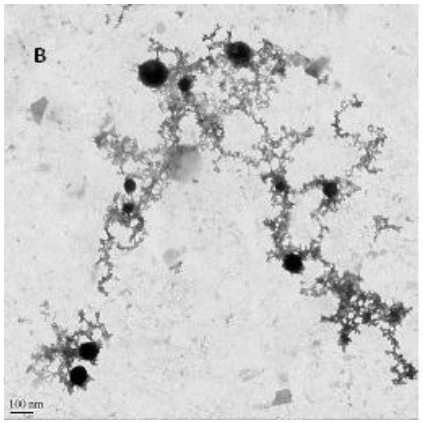

Mass ratio of CS/CPPs=0.25

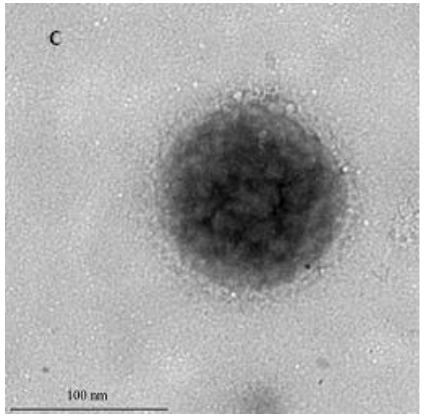

Mass ratio of CS/CPPs=1.0

Absorption of EGCG in Caco-2 Cells

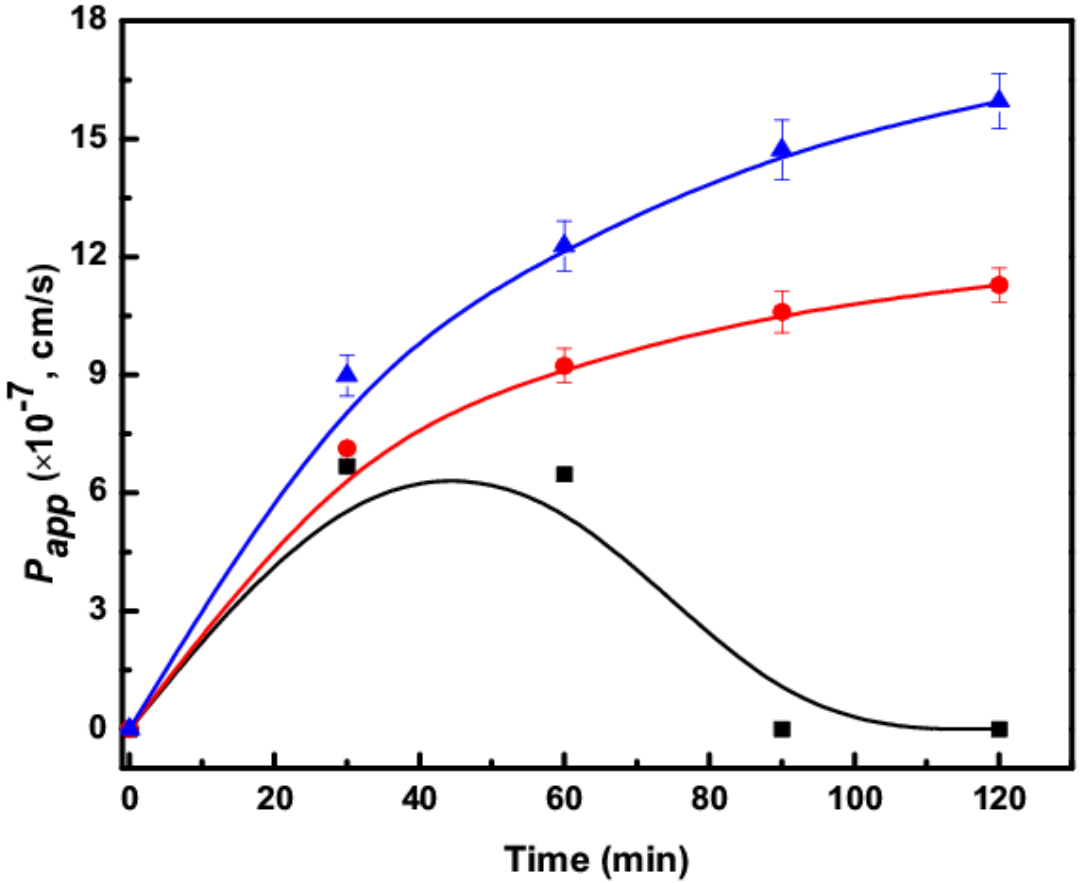

Transport of non-encapsulated (■) and CS-CPP nanoparticles encapsulated EGCG (●,1mg/mL CS; ▲,2mg/mL CS) through Caco-2 cell monolayers

Intellectual Merit

• This project investigates the mechanism which contributes to the assembly of protein/polysaccharide-based particles with the sizes ranging from a few nanometers to several micrometers, nanoscale interactions between proteins and polyelectrolytes, and macroscopic rheological properties of protein/polyelectrolyte coacervates—a theme which is of enormous importance in both fundamental understanding of colloid-polyelectrolyte interactions and industrial applications ranging from drug/gene delivery, cosmetics, functional food, dietary supplements, protein separation, to biosensors.

• Provide experimental basis for further theoretical studies.

-Right figure is a Snapshot of our recent Monte Carlo simulation configuration at pH 5.0.

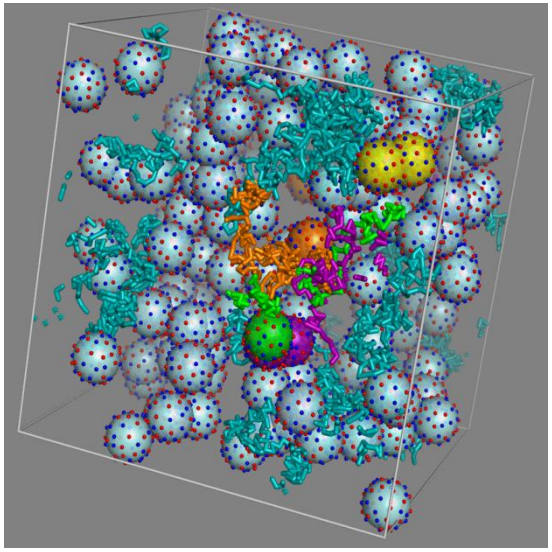

Broader Impact

- Economic impact

- Broad applications in the formulation of multicomponent functional foods, drug, personal care products, waste water management etc.

- Student training

- International collaboration

- Dissemination

Nanoporous Silicon Based Sensor Array for Bacteria Detection

Chang Lu (PI), Chemical Engineering, Virginia Tech, Blacksburg, VA

Arun Bhunia (co-PI), Food Science, Purdue University, West Lafayette, Indiana

Nanoporous silicon sensor for biosensing based on Interferometry

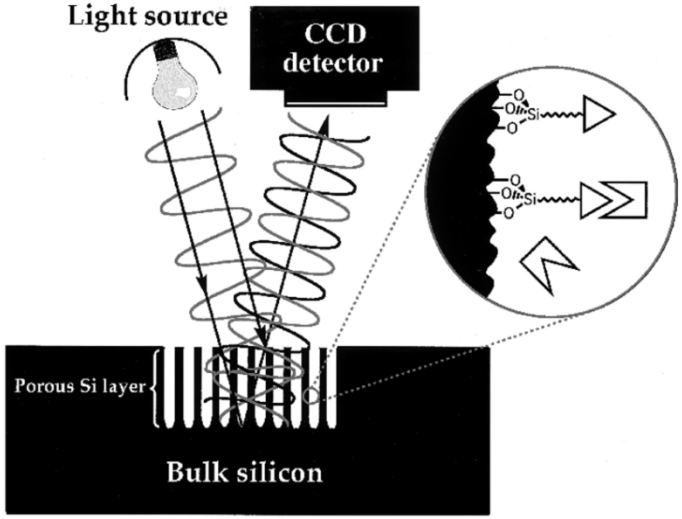

Overview

Cross section

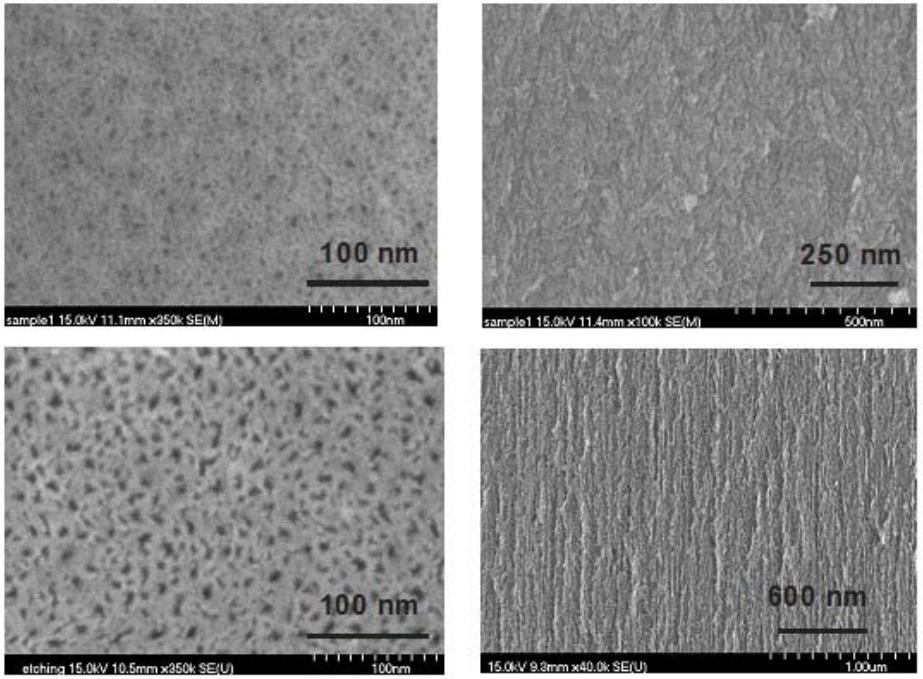

- Fabry–Pérot interference fringes due to light reflection at both top and bottom of the nanoporous silicon layer
- Shift in the interference fringes upon entry of biomolecules (DNA or protein)
- Molecular recognition elements coated on the interior surface for specific detection

Aad as an intracellular antigen for *Listeria* detection

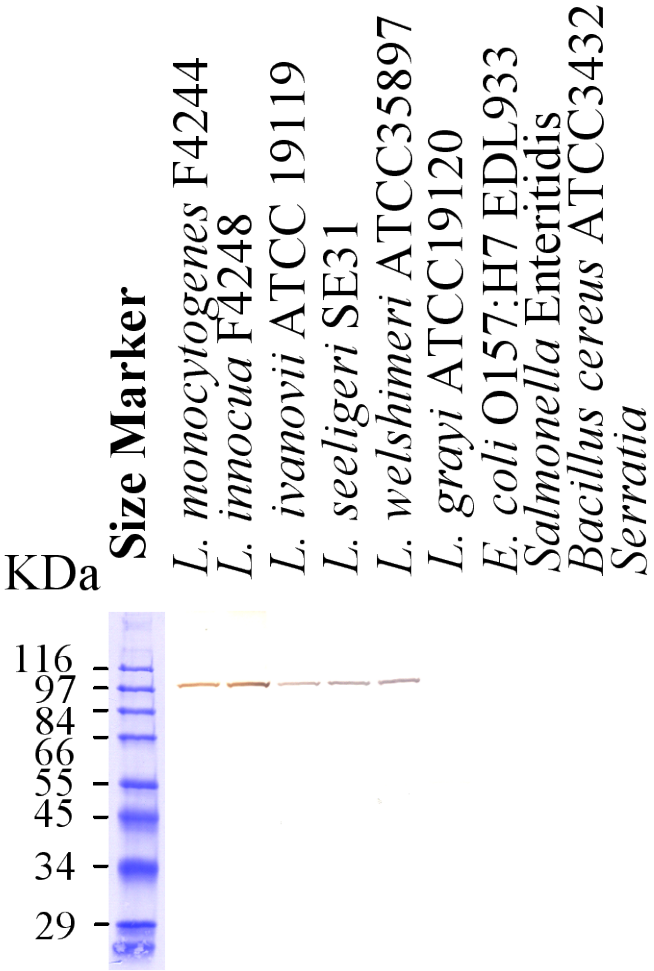

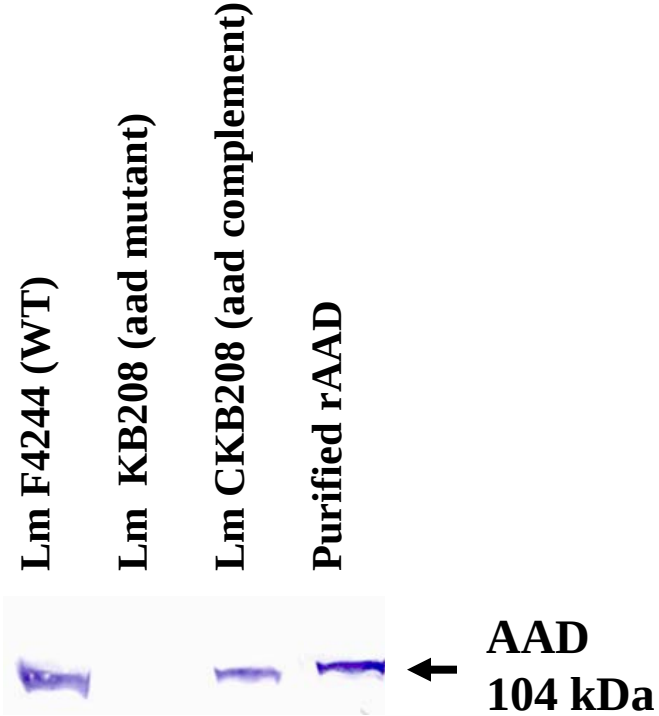

Western blot analysis of AAD (alcohol acetaldehyde dehydrogenase) expression in WT and mutant strains

Cell lysis and intracellular component release

GFP

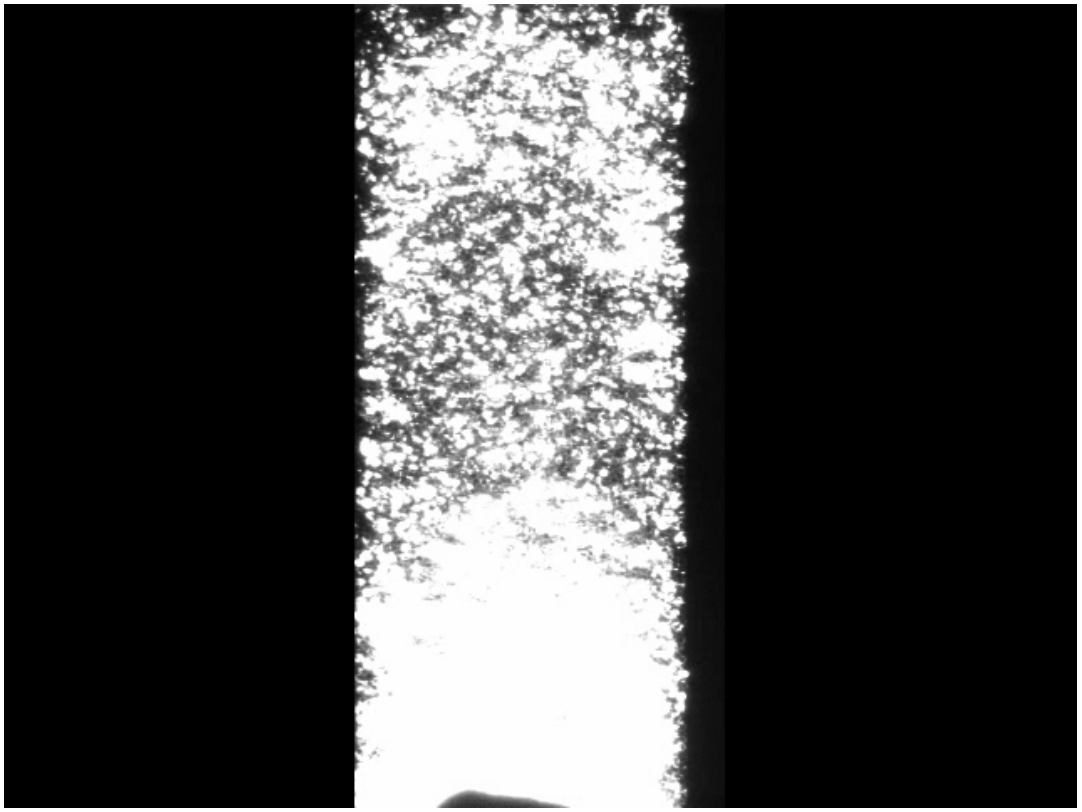

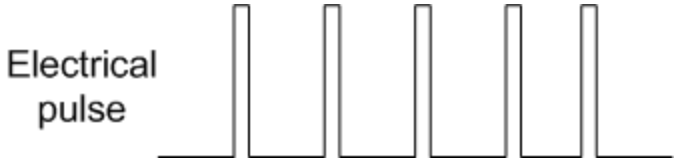

Interferometric measurements on nanoporous silicon for detecting antigen presence

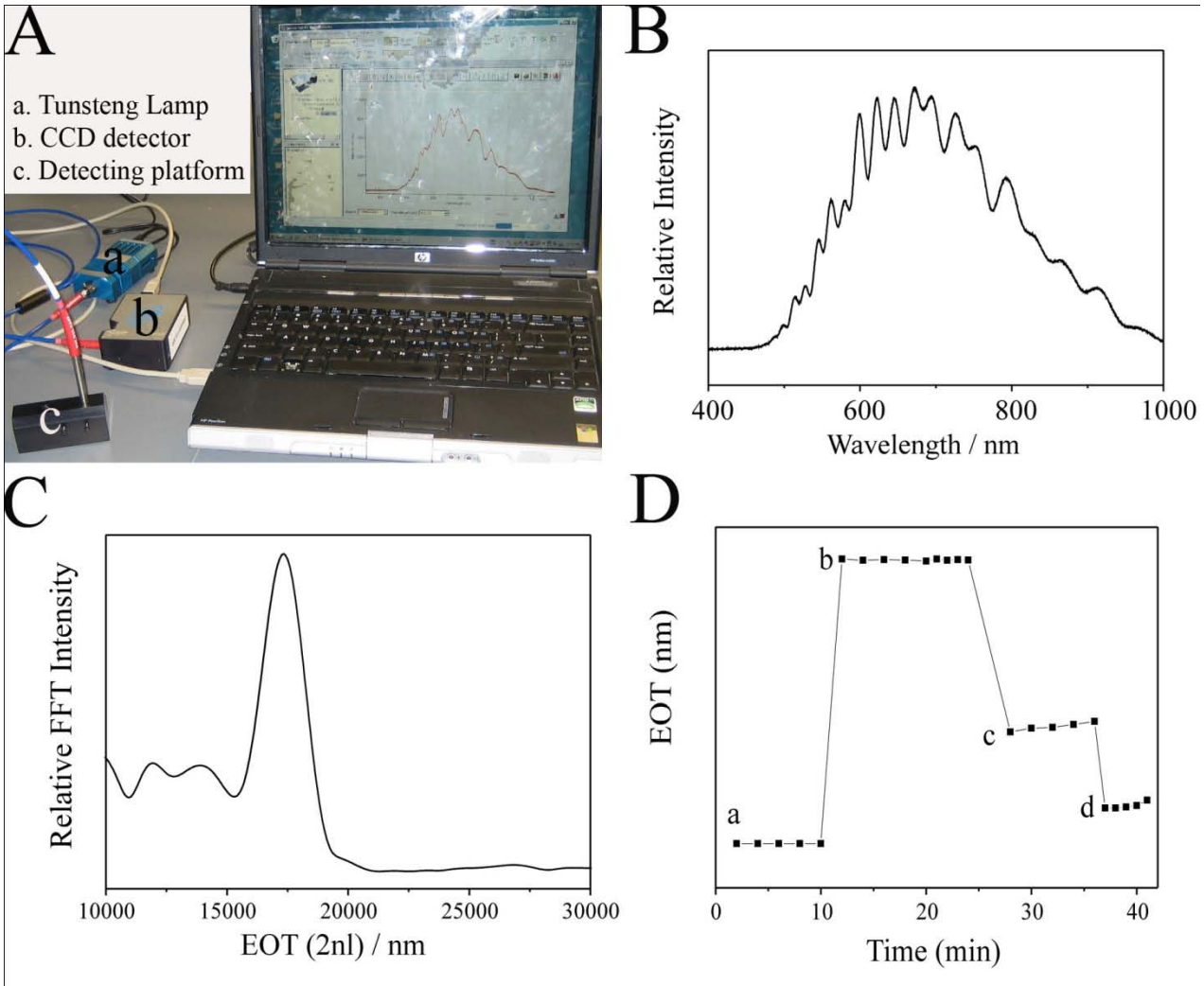

The nonspecific adsorption of 1 mg/mL antibody MAb-H7 in oxidized nanoporous silicon and subsequent removal by washing, reflected by the change in effective optical thickness (EOT). (a) Nanoporous silicon sensor in PBS buffer; (b) The antibody solution introduced; (c) First wash using PBS buffer; (d) Second wash using PBS buffer.

Detection based on DNA: Microchip design for releasing DNA

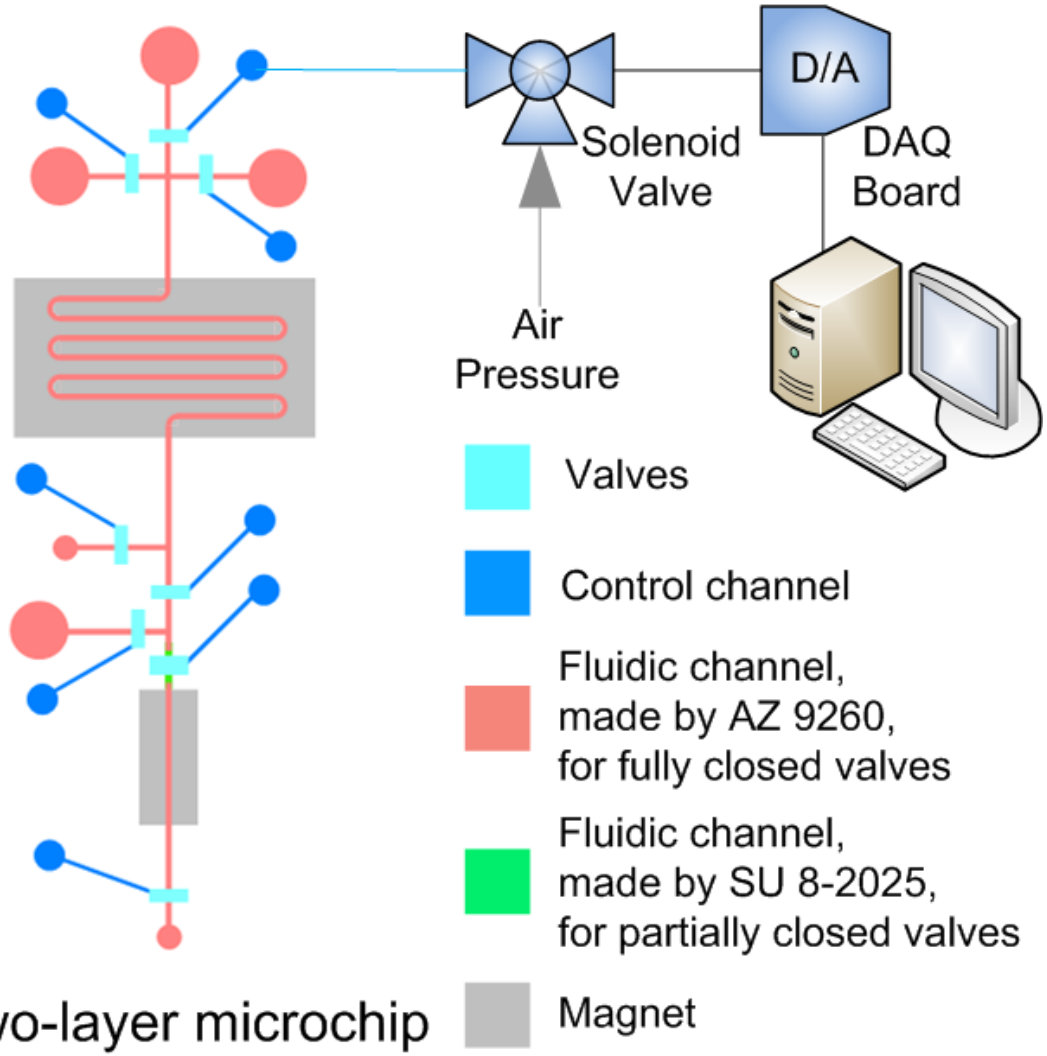

Two-layer microchip

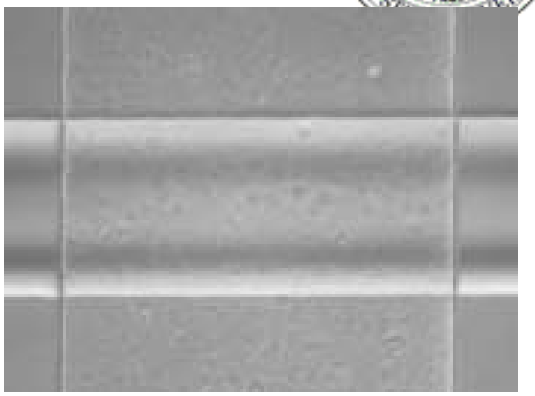

Fully closed valve (rounded channel)

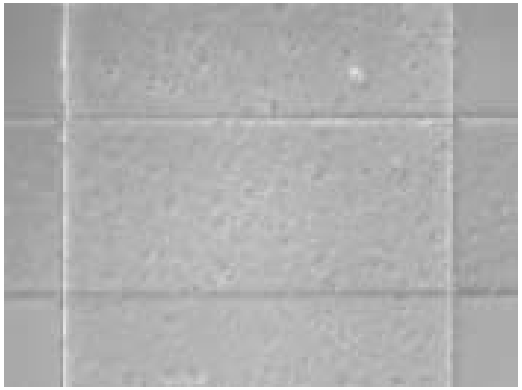

Partially closed valve (rectangular channels)

On-chip cell concentration, lysis and DNA purification

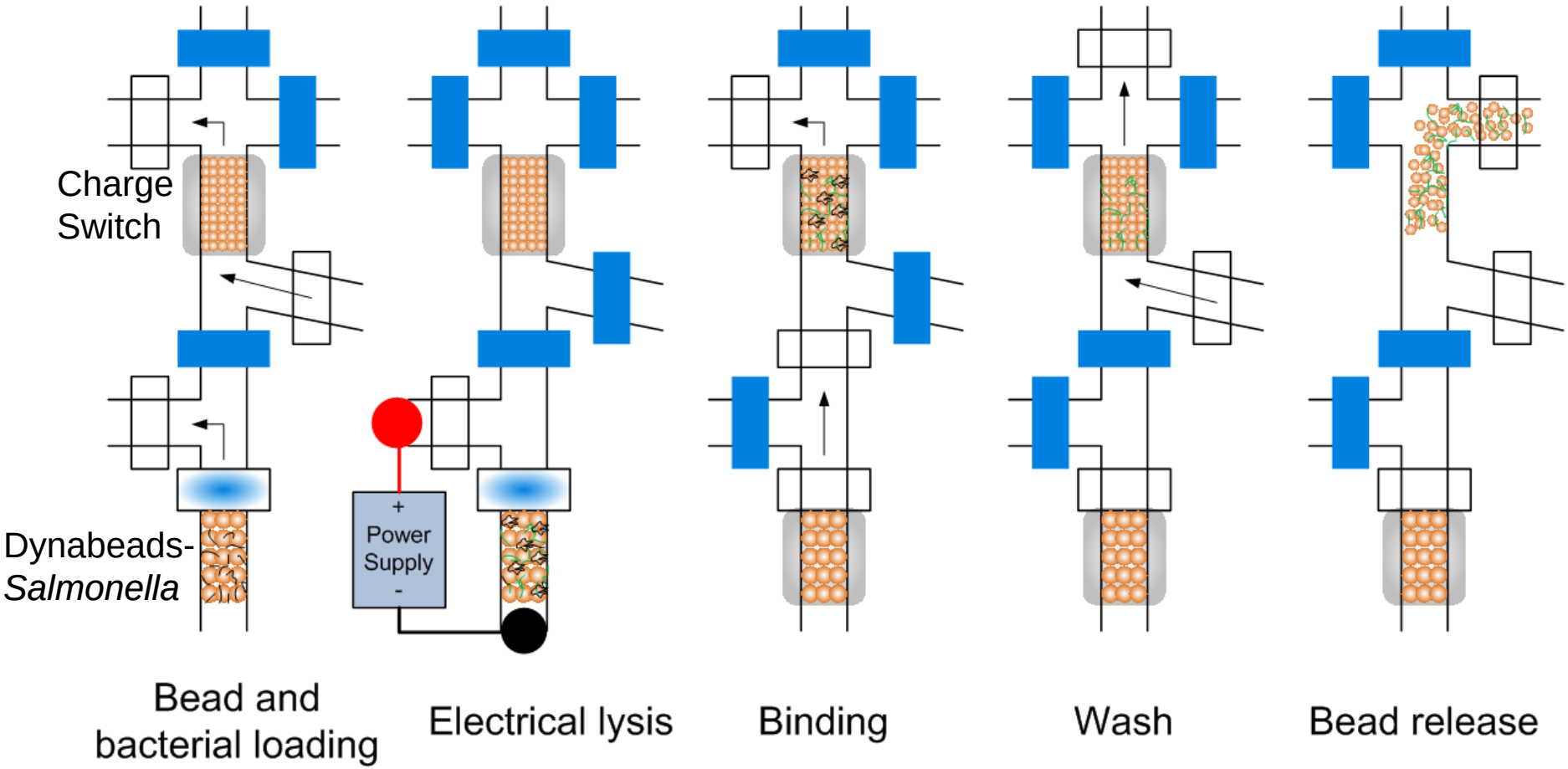

Immunomagnetic separation (IMS)

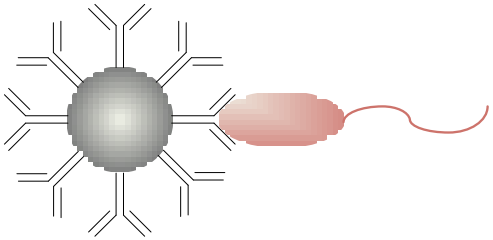

Dynabeads® anti-*Salmonella*

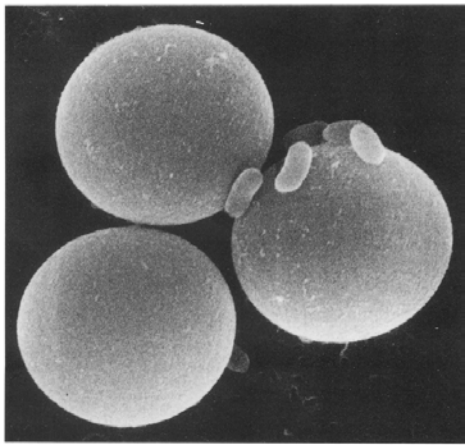

Olsvik O., Popovic T., Skjerve E., Cudjoe K.S., Hornes E., Ugelstad J., Uhlén M. **Clinical Microbiology Review** 7 (1994) 43-54.

Purification and concentration of bacteria

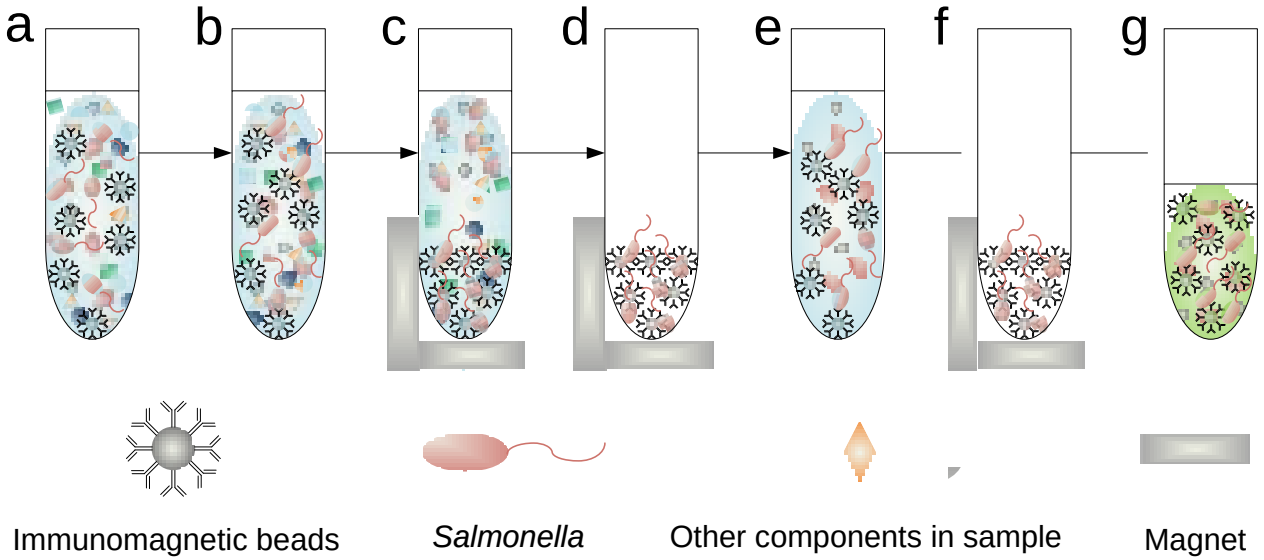

ChargeSwitch® magnetic beads for DNA purification

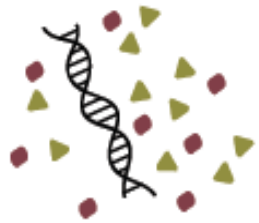

Step 1—Cellular lysis.

Bead charge

Charge on

pH < 6.5

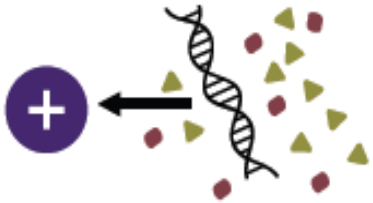

Step 2—DNA binding. To bind DNA, the pH is dropped to <6.5. At this pH, the ChargeSwitch® Magnetic Beads become positively charged and selectively bind DNA in the presence of optimized buffers.

Charge on
pH = 7.0

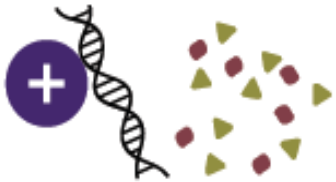

Step 3—Contaminant removal. Proteins and other contaminants are washed away in an aqueous wash buffer.

Charge off
pH = 8.5

Step 4—DNA elution. To elute DNA, the pH is raised to >8, changing the surface charge of the ChargeSwitch® Magnetic Beads and releasing the purified DNA directly into solution.

http://www.invitrogen.com/site/us/en/home/brands/Product-Brand/ChargeSwitch.html

Manipulation of magnetic beads on chip

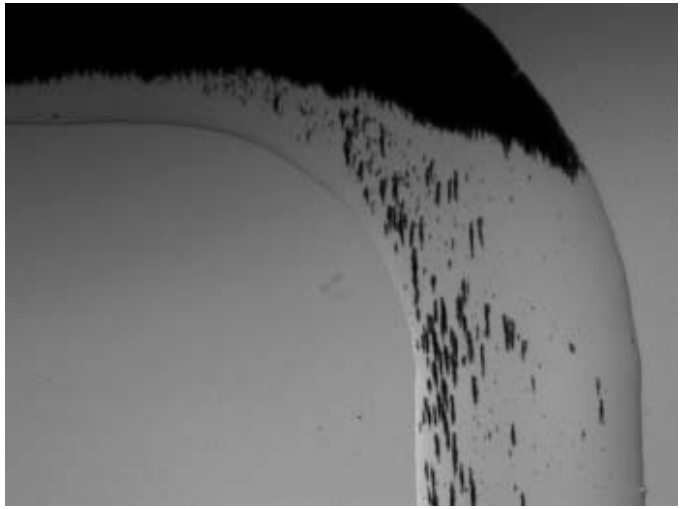

Beads loading

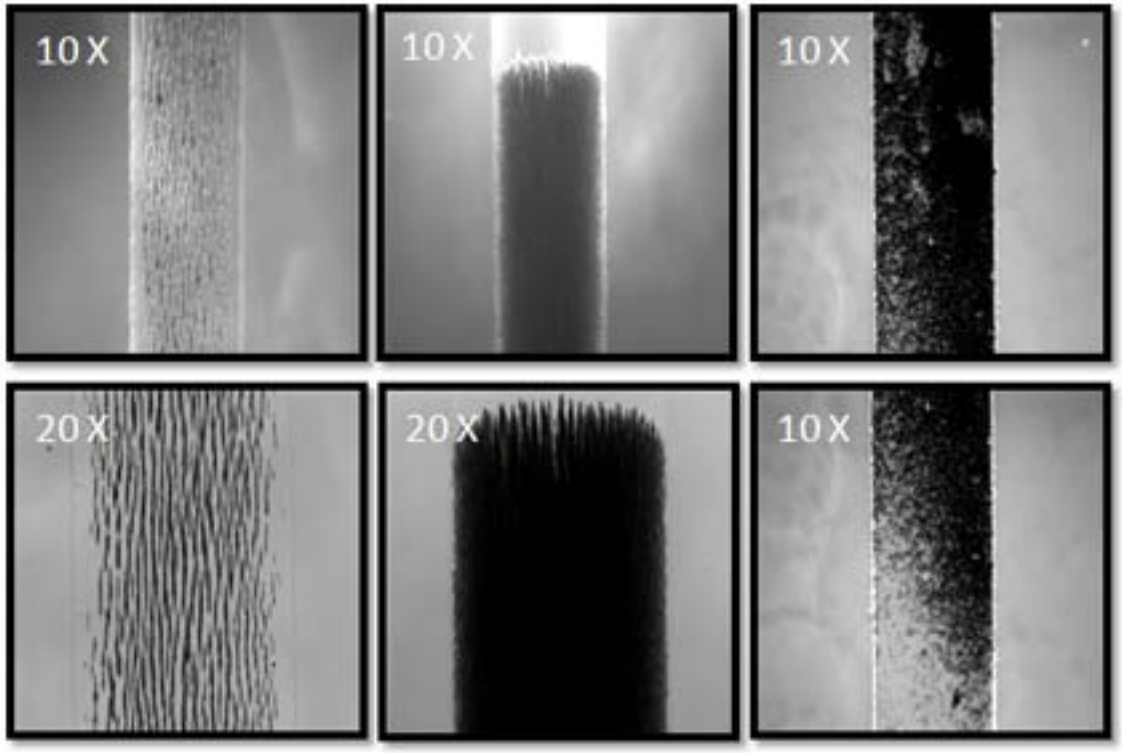

Flowing magnetic beads under magnetic field

Magnetic bead plug

Magnetic beads without magnetic field

Electrical lysis to release intracellular DNA

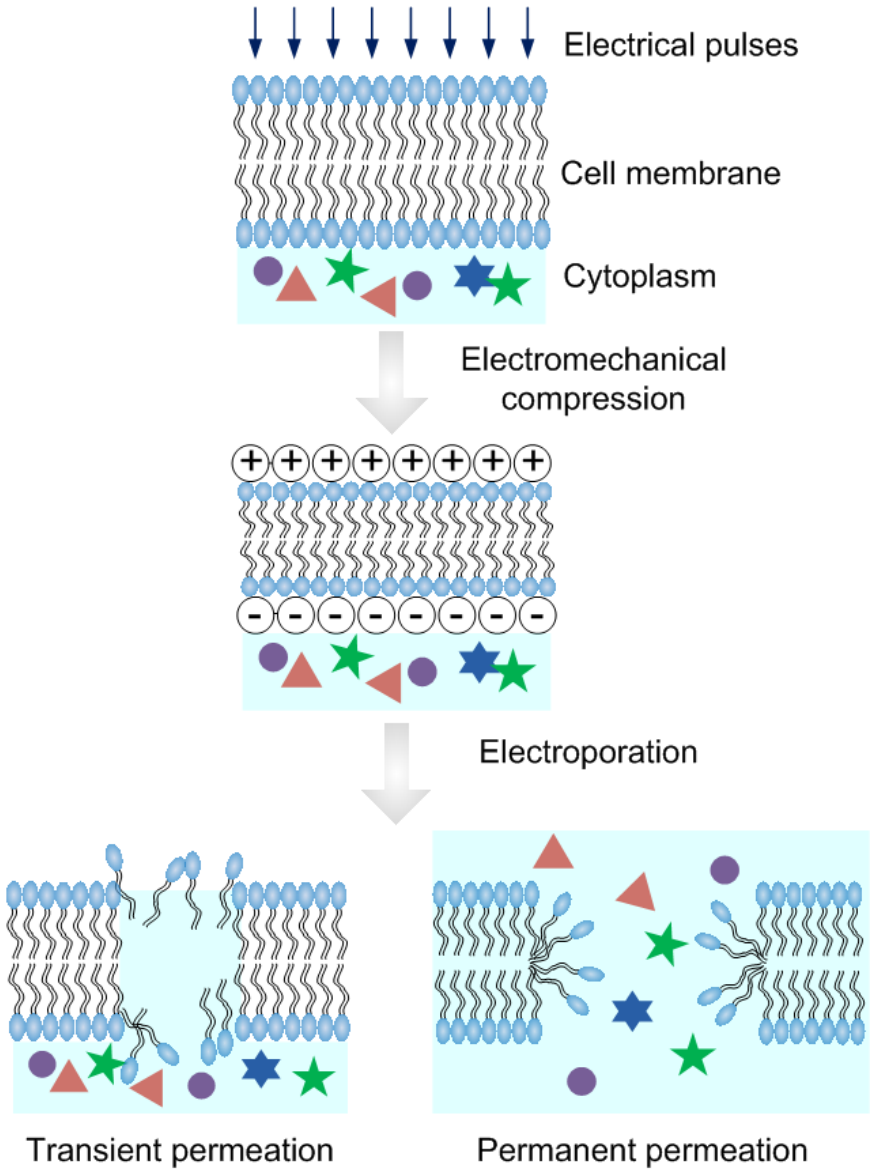

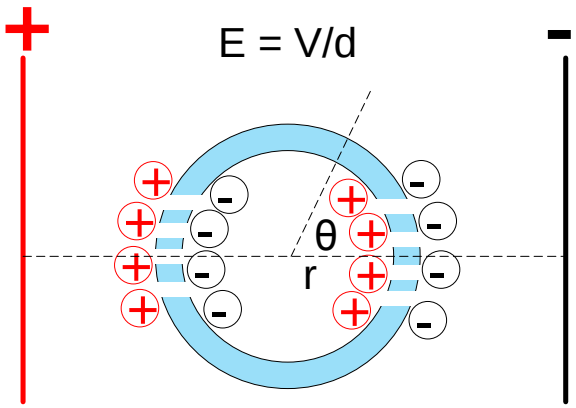

$$\Delta\psi = fg(\lambda)Er\cos\vartheta$$

$\Delta\psi$: transmembrane potential;
f: the shape of the cell;
$g(\lambda)$: the conductivity of the media;
E: the external electric field intensity;
r: cell radius;
ϑ: polar angle with respect to external field.

PCR assay to confirm DNA release

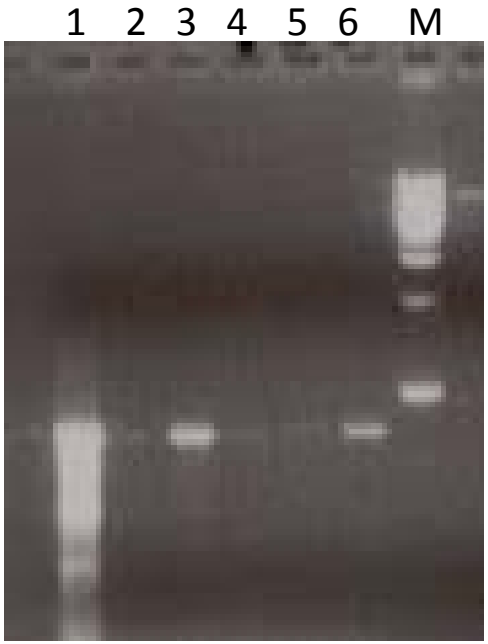

***invA* gene**

PCR conditions:

initially at 94 °C for 1 min, 29 cycles at 94 °C for 1 min, at 50 °C for 1 min, at 72 °C for 1 min, and a final extension at 72 °C for 10 min

Primers:

Farward: CGGTGGTTTTAAGCGTACTCTT

Reverse : CGAATATGCTCCACAAGGTTA

Lane 1: Positive control, cells were lysed by heathing for 10 min at 90 °C, and DNA were not purified, 10^6 CFU

Lane 2: 1500 V/cm, 10^6 CFU

Lane 3: 1200 V/cm, 10^6 CFU

Lane 4: 1000 V/cm, 10^4 CFU

Lane 5: 1000 V/cm, 10^4 CFU, from wash

Lane 6: 1000 V/cm, 10^6 CFU

Pulses: monopolar square, 16, 1 s

Interval: 10 s

Total time: 3 min

A different approach: macroporous silicon for amperometric detection of bacteria

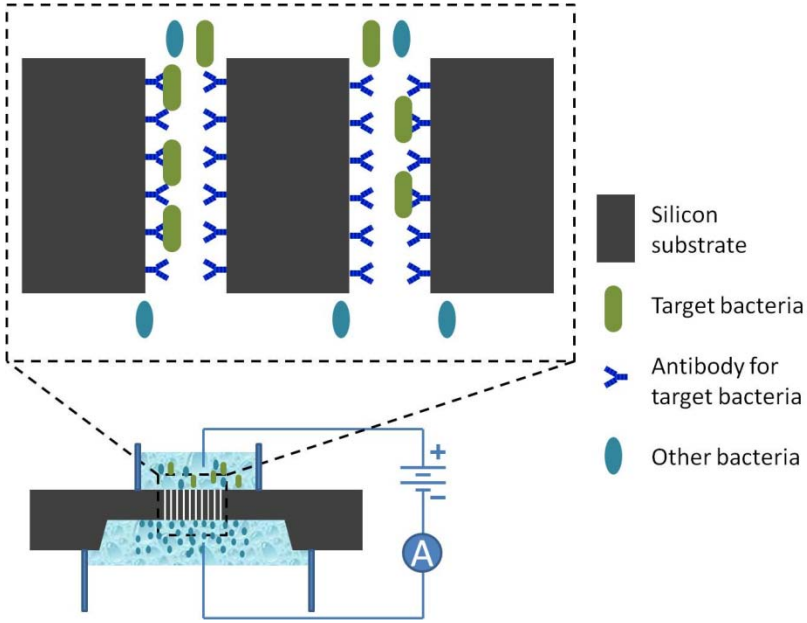

Specific detection of a bacterium based on blocking of the current

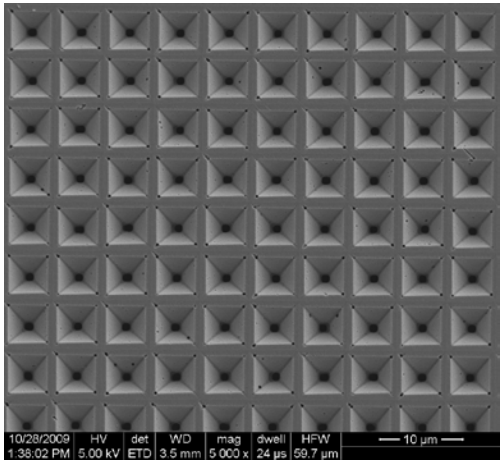

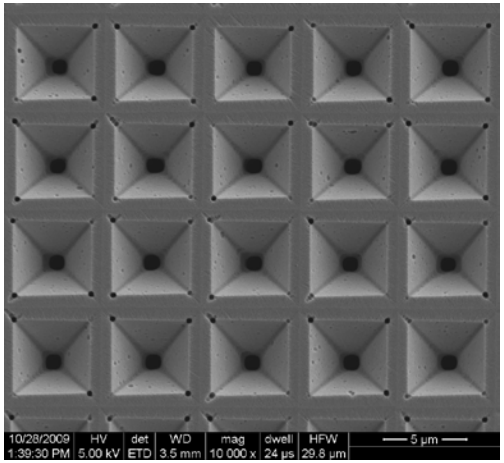

Fabricated by combination of microfabrication and photoactivated electrochemical etching; pore size: 200 nm-several microns

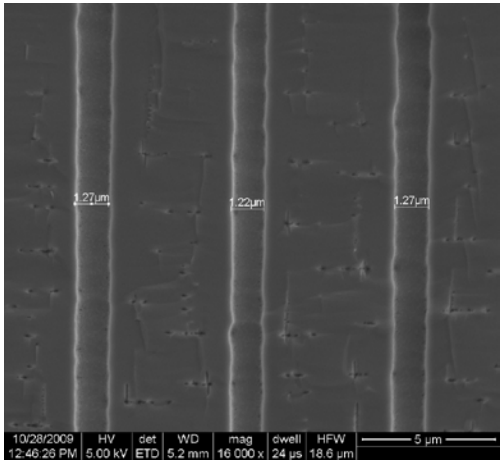

Publications and presentations in 2010 supported by the grant

Journal publications

- Wang, J., Zhan, Y., Ugaz, V.M. and Lu, C. ***Lab on a Chip*** 10 (2010) 2057-2061.
- Bao, N., Le, T.T., Cheng, J.X. and Lu, C. ***Integrative Biology*** 2 (2010) 113-120.

Conference presentations

- Geng, T., Mishra, K. Bhunia, A.K., Lu, C. Rapid and Sensitive Detection of Salmonella Using An Integrated Microfluidic Chip and Real-Time PCR. AIChE Annual Meeting, Nov. 7-12, 2010, Salt Lake City, UT, USA.
- Geng, T., Bao, N., Litt, M., Lu, C. Microfluidic Native Chromatin Immunoprecipitation (µNChIP) Assay for Histone Acetylation Detection. AIChE Annual Meeting, Nov. 7-12, 2010, Salt Lake City, UT, USA.
- Zhan, Y., Bao, N., Wang, J., Lu, C. Flow-through Electroporation for Transfection Based On Low-Frequency AC Voltage. AIChE Annual Meeting, Nov. 7-12, 2010, Salt Lake City, UT, USA.

News media coverage

- Research highlight in *Nature* (Vol 466, page 163, July 8, 2010): "Biotechnology: Swirling cells."
- Update in *Chemical Engineering Progress* (CEP) (August 2010).
- Virginia Tech News (July 12, 2010).
- *Highlights in Chemical Biology* (Jan 13, 2010).

Future work

- Improve the release efficiency of DNA and couple nanoporous silicon detection of DNA sequence to the DNA release
- Continue exploration of amperometric bacteria detection based on macroporous silicon
  - Fabricate nanoscale to microscale pores with consistency and reproducibility
  - Functionalize electrochemically etched silicon surfaces

Nanoliter/Picoliter Scale Fluidic Arrays for Rapid Identification of Pathogenic Bacteria

Jong Wook Hong and Omar Oyarzabal

Materials/Mechanical Engineering, Auburn University♪

AUBURN

UNIVERSITY

Contents

1. *Listeria monocytogenes*
2. Principle of nanoliter fluidic array
3. Current detection methods and nanoliter fluidic array
4. Detection of *L. monocytogenes*
   a. Development of nanoliter fluidic array
   b. Design and evaluation of primer sets and probes
   c. Detection of single template of *L. monocytogenes*
5. Future Works

AUBURN UNIVERSITY

Listeria monocytogenes

- Gram positive rod
- Isolated from soil, water, effluents, foods, humans/animal feces
- Ruminants maintain *Listeria* spp in rural environment via continuous fecal-oral enrichment

- Well evolutionized to survive under extreme conditions
  - Temperature range: 30 to 113°F (-1 to 45°C)
  - pH range: 5.0 to 9.6
  - Salt concentration : Growth at 10% and survival at 25.5%

- Causative agent of **listeriosis**

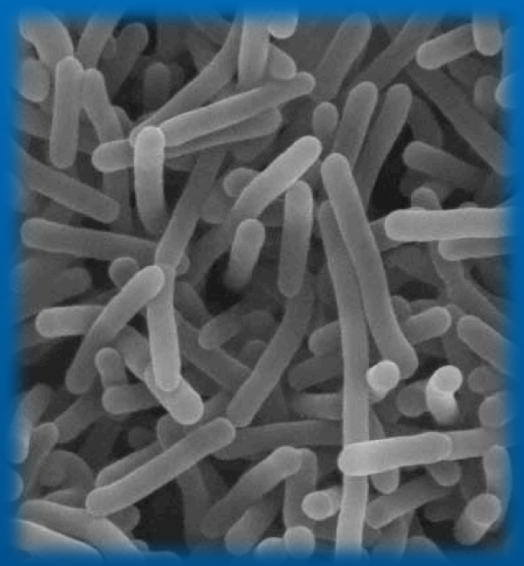

http://www.koolielu.edu.ee/.../Listeria%20monocytogenes.jpg

AUBURN UNIVERSITY

Listeriosis

- Caused by virulence factor, listeriolysin O
- Severely effects immuno-comprimised individuals, such as pregnant women, newborns, and others.
- Incidence rate of 0.33 cases/100,000 population

Pathogen	Illnesses	Deaths	Mortality rate
Campylobacter	2,453,926	124	0.1%
Salmonella	1,412,498	582	0.8%
E. coli O157:H7	73,480	61	0.8%
Listeria ♪	2,518♪	504 ♪	20.0%♪

Mead P, et al, *Emerging Infectious Diseases, 1999*

Because of high mortality rate of listeriosis there is a great need to find more rapid and sensitive methods of detection

AUBURN UNIVERSITY

Nanoliter/Picliter fluidic array

- **Number of panels (samples): 10**
- **Number of reactors: 10,000**
- **Volume of a reactors: 5 nL**
- The use of nanoliter reaction volumes can **increase the specific template concentration** by approximately **three or four orders of magnitude**, if a template was included in a reactor.

Design of microfluidic reactor arrays

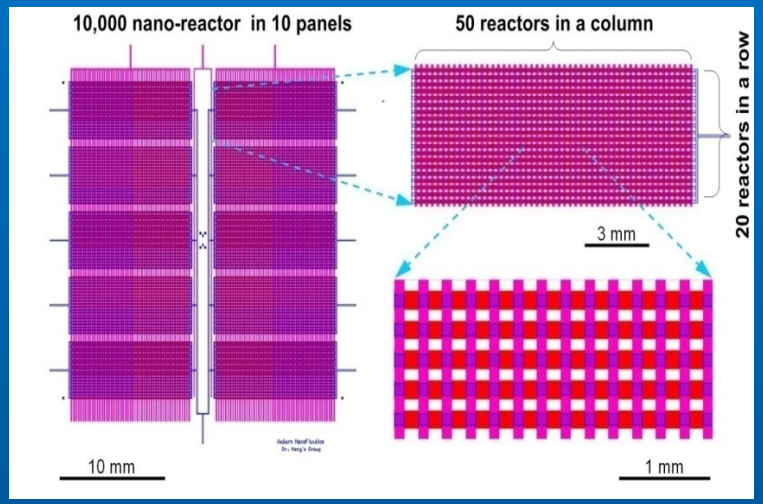

Table. Comparisons between conventional tube PCR and microfluidic digital PCR

Parameters	Macro-scale reactor	10,000 nanoliter array
Total reaction volume	50 µL	50 µL
Reaction volume in a reactor	50 µL	5 nL
Number of reactions in a single experiment	1 reaction	10,000 reactions
Relative concentration of template in a reactor♪	3×10^{-18} M (≈ 10^2 copies/50 µL)♪	3×10^{-14} M (≈ 10^2 copies/5 nL)♪

BURN UNIVERSITY

Current detection methods vs. nanoliter fluidic array

Culture and colony counting method

- Advantages
  - Most sensitive and accurate
  - Resolution of single bacterium
  - Discriminating viable and non-viable cell
  - Providing common units of measure: CFU
- Disadvantages
  - Extremely time-consuming

Biosensors

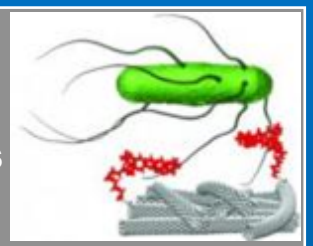

- Advantages
  - Rapid detection within few minutes
  - Detect a single bacterium in theory
- Disadvantages
  - Not be proved with real samples
  - Requiring signal transducers
  - Including background noise

Real-time tube PCR

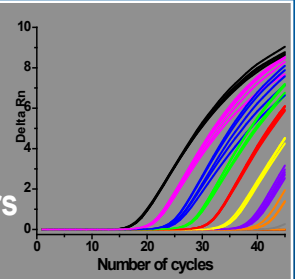

- Advantages
  - Detect a single bacterium in theory
  - Rapid detection within 30 min ~ 2 hrs
- Disadvantages
  - Sensitive to the quality of starting materials
  - Can't discriminate between viable and non-viable cell
  - Need to be translated into CFU

Nanoliter fluidic array

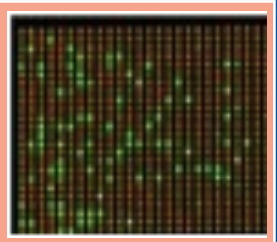

- Advantages
  - Identical sensitivity to colony counting method
  - Resolution of single bacterium
  - Rapid detection within 30 min ~ 2 hrs
  - Providing CFU without translation

This method covers the advantages of colony counting methods and real-time tube PCR

AUBURN UNIVERSITY

Research design

- **Specific goals of this research are to:**
- Develop nanoliter fluidic arrays for the detection of pathogenic bacterial cells.
- Develop specific primer sets and fluorescently labeled probes for specific detection of *Campylobacter jejuni* and *Listeria monocytogenes*.
- Accomplish bacterial detection with a detection limit of less than 10 CFU/ml on nanoliter fluidic arrays within eight hours.

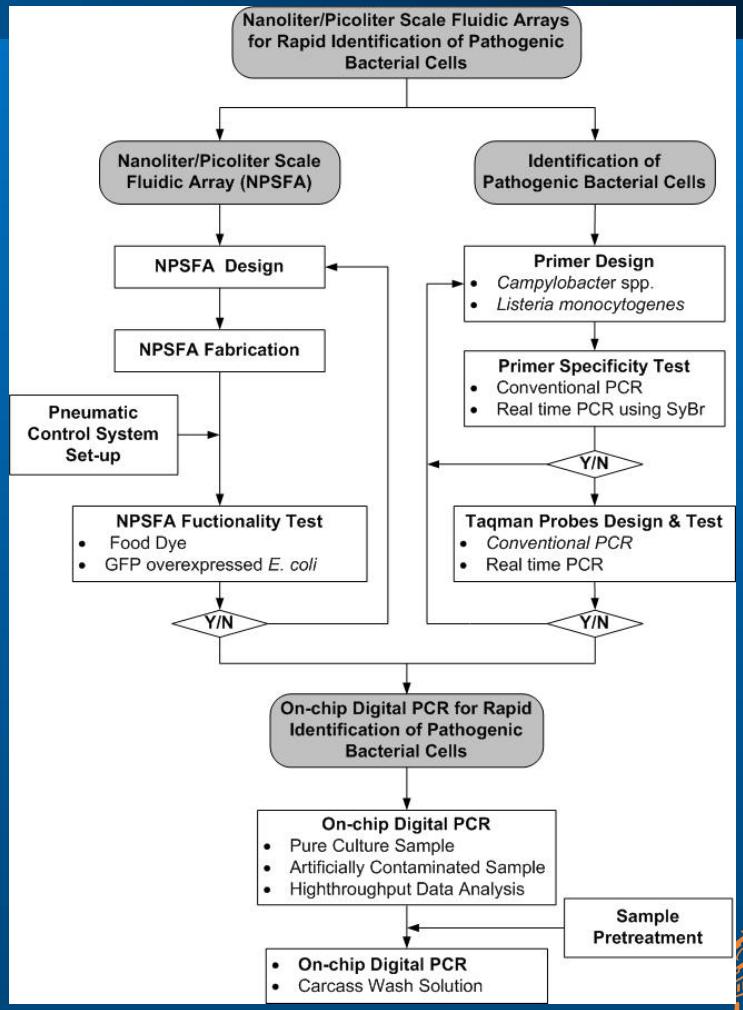

AUBURN UNIVERSITY

Device fabrication process

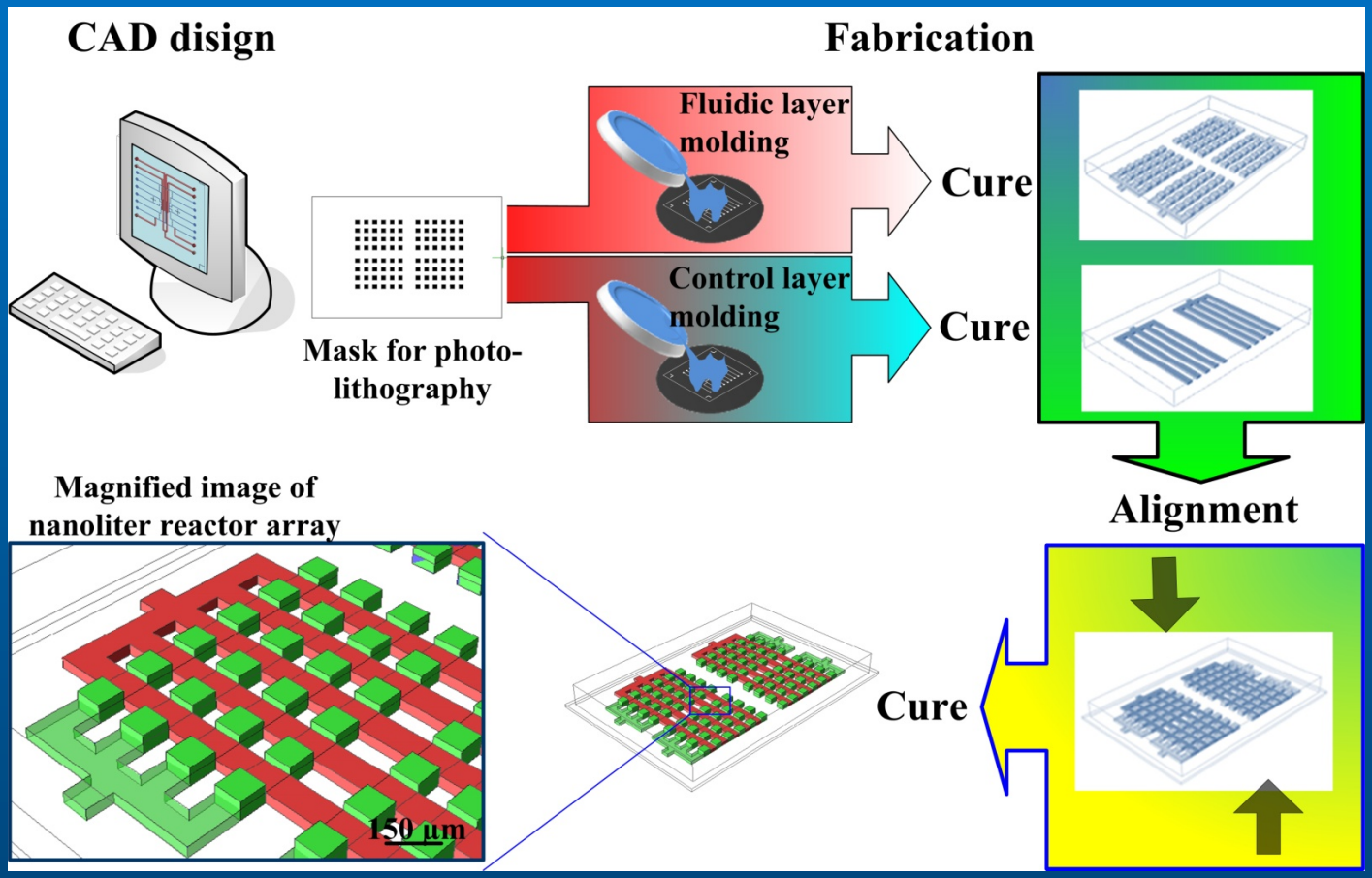

AUBURN UNIVERSITY

Fabricated nanoliter fluidic array

- **A fabricated nanoliter fluidic array and the chip-to-world interface**
- a) A nanoliter fluidic array chip on an inverted fluorescent microscope stage. The chip was designed and fabricated by the Auburn Systems and Nanomaterials Engineering Laboratories
- b) Example of nanofluidic detection of single-bacterial cells using a biochip array scanner. Bright spots indicate the presence of target bacteria in the sample.

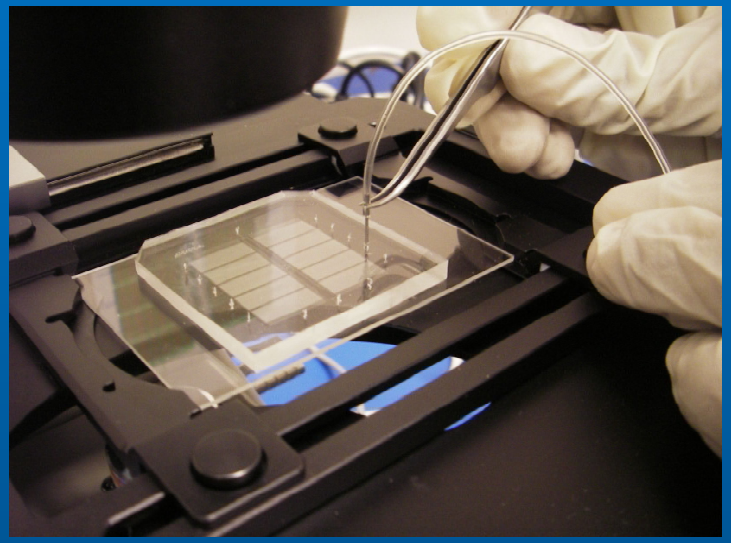

AUBURN
UNIVERSITY

Operation of nanoliter fluidic array

- **a) Preloading**
  - Introduce the control solution, such as polyethylene glycol (PEG) into control channel, to operate or close the control valves located among each nanoliter fluidic reactor
- **b) Sample loading**
  - Introduce the mixture of suspect samples, which may include target pathogenic bacterium, and PCR reagent, such as Taq polymerase, forward and reverse primers, probe, dNTPs, $MgCl_2$ etc.
- **c) Nanoliter digital PCR**
  - Perform thermal cycling with the nanoliter fluidic array on a modified thermal stage.
- **d) Bacteria detection**
  - Detect fluorescence signal that is specific to target pathogenic bacteria

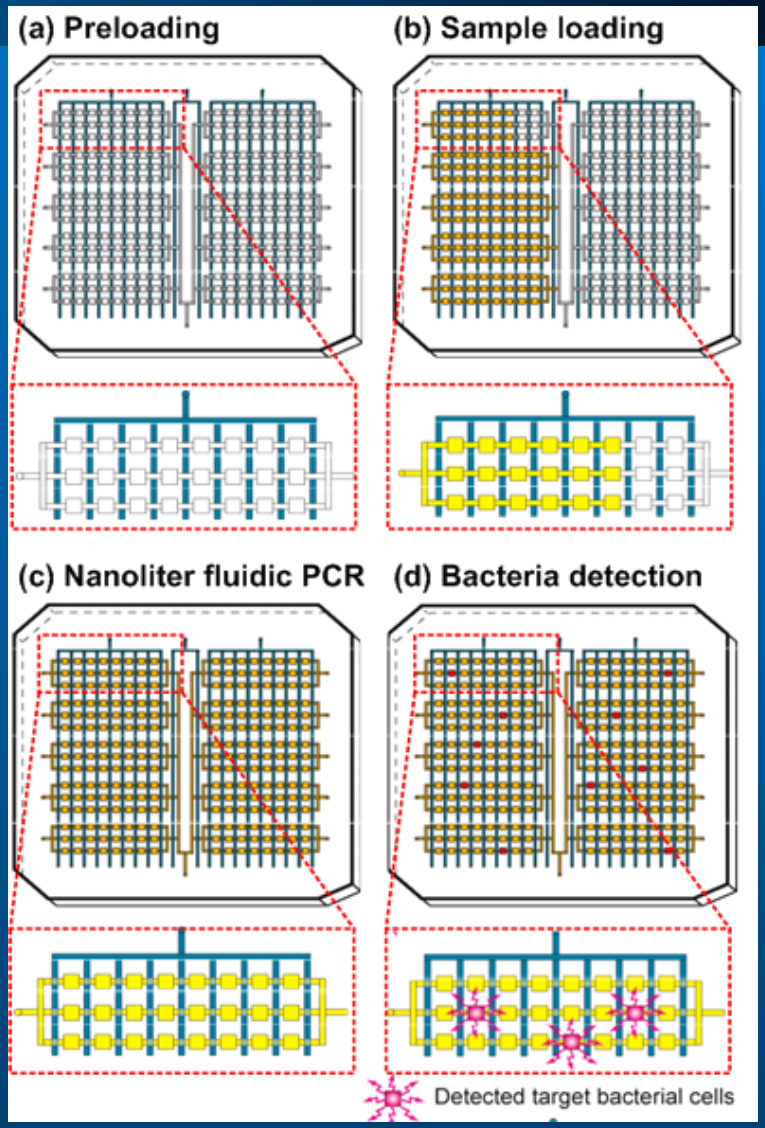

Amplicon size and locations of the designed primer sets and probes

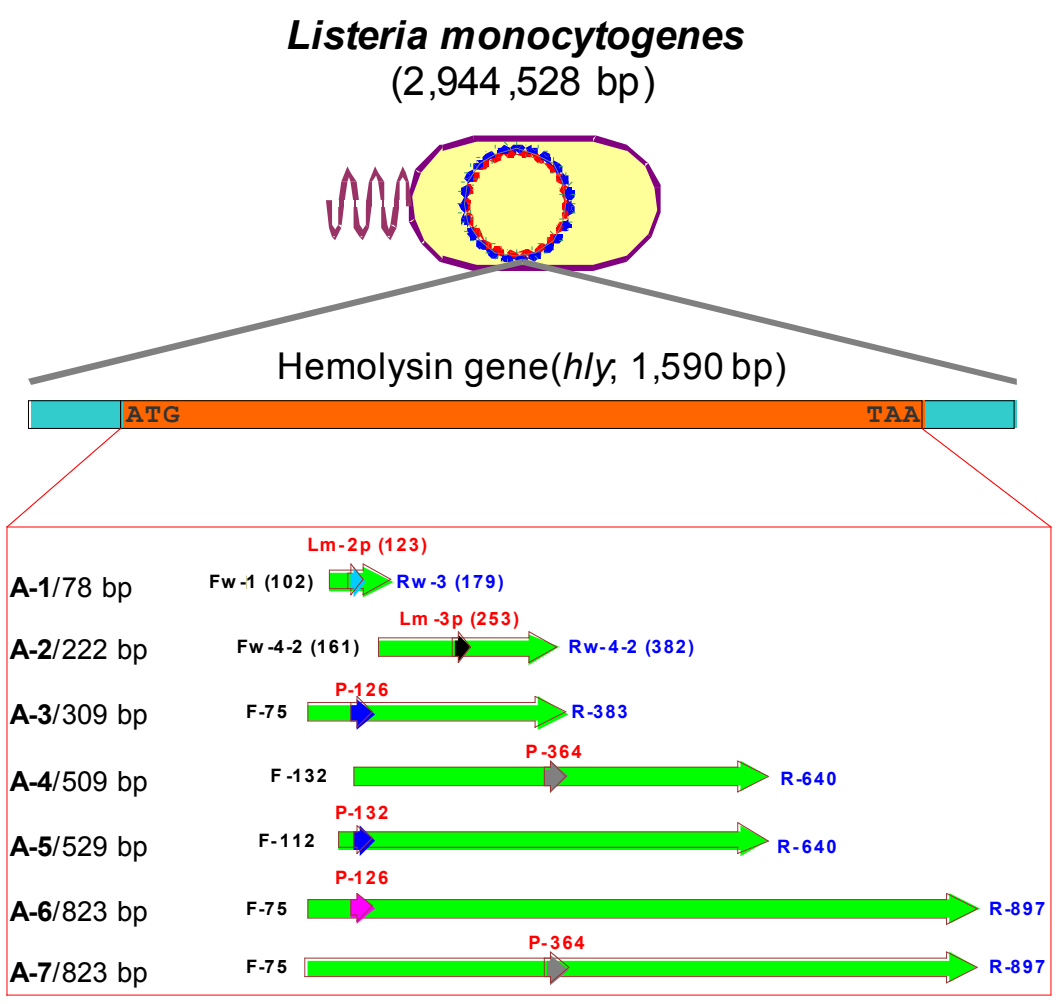

AUBURN UNIVERSITY

Off-chip specificity evaluation with purified genomic DNA

- **Template:**
- 10^6 copies/reaction of genomic DNA
- Strains: *L. ivanovii, L. welshimeri, L. innocua, L. grayi, L. seeligeri and L. monocytogenes*
- **Primer sets and probes:**
- 4 combinations of primarily screened primer sets and probes
- **Number of reactions**
- combinations × (strains + 1N.C.) × number of replications = 4 × 7 × 3 = 84 reactions
- **Reagents and machine**
- ABI 7500 PCR machine
- 2 X Taqman Universal Master mix

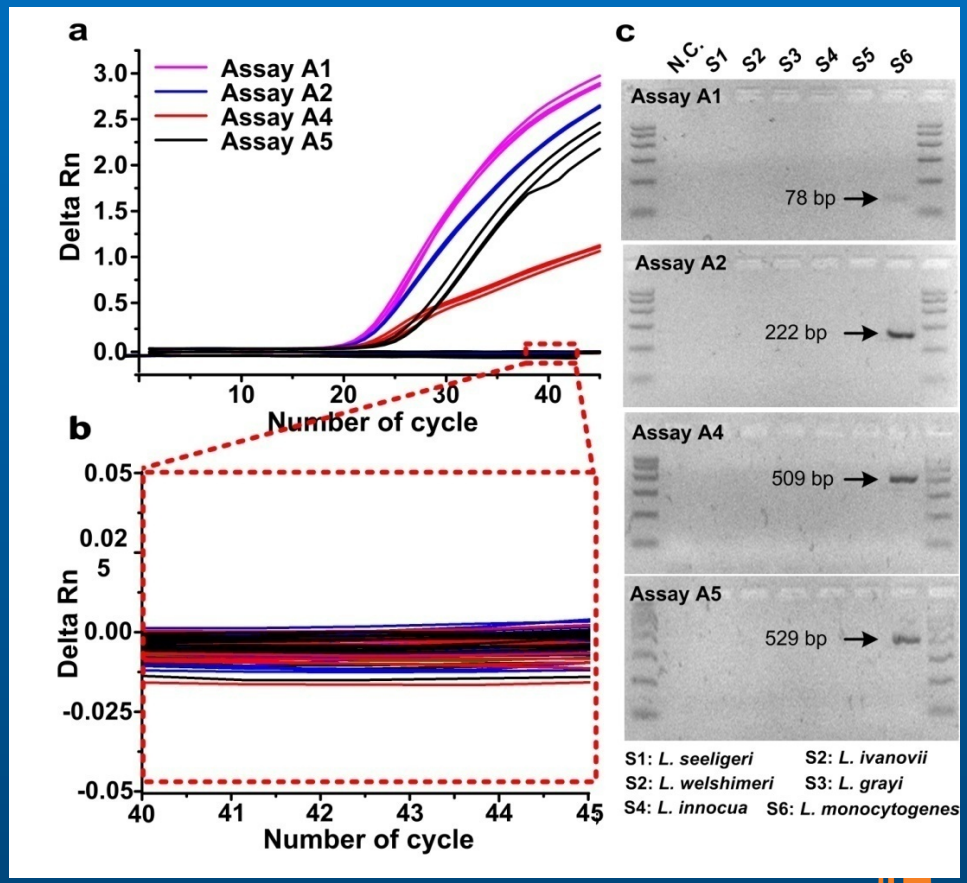

AUBURN UNIVERSITY

Off-chip specificity evaluation with raw cells

- **Template:**
- 5 X10^4 copies/reaction of raw cells
- Strains: *L. ivanovii, L. welshimeri, L. innocua, L. grayi, L. seeligeri and L. monocytogenes*
- **Primer sets and probes:**
- 4 combinations of primarily screened primer sets and probes
- **Number of reactions**
- combinations × (strains + 1N.C.) × number of replications = 4 × 7 × 3 = 84 reactions
- **Reagents and machine**
- ABI 7500 PCR machine
- 2 X Taqman Universal Master mix

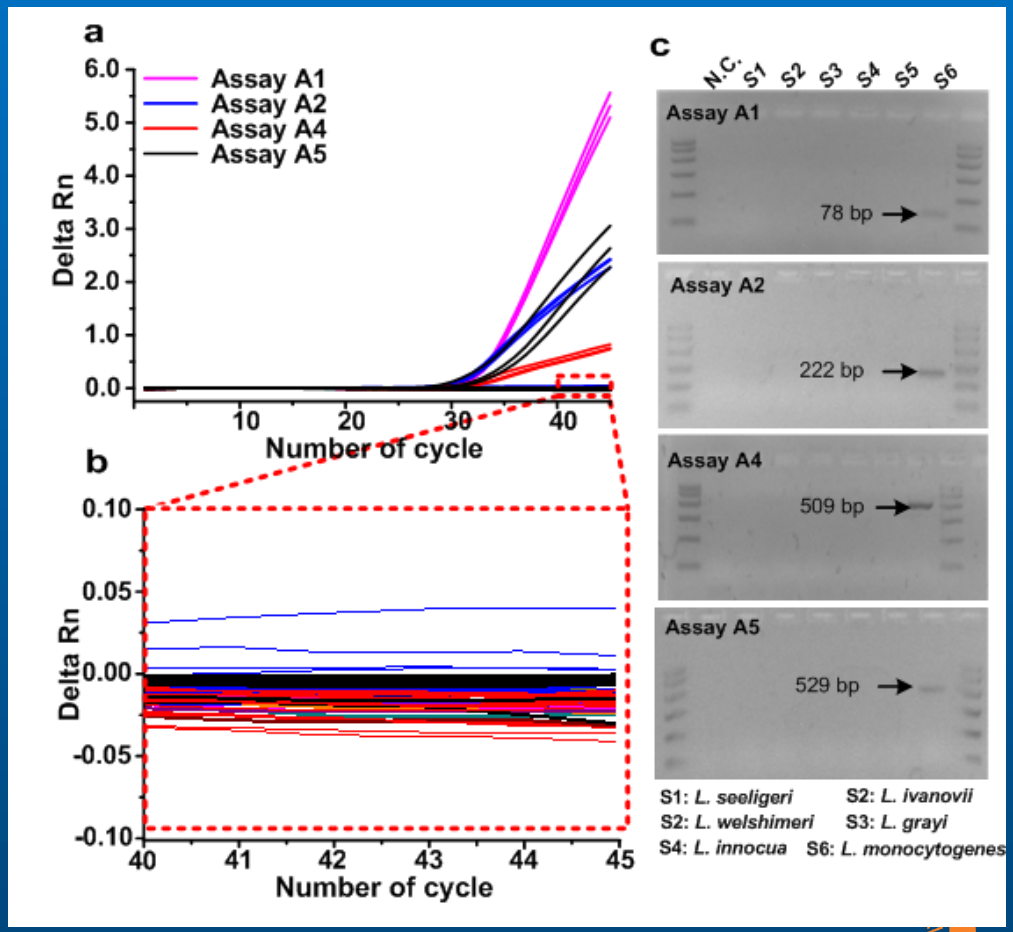

AUBURN UNIVERSITY

Relationship between template concentration and C_T values

- **Template:**
  - Purified genomic DNA of *L. monocytogenes* with *Qiagen* kit
  - Raw cell of *L. monocytogenes* in PBS buffer (pH 7.4)
  - Crude cell extract of *L. monocytogenes* in PBS buffer (pH 7.4)
- **Primer sets and probes:**
  - Combination A-1
  - Primer concentration: 900/900 nM
  - Probe concentration: 400 nM
- **Reagents and machine**
  - ABI 7500 PCR machine
  - 2 X Taqman Universal Master mix

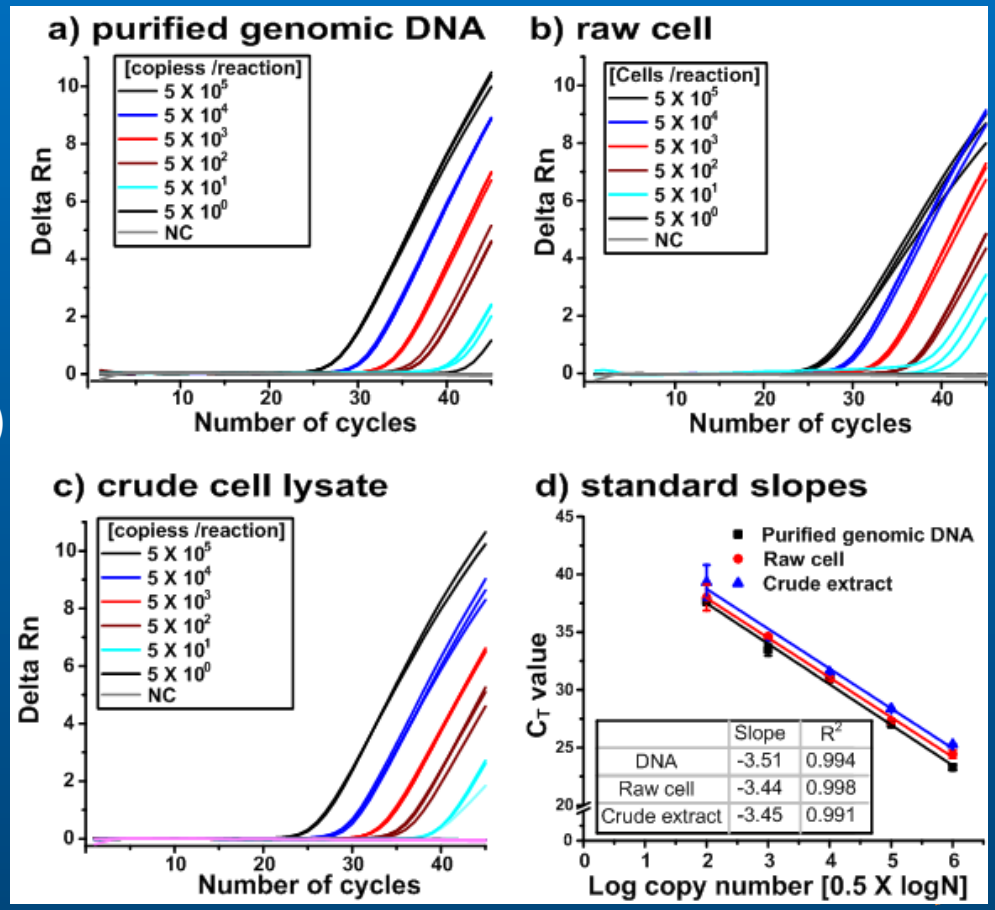

AUBURN UNIVERSITY

Plating on agar

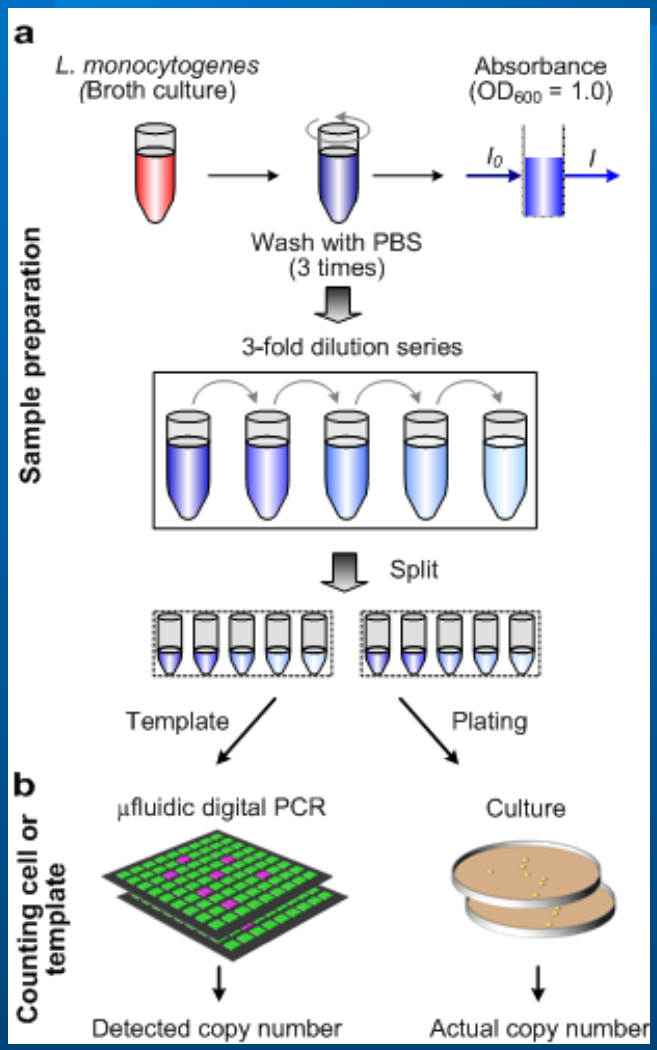

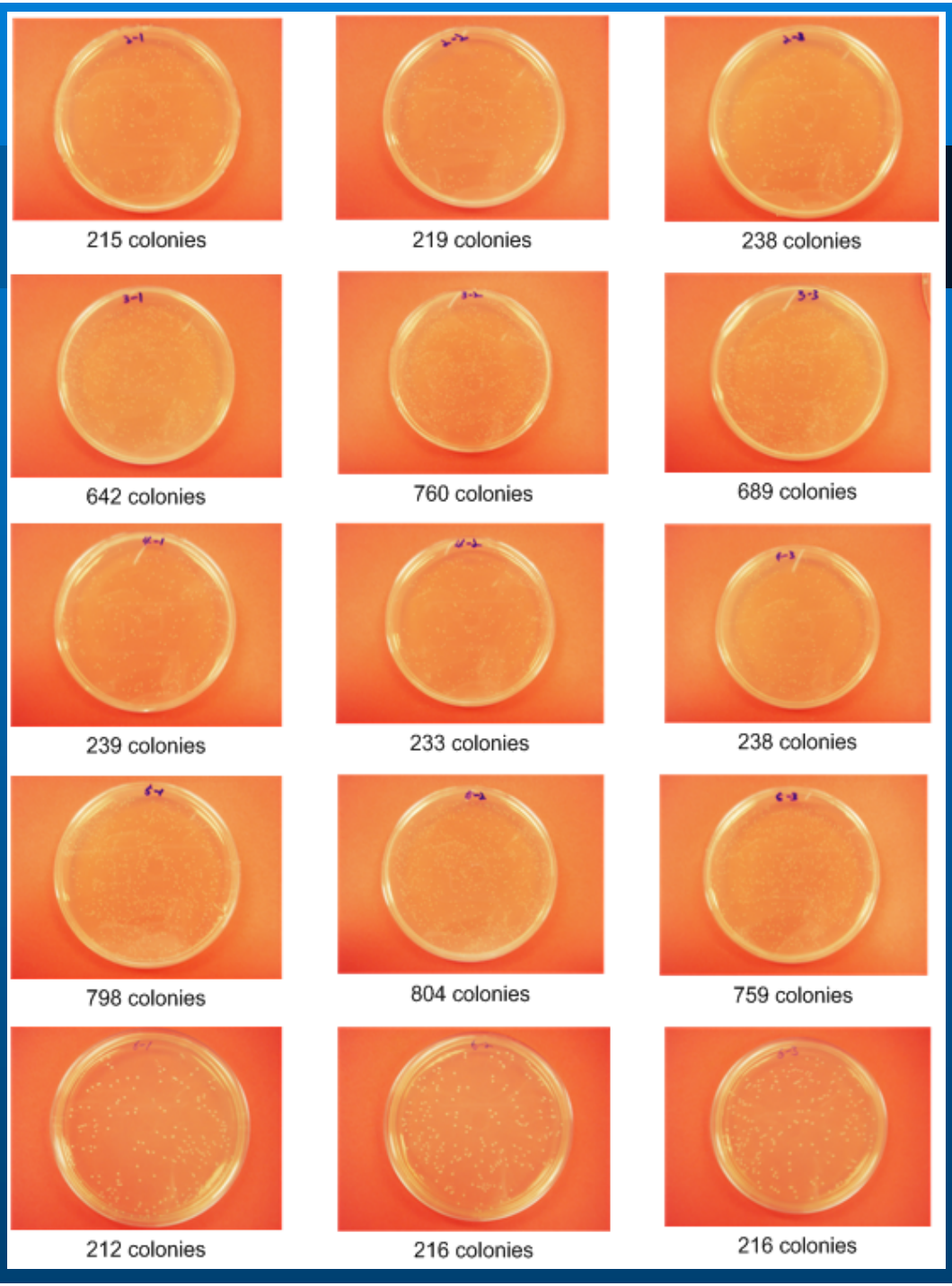

Enumeration: Sensitivity of nanoliter arrays

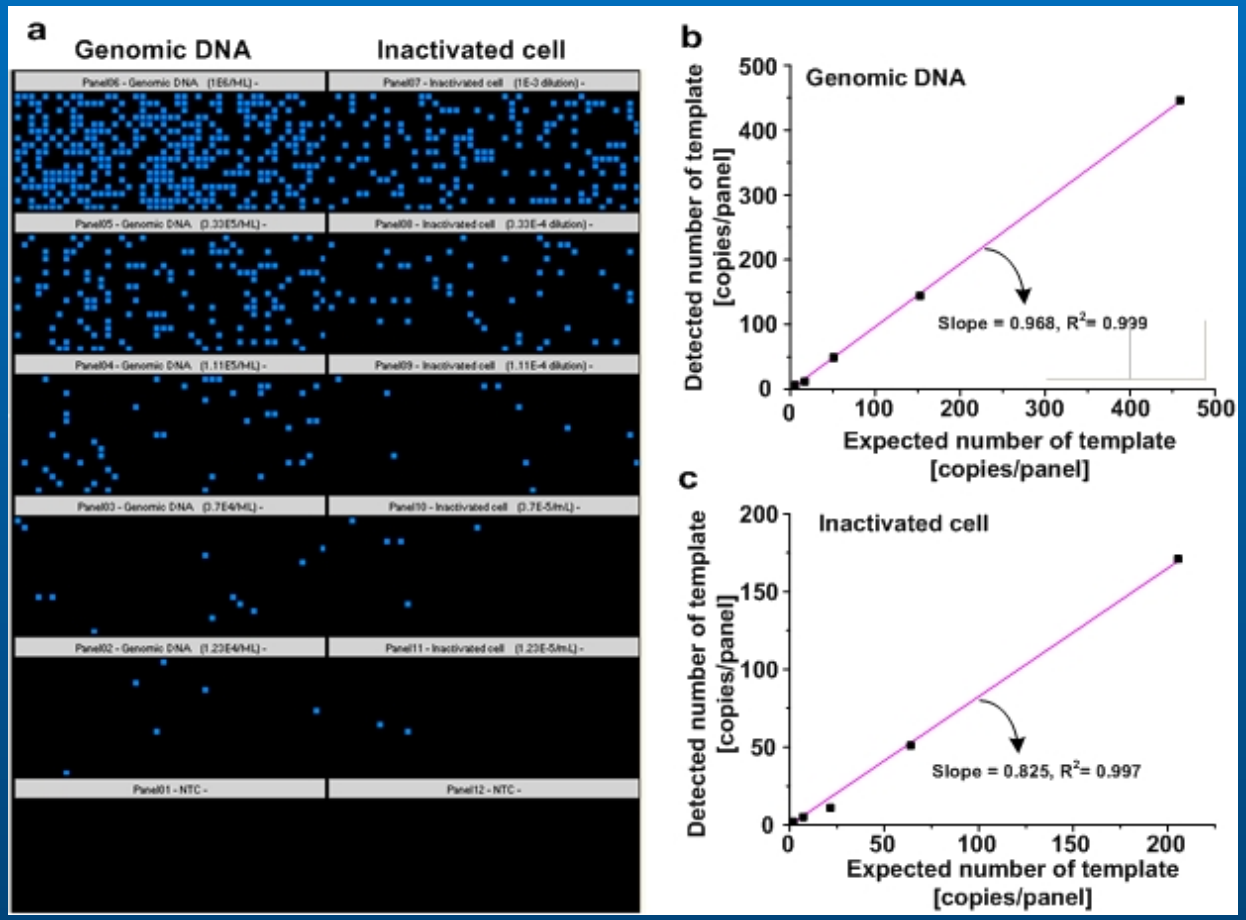

AUBURN UNIVERSITY

Further Work

- Detection of pathogenic bacteria from enriched carcass rinse

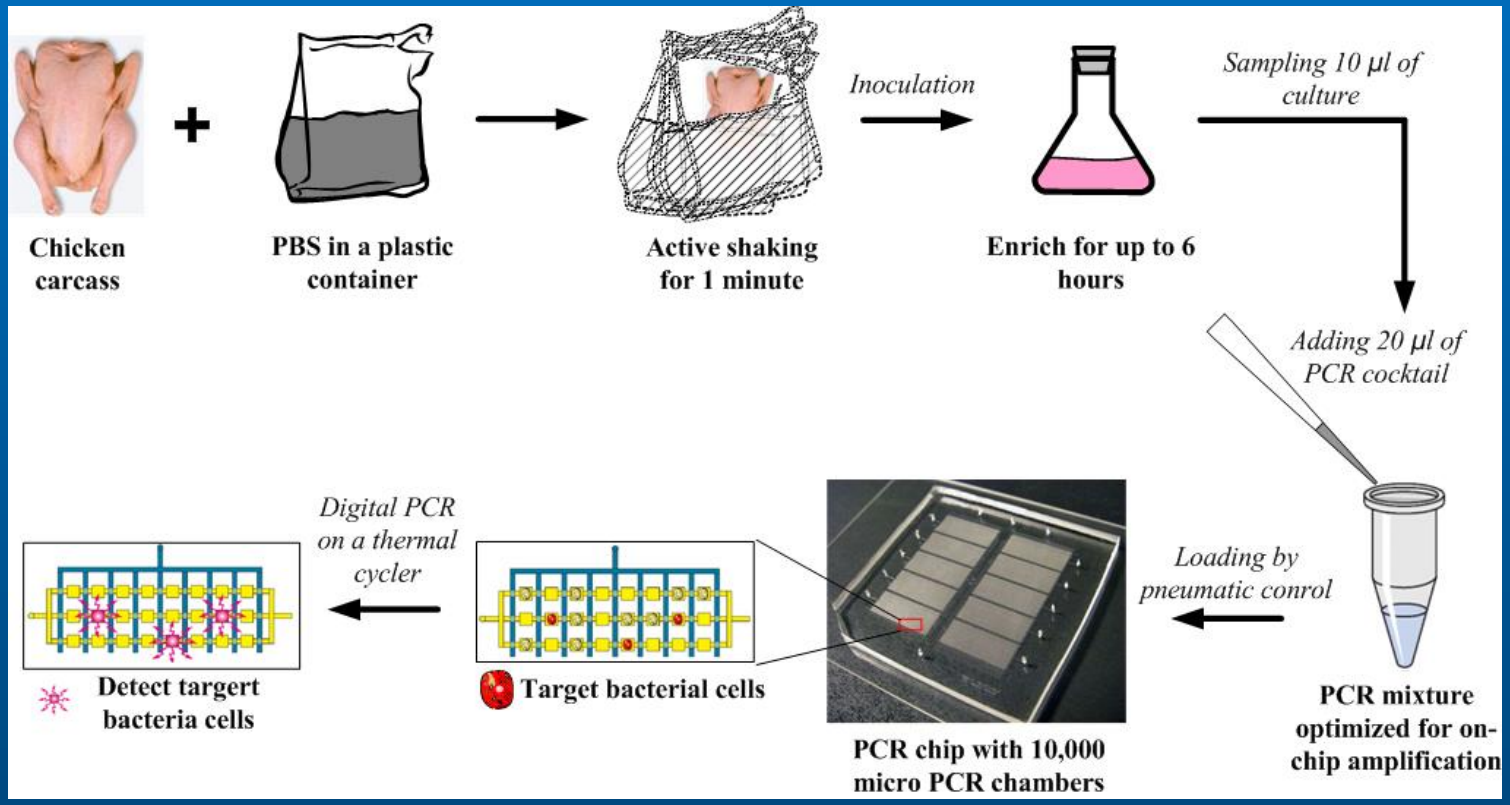

AUBURN UNIVERSITY

Summary

- Nanoliter fluidic array was designed and fabricated.
- 4 combinations of primer sets and probes were developed for specific detection of *L. monocytogenes.*
- *C*ombination A-1 was selected and the reaction conditions were then optimized.
- The detection of single templates of DNA and inactivated cells of *L. monocytogenes* has achieved by using a nanoliter fluidic array.
- The detection of *L. monocytogenes* from poultry carcass rinse will be evaluated by using a nanoliter fluidic array.

AUBURN
UNIVERSITY

Acknowledgments

- USDA NIFA NRI program
- Mechanical Engineering, Auburn University
  - Dr. Jae Young Yun
  - Jing Zou
- Alabama State University
  - Dr. Omar A. Oyarzabal
- Biology, Brigham Young University-Idaho
  - Eliseo Garcia

AUBURN UNIVERSITY

Comments &

Questions

AUBURN
UNIVERSITY